

Dissertation
submitted to the
Combined Faculties for the Natural Sciences and for Mathematics
of the Ruperto-Carola University of Heidelberg, Germany
for the degree of
Doctor of Natural Sciences

presented by

Diplom-Biochem.: Rudolf Walczak

born in: Hamburg, Germany

Oral examination:

The role of MEL-28 in nuclear pore complex formation

PhD student:

Rudolf Walczak

Group leader:

Prof. Dr. Iain W. Mattaj

Referees:

Dr. Jan Ellenberg

Prof. Dr. Elmar Schiebel

INAUGURAL - DISSERTATION

zur
Erlangung der Doktorwürde
der
Naturwissenschaftlich-Mathematischen Gesamtfakultät
der
Ruprecht – Karls – Universität
Heidelberg

vorgelegt von

Diplom-Biochem.: Rudolf Walczak

aus: Hamburg, Deutschland

Tag der mündlichen Prüfung:

Die Rolle von MEL-28 bei der Bildung des Kernporenkomplexes

Doktorand:

Rudolf Walczak

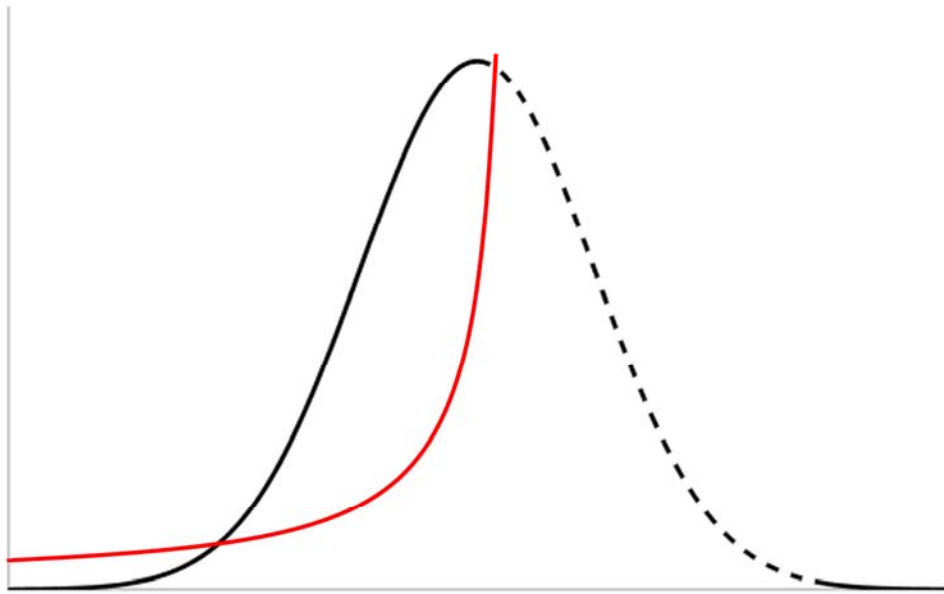
Betreuer:

Prof. Dr. Iain W. Mattaj

Gutachter:

Dr. Jan Ellenberg

Prof. Dr. Elmar Schiebel



"The greatest shortcoming of the human race is our inability to understand the exponential function."

(A. A. Bartlett)

Table of contents

Short summary	9
Zusammenfassung	11
List of figures	13
Abbreviations	14
1 Introduction	17
1.1 The nuclear envelope	18
1.2 The nuclear pore complex	20
1.3 Nucleocytoplasmic transport.....	24
1.4 Functions of the NE and NPCs other than transport	27
1.5 The nuclear lamina	28
1.6 Dynamics of the nuclear envelope during the cell cycle.....	29
1.6.1 Nuclear envelope breakdown	29
1.6.2 Functions of NE and NPC components during mitosis	31
1.6.3 Nuclear envelope and nuclear pore complex formation	31
1.7 MEL-28 and NET5	37
1.7.1 MEL-28	37
1.7.2 NET5.....	39
1.8 Aim of the thesis	40
2 Results	41
2.1 MEL-28	42
2.1.1 Generation of specific reagents against human MEL-28	42
2.1.2 Human MEL-28 is a nuclear envelope and kinetochore protein.....	44
2.1.3 MEL-28 localizes to nuclear pores and the INM.....	44
2.1.4 MEL-28 is required for NPC maintenance in human cells.....	49
2.1.5 Annulate lamellae can form independently of MEL-28.....	51
2.1.6 MEL-28 is required for postmitotic NPC assembly.....	54
2.1.7 MEL-28 interacts with the Nup107-160 complex.....	57
2.1.8 Identification of proteins bound to MEL-28.....	59
2.1.9 MEL-28 acts upstream of the Nup107-160 complex in NPC assembly.....	62
2.1.10 Mapping the NE-localization domain in MEL-28	64
2.1.11 Interplay with the Ran GTPase system.....	67
2.1.12 Expression and purification of full length MEL-28	70
2.1.13 Recombinant MEL-28 rescues the MEL-28 depletion phenotype in the first steps of NPC assembly	72
2.1.14 Investigating the function of the MEL-28 AT hook.....	75
2.1.15 Inhibition of nuclear assembly with an excess of AT hook recapitulates the MEL-28 depletion phenotype.....	78
2.1.16 The C-terminus of MEL-28 contains at least one chromatin binding motif besides the AT hook	82
2.1.17 MEL-28 binding to chromatin is regulated during the cell cycle	86

2.2 NET5.....	89
2.2.1 NET5 is a conserved transmembrane protein with a well defined domain organization	89
2.2.2 Human NET5 localizes to foci in the nuclear envelope	90
2.2.3 RNAi depletion of NET5 causes aberrant nuclear and cytoskeletal morphology and folding of the nuclear envelope	94
2.2.4 Mapping the sequence requirements for NET5 localization.....	97
2.2.5 Additional approaches and experiments	100
3 Discussion.....	102
3.1 MEL-28	103
3.1.1 MEL-28 is a conserved NPC/INM protein in metazoa.....	103
3.1.2 MEL-28 is essential for NPC formation	104
3.1.3 MEL-28 interacts with the Nup107-160 complex.....	104
3.1.4 MEL-28 functions in postmitotic NPC formation by recruiting nucleoporins to chromatin	105
3.1.5 Recombinant MEL-28 rescues Nup107-160 complex binding to chromatin.....	107
3.1.6 The MEL-28 AT hook binds to chromatin and is important for NPC formation.....	107
3.1.7 Regulation of MEL-28 function by the GTPase Ran	110
3.1.8 The function of MEL-28 is regulated during the cell cycle.....	110
3.1.9 Model for MEL-28 in postmitotic NPC formation	111
3.2 NET5.....	114
3.2.1 NET5 is a conserved transmembrane protein of the INM	114
3.2.2 Specific domains mediate correct NET5 localization	114
3.2.3 Loss of NET5 perturbs nuclear integrity.....	115
3.2.4 Future perspectives regarding NET5	117
4 Materials and methods	118
4.1 Materials	119
4.1.1 Chemicals and reagents	119
4.1.2 Commonly used buffers, solutions and media	122
4.1.3 Materials	123
4.1.4 Instruments	124
4.1.5 Animals and cell lines	125
4.1.6 Bacterial strains	125
4.1.7 Antibodies	125
4.1.8 Clones.....	126
4.1.9 Oligonucleotides	127
4.1.10 Plasmids	128
4.1.11 Constructs.....	129
4.1.11.1 Foreign constructs	129
4.1.11.2 Constructs generated as part of this thesis.....	129
4.2 Methods	130
4.2.1 Molecular biology methods	130
4.2.1.1 Purification of plasmid DNA	130

4.2.1.2 Restriction digest	130
4.2.1.3 Ligation of DNA fragments	131
4.2.1.4 Preparation of chemically competent cells	131
4.2.1.5 Transformation of chemically competent bacteria	131
4.2.1.6 PCR	131
4.2.1.7 RT-PCR	132
4.2.1.8 Real time quantitative PCR	132
4.2.2 Biochemical methods	132
4.2.2.1 Biochemical standard methods	132
4.2.2.1.1 Protein expression in <i>E. coli</i>	132
4.2.2.1.2 Purification of His ₆ -tagged proteins	132
4.2.2.1.3 Purification of GST-tagged proteins	133
4.2.2.1.4 Determination of protein concentration	133
4.2.2.1.5 Sodium dodecyl sulfate polyacrylamide gel electrophoresis (SDS-PAGE)	133
4.2.2.1.6 Silver staining	134
4.2.2.1.7 Western blotting	134
4.2.2.1.8 Affinity purification of polyclonal antibodies	135
4.2.2.1.9 Preparation of antibody beads	135
4.2.2.1.10 Immunodepletion of MEL-28 or the Nup107-160 complex from egg extract	136
4.2.2.1.11 Immunoprecipitation	136
4.2.2.2 Specific biochemical methods	136
4.2.2.2.1 Protein expression and purification using the Baculo system	136
4.2.2.2.2 Preparation of interphase <i>Xenopus leavis</i> egg extract	137
4.2.2.2.3 Preparation of mitotic <i>Xenopus leavis</i> egg extract	140
4.2.2.2.4 Floatation of interphase membranes	140
4.2.2.2.5 Labeling of floated membranes	140
4.2.2.2.6 Preparation of sperm chromatin	141
4.2.2.2.7 <i>In vitro</i> nuclear assembly	141
4.2.2.2.8 Formation of annulate lamellae <i>in vitro</i>	141
4.2.2.2.9 Re-isolation of chromatin for Western blotting	143
4.2.3 Other methods	143
4.2.3.1 Generation of polyclonal antibodies in rabbits	143
4.2.3.2 Cell culture	144
4.2.3.3 Transient transfection of human cells	144
4.2.3.4 Immunofluorescence	144
4.2.3.5 Light microscopy	144
4.2.3.6 Electron microscopy	145
4.2.3.7 Bioinformatic tools	145
5 References	146
Declaration / Erklärung	158
Publications	159
Acknowledgements	160

Short summary

The nuclear envelope (NE) is a highly specialized membrane system that surrounds the interphase nucleus of eukaryotic cells. Nuclear pore complexes (NPCs) form gated channels through the NE and mediate nucleocytoplasmic transport. In metazoan cells, the NE breaks down and reforms during each cell cycle. These events are tightly coordinated in space and time with the formation of the mitotic spindle and the segregation of chromosomes to the two daughter cells. At the end of mitosis, new NPCs begin to assemble on chromatin and an intact NE reforms around the decondensing chromosomes.

MEL-28/ELYS is a recently identified NE protein essential for nuclear integrity and function in many organisms. Genetic mutation or RNAi depletion of MEL-28 severely impair nuclear morphology and lead to loss of NPCs from the NE in a variety of cells and organisms. Our work and that of others shows that MEL-28 is critically involved in postmitotic NPC formation, but at the same time links between MEL-28 and other cellular processes are emerging.

This thesis aims at thoroughly characterizing the role of MEL-28 in nuclear assembly. It addresses the function of MEL-28 in living cells and examines the contribution of MEL-28 to nuclear assembly *in vitro*.

MEL-28 is an NPC/INM protein in interphase and partly localizes to kinetochores in mitosis. RNAi knockdown of MEL-28 in human cells results in loss of nucleoporins (nups) from the NE, but leaves the NE membranes intact, suggesting that it is specifically involved in NPC assembly. This phenotype is mirrored by employing MEL-28-immunodepleted *Xenopus laevis* egg extract for nuclear assembly *in vitro*, which gives rise to nuclei devoid of pores. MEL-28 acts in NPC formation by targeting nups to chromatin. It interacts with a subset of nups, the Nup107-160 complex, which is a central building block of the NPC. MEL-28 binds directly to chromatin through its AT hook and additional chromatin binding motifs in its C-terminus. My data show that MEL-28 anchors the forming NPC to chromatin. Addition of high concentrations of AT hook to a nuclear assembly reaction leads to inhibition of NPC assembly and

recapitulates the MEL-28 depletion phenotype. Recombinant MEL-28 rescues the recruitment of the Nup107-160 complex to chromatin, indicating that the depletion phenotype in nuclear assembly can be specifically attributed to MEL-28. The function of MEL-28 is under control of the Ran GTPase. RanGTP enhances MEL-28 and nup binding to chromatin and thus triggers NPC formation. Moreover, MEL-28 chromatin binding is regulated during the cell cycle, possibly by phosphorylation.

In conclusion, this study extends our current model of postmitotic NPC formation by demonstrating that targeting of nups to chromatin is mediated by and requires MEL-28. MEL-28 function is regulated spatially by the Ran GTPase and coordinated temporally with the cell cycle. The involvement of MEL-28 in NPC formation is its best characterized function to date, but it is likely that MEL-28 has additional roles in other cellular processes.

In addition, this thesis contains an initial characterization of NET5, a conserved transmembrane protein of the INM. NET5 has a well defined domain topology and localizes to foci in the NE which are not identical to nuclear pores. RNAi knockdown of NET5 in human cells perturbs nuclear integrity and leads to distortion of the NE, suggesting that it has an essential role in nuclear organization.

Part of this thesis was published in:

Franz C*, **Walczak R***, Yavuz S, Santarella R, Gentzel M, Askjaer P, Galy V, Hetzer M, Mattaj IW and Antonin W (2007). "MEL-28/ELYS is required for the recruitment of nucleoporins to chromatin and postmitotic nuclear pore complex assembly." EMBO Rep **8**: 165-72.

* authors contributed equally

Zusammenfassung

Die Kernhülle stellt ein hochgradig spezialisiertes Membransystem dar, welches den Zellkern eukaryontischer Zellen in der Interphase umgibt. Kernporenkomplexe bilden Kanäle durch die Kernhülle und vermitteln den Transport von Molekülen zwischen Zellkerninnerem und Zytoplasma. In Vielzellern wird die Kernhülle bei jeder Zellteilung abgebaut, und bildet sich danach neu. Diese Vorgänge sind räumlich und zeitlich eng mit der Bildung der mitotischen Spindel und der Verteilung der Chromosomen auf die beiden Tochterzellen abgestimmt. Am Ende der Mitose bilden sich neue Kernporenkomplexe auf dem Chromatin, und eine intakte Kernhülle baut sich um die dekodensierenden Chromosomen auf.

MEL-28/ELYS ist ein kürzlich identifiziertes Kernhüllenprotein, das in zahlreichen Organismen für die Integrität und Funktion des Zellkerns essentiell ist. Die genetische Mutation oder RNAi Depletion von MEL-28 beeinträchtigen die Gestalt des Zellkerns und führen in einer Vielzahl von Zellen und Organismen zu einem Verlust von Kernporenkomplexen von der Kernhülle. Unsere Arbeit und diejenige anderer zeigen, dass MEL-28 an der Bildung von Kernporenkomplexen am Ende der Mitose beteiligt ist. Gleichzeitig wird jedoch, deutlich, dass MEL-28 auch in andere zelluläre Vorgängen eingebunden ist.

Die vorliegende Arbeit hatte das Ziel, die Rolle von MEL-28 bei der Bildung des Zellkerns umfassend zu charakterisieren. Sie beinhaltet Experimente zur Funktion von MEL-28 in lebenden Zellen und zum Beitrag von MEL-28 zur Zellkernbildung *in vitro*.

MEL-28 ist Teil der Kernpore und der inneren Kernmembran in der Interphase, und ein Teil des zellulären MEL-28 bindet an Kinetochore in der Mitose. Die RNAi Depletion von MEL-28 in menschlichen Zellen hat den Verlust von Nukleoporinen von der Kernhülle zur Folge, nimmt jedoch keinen Einfluss auf die Kernmembran. Dieses Ergebnis legt nahe, dass MEL-28 spezifisch an der Bildung von Kernporenkomplexen beteiligt ist. Ein vergleichbares Ergebnis erhält man mit dem *in vitro* Kernbildungssystem, bei dem die Verwendung von MEL-28-immundepletiertem *Xenopus laevis* Eiextrakt zur Bildung von kernporenfreien Zellkernen führt. Die

Funktion von MEL-28 besteht darin, Nukleoporine bei der Bildung des Kernporenkomplexes zum Chromatin zu führen. MEL-28 interagiert mit einer Gruppe von Nukleoporinen, dem Nup107-160 Komplex, einem zentralen Baustein des Kernporenkomplexes. Es bindet mittels seines AT hook Motifs und weiterer Chromatinbindungsmotive in seinem C-Terminus direkt an Chromatin. Meine Daten zeigen, dass MEL-28 den sich bildenden Kernporenkomplex am Chromatin verankert. Die Zugabe hoher Konzentrationen von AT hook zu einer Kernbildungsreaktion hemmt die Bildung von Kernporenkomplexen und führt zum gleichen Phänotyp wie die Depletion von MEL-28. Rekombinantes MEL-28 rettet die Bindung des Nup107-160 Komplexes an Chromatin, was verdeutlicht, dass der Depletionsphänotyp bei der Zellkernbildung spezifisch auf MEL-28 zurückzuführen ist. Die Funktion von MEL-28 wird durch die GTPase Ran reguliert. RanGTP verstärkt die Bindung von MEL-28 und Nukleoporinen an Chromatin und fördert so die Bildung von Kernporenkomplexen. Zusätzlich ist die Bindung von MEL-28 an Chromatin im Laufe des Zellzyklus reguliert, möglicherweise durch Phosphorylierung.

Die vorliegende Arbeit erweitert unser Modell der Bildung von Kernporenkomplexen um die Erkenntnis, dass MEL-28 die Bindung von Nukleoporinen an Chromatin vermittelt. Die Funktion von MEL-28 ist räumlich durch die GTPase Ran reguliert und zeitlich mit dem Zellzyklus abgestimmt. Die Beteiligung an der Kernporenbildung ist die bisher bestcharakterisierte Funktion von MEL-28, aber es ist wahrscheinlich, dass es an weiteren zellulären Vorgängen beteiligt ist.

Diese Arbeit umfasst zusätzlich eine initiale Charakterisierung von NET5, einem konservierten Protein der inneren Kernmembran. NET5 verfügt über eine klar definierte Topologie und ist in Foci in der Kernhülle zu finden, bei denen es sich nicht um Kernporen handelt. Die RNAi Depletion von NET5 in menschlichen Zellen zerstört die Integrität des Zellkerns und führt zu einer Auffaltung der Kernhülle. Diese Ergebnisse legen nahe, dass NET5 eine essentielle Funktion für die Organisation des Zellkerns besitzt.

List of figures

Figure 1-1.	Schematic illustration of a metazoan nucleus.	19
Figure 1-2.	3D-model of the NPC from <i>Dictyostelium discoideum</i>	21
Figure 1-3.	Nucleoporin organization within the metazoan NPC.	22
Figure 1-4.	The events of nuclear envelope breakdown (NEBD).	30
Figure 1-5.	Schematic illustration of postmitotic NE and NPC formation.	33
Figure 2-1.	Generation of specific antibodies against human MEL-28.	43
Figure 2-2.	Human MEL-28 is a nuclear envelope and kinetochore protein.	45
Figure 2-3.	MEL-28 localizes to nuclear pores and the INM.....	46
Figure 2-4.	The C-terminus of MEL-28 faces the inner side of the NE.	48
Figure 2-5.	MEL-28 is required for NPC maintenance in human cells.....	50
Figure 2-6.	RNAi depletion of MEL-28 leads to annulate lamellae formation.	52
Figure 2-7.	MEL-28 is neither part of annulate lamellae nor required for AL formation.	53
Figure 2-8.	MEL-28 is required for postmitotic NPC formation.	56
Figure 2-9.	MEL-28 interacts with the Nup107-160 complex.....	58
Figure 2-10.	Proteins bound to MEL-28 in <i>Xenopus laevis</i> egg extract.....	60
Figure 2-11.	MEL-28 is required for recruitment of the Nup107-160 complex to chromatin but not vice versa.	63
Figure 2-12.	Mapping the minimal region for NE localization in MEL-28.	65/66
Figure 2-13.	RanGTP-mediated recruitment of nucleoporins to chromatin is dependent on MEL-28.....	69
Figure 2-14.	Expression and purification of full length MEL-28 from insect cells..	71
Figure 2-15.	Recombinant MEL-28 partially rescues the MEL-28 depletion phenotype in NPC assembly.....	74
Figure 2-16.	The AT hook in MEL-28 binds to chromatin.	76
Figure 2-17.	Inhibition of nuclear assembly with an excess of AT hook recapitulates the MEL-28 depletion phenotype.	79
Figure 2-18.	The MEL-28 AT hook does not displace endogenous MEL-28 from chromatin.	81
Figure 2-19.	The endogenous MEL-28 concentration in <i>Xenopus laevis</i> egg extract is ≈ 75 nM.....	83
Figure 2-20.	The C-terminus of MEL-28 contains at least one chromatin binding motif besides the AT hook.....	85
Figure 2-21.	MEL-28 binding to chromatin is regulated during the cell cycle.	87
Figure 2-22.	Topology of NET5.	89
Figure 2-23.	Human NET5 localizes to foci in the nuclear envelope.	91
Figure 2-24.	The NET5 foci are not identical to nuclear pores.	93
Figure 2-25.	RNAi depletion of NET5 causes aberrant nuclear morphology and leads to invagination of the nuclear envelope.	95
Figure 2-26.	RNAi depletion of NET5 results in distortion of nuclear shape and perturbs cytoskeletal organization.....	96
Figure 2-27.	Mapping the requirements for NET5 localization.....	99
Figure 3-1.	Model for early events in postmitotic NPC formation.....	112
Figure 4-1.	Preparation of interphase <i>Xenopus laevis</i> egg extract.	139
Figure 4-2.	Steps of nuclear assembly <i>in vitro</i>	142

Abbreviations

µm	Micrometer
µM	Micromole
aa	Amino acid
AL	Annulate lamellae
ATP	Adenosine triphosphate
BAF	Barrier to autointegration factor
BAPTA	1,2-Bis(2-aminophenoxy) ethane-N,N,N',N'-tetraacetic acid
BSA	Bovine serum albumin
<i>C. elegans</i>	<i>Caenorhabditis elegans</i>
Cdk	Cyclin-dependent kinase
cDNA	Complementary DNA
Conc.	concentration
Crm1	Chromosome region maintenance 1
DAPI	4',6-Diamidino-2-phenylindole
DNA	Deoxyribonucleic acid
DTT	Dithiothreitol
<i>E. coli</i>	<i>Escherichia coli</i>
EDTA	1-(4-Aminobenzyl)ethylenediamine-N,N,N',N'- tetraacetic acid
EGFP	Enhanced green fluorescent protein
EGTA	Ethylene glycol-bis(2-aminoethyl)-N,N,N',N'-tetraacetic acid
ELYS	Embryonic large molecule derived from yolk sac
EM	Electron microscopy
ER	Endoplasmic reticulum
ESPRIT	Expression of Soluble Proteins by Random Incremental Truncation
FG	Phenylalanine glycine dipeptide
GAP	GTPase activating protein
GAPDH	Glyceraldehyde 3-phosphate dehydrogenase
GDP	Guanosine diphosphate
GEF	Guanine-nucleotide exchange factor
GFP	Green fluorescent protein
GSH	Glutathione
GST	Glutathione-S-transferase
GTP	Guanosine triphosphate
hCG	Human chorionic gonadotropin
HeLa cells	Henrietta Lacks' cells
HMGA	High-mobility group A
<i>Hs</i>	<i>Homo sapiens</i>
iFRAP	Inverse fluorescence-recovery after photobleaching
INM	Inner nuclear membrane
IP	Immunoprecipitation
IPTG	Isopropyl-β-D-1-thiogalactopyranoside
KASH	Klarsicht, ANC-1, Syne homology domain
Kb	kilobase
kDa	Kilodalton
Lap	Lamina associated peptide

LBR	Lamin B receptor
LEM	Protein domain found in <u>L</u> AP2, <u>E</u> merin and <u>M</u> AN-1
LHX	LIM homeobox protein
mAb	Monoclonal antibody
Mcm	Minichromosome maintenance
MDa	Megadalton
mel-28	Maternal-effect embryonic-lethal
mRNA	Messenger RNA
MTOC	Microtubule organizing center
MS	Mass spectrometry
MT	Microtubule
NE	Nuclear envelope
NEBD	Nuclear envelope breakdown
NES	Nuclear export signal
NET	Nuclear envelope transmembrane protein
NIMA	Never in mitosis
Ni-NTA	Nickel-nitrilo triacetic acid
NLS	Nuclear localization signal
nm	Nanometer
NMR	Nuclear magnetic resonance
NPC	Nuclear pore complex
NTF2	Nuclear transport factor 2
NTP	Nucleoside triphosphate
Nup	Nucleoporin
OD	Optical density
Oligo	Oligonucleotide
ONM	Outer nuclear membrane
ORC	Origin recognition complex
ORF	Open reading frame
PAGE	Polyacrylamide gel electrophoresis
PCR	Polymerase chain reaction
PFA	Paraformaldehyde
pI	Isoelectric point
PI	Protease inhibitors
PMSG	Pregnant mare serum gonadotropin
POM	Pore membrane
Ran	Ras-related nuclear protein
RanBP	Ran binding protein
RanGAP	Ran GTPase activating protein
RanGEF	Ran guanine-nucleotide exchange factor
RCC1	Regulator of chromosome condensation
RNA	Ribonucleic acid
RNAi	RNA interference
rRNA	Ribosomal RNA
RT	Room temperature
RT-PCR	Reverse transcriptase PCR
RZPD	Deutsches Ressourcenzentrum für Genomforschung
SAP	Shrimp alkaline phosphatase
SDS	Sodium dodecyl sulfate

siRNA	Small interfering RNA
SUMO	Small ubiquitin-related modifier
SUN	<u>Sad1</u> , <u>UNC-84</u> homology domain
TEM	Transmission electron microscopy
TPR	Translocated promoter region
u	Unit
UTR	Untranslated region
VRK	Vaccinia-related kinase
<i>Xl</i>	<i>Xenopus laevis</i>

1 Introduction

The hallmark of eukaryotic cells is their elaborate subdivision into structurally and functionally distinct membrane-enclosed compartments. The most prominent of these organelles is the cell nucleus, which harbors the genetic material during interphase of the cell cycle. The nucleus is delimited by the nuclear envelope (NE), which provides the physical barrier between the nuclear interior and the cytoplasm and constitutes a central component of nuclear architecture. Compartmentalization into nucleus and cytoplasm provides eukaryotic cells with unique and complex possibilities for regulating gene expression. At the same time, the need for selective exchange of molecules between the different compartments arises. DNA replication, transcription, RNA processing and ribosomal subunit maturation occur in the nucleus, while proteins are synthesized in the cytoplasm. Therefore, mRNAs, rRNAs and ribosomes must be exported from the nucleus whereas nuclear and ribosomal precursor proteins have to be imported. These transport events are exclusively mediated by nuclear pore complexes (NPCs) in the NE and selective and efficient nucleocytoplasmic transport is essential for proper functioning and survival of eukaryotic cells. The transport mechanism will be discussed in greater detail below, but first I will describe the crucial elements of NE architecture.

1.1 The nuclear envelope

The NE is composed of four distinct elements: the inner (INM) and outer (ONM) nuclear membranes, NPCs and, in metazoa, the nuclear lamina. INM and ONM contain two different sets of membrane proteins and are separated by the perinuclear space, which topologically corresponds to the lumen of the endoplasmic reticulum (ER). While the ONM is continuous with, although not identical to, the ER, the INM harbors a unique set of integral membrane proteins which form contacts with the underlying lamina and chromatin. One group of INM proteins are the so-called LEM domain (Lap2, Emerin and MAN-1) containing proteins, which interact with the small dimeric DNA-binding protein Barrier-to-autointegration factor (BAF) and are associated with the nuclear lamina. BAF acts in concert with vaccinia-related kinase (VRK) and is required for NE formation in *C. elegans* (Gorjanacz *et al.*, 2007). Lamin B receptor, another conserved integral INM protein, binds to lamin B and

transcriptionally silent chromatin via heterochromatin protein 1 (Ye and Worman, 1996).

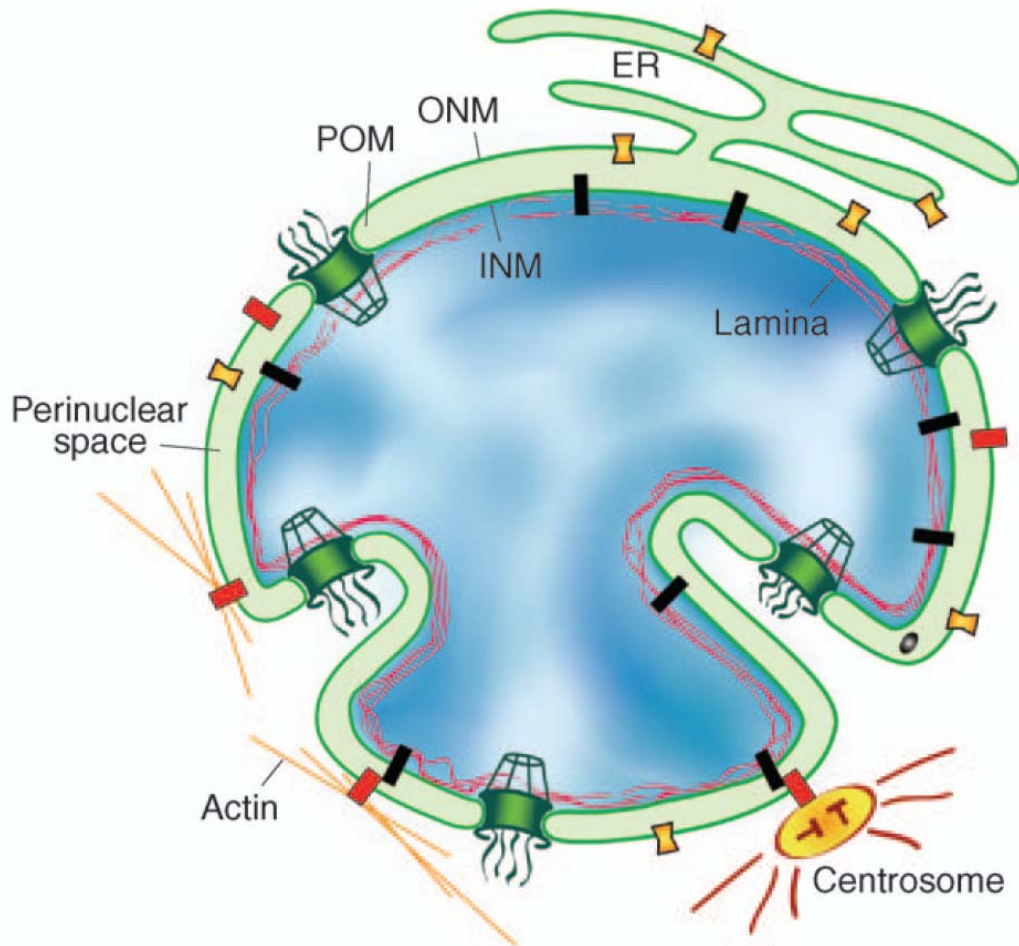


Figure 1-1. Schematic illustration of a metazoan nucleus. ER: endoplasmic reticulum; ONM: outer nuclear membrane; INM: inner nuclear membrane; POM: pore membrane; INM-specific proteins are depicted in black, ONM-specific proteins in red and ER/ONM proteins in yellow. (Modified from Prunuske and Ullman, 2006)

In recent years, an intriguing link between the INM and ONM has emerged with the discovery and characterization of proteins from the SUN (Sad1, UNC-84 homology) and KASH (Klarsicht, ANC-1, Syne homology) families. SUN proteins reside in the INM, while KASH-domain proteins are specific for the ONM. Both form an interaction that bridges the perinuclear space and is essential for proper spacing of the nuclear membranes (Crisp *et al.*, 2006). At the same time, SUN proteins bind to lamins A and

C (Haque *et al.*, 2006), whereas KASH proteins associate with the cytoskeletal actin network and centrosome (Starr and Han, 2002; Malone *et al.*, 2003). In this way they have been implicated in nuclear positioning and migration and in transmitting forces between the cytoskeleton and nuclear lamina (Starr, 2007).

1.2 The nuclear pore complex

The NE is perforated by nuclear pores, aqueous channels that connect the nucleoplasm and the cytoplasm. These openings are occupied by NPCs, large protein assemblies, which span the ONM and INM. NPCs are the sole known mediators of nucleocytoplasmic transport and their general architecture is conserved among eukaryotes. Early structural studies revealed that NPCs possess an eightfold rotational symmetry perpendicular to the plane of the NE (Watson, 1959; Franke, 1966). Today, with the help of powerful imaging methods, such as cryoelectron tomography and three-dimensional reconstruction, the NPC structure has been refined significantly and several distinct structural elements within the NPC have been identified (Beck *et al.*, 2004; Beck *et al.*, 2007). The NPC can be divided into three main parts, a central circular core in the plane of the NE, cytoplasmic filaments and a nuclear basket. The central core, which measures roughly 100 nm in diameter, consists of three distinct ring structures: a cytoplasmic ring, a luminal spoke ring and a nuclear ring. It has been a matter of debate whether the central plug or transporter, which appears to be highly variable in shape (Beck *et al.*, 2004), is an integral part of the NPC or represents cargo in transit through the nuclear pore. A diverse set of biophysical and proteomic data were combined in an effort to obtain a comprehensive model of the yeast NPC with better definition of the position of individual proteins than has been possible from the EM studies (Alber *et al.*, 2007). This model needs to be tested as additional information on the NPC emerges. Until recently, only few crystal structures of nuclear pore proteins had been determined, but new studies are adding to our understanding of the fine structure of NPCs (Napetschnig *et al.*, 2007; Melcak *et al.*, 2007; Hsia *et al.*, 2007; Schrader *et al.*, 2008; Böhmer *et al.*, 2008; Brohawn *et al.*, 2008; Debler *et al.*, 2008). The future challenge for structural biologists will be to determine the structures of NPC subcomplexes, to fit the obtained crystal structures

into the EM structures to complete our model of the NPC and to understand the dynamics of NPC components.

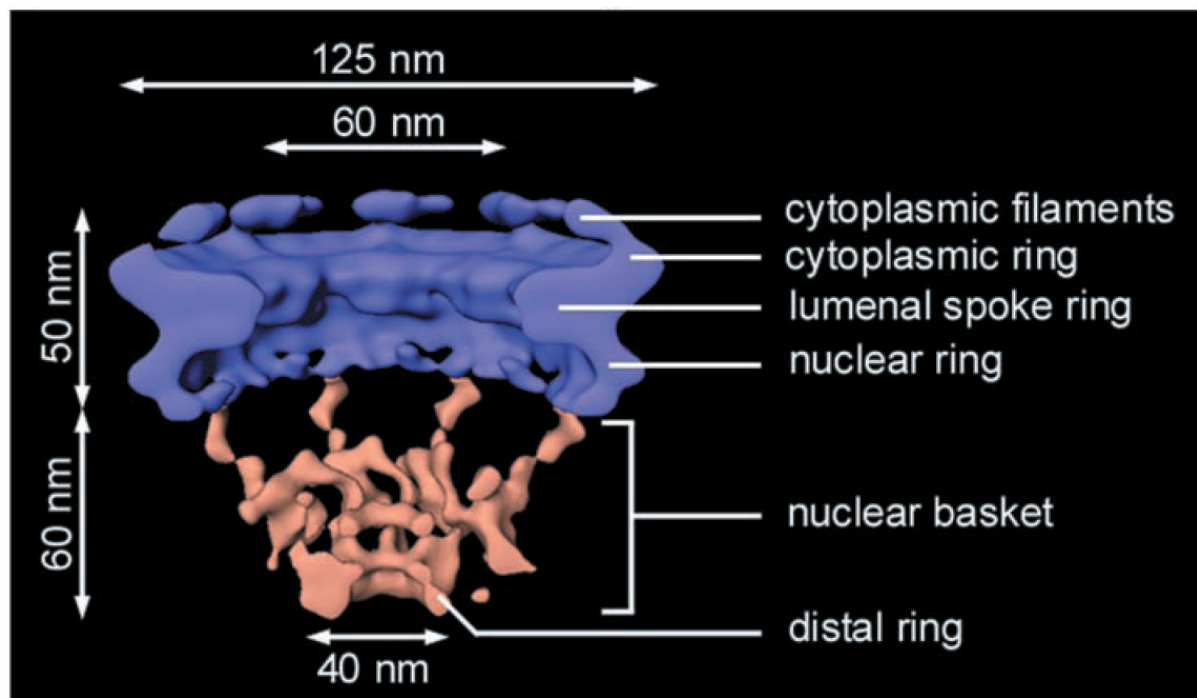


Figure 1-2. 3D-model of the NPC from *Dictyostelium discoideum*. This structure was determined by cryoelectron tomography and three-dimensional reconstruction and highlights the main morphological features of eukaryotic NPCs. (Adapted from Beck *et al.*, 2004)

NPCs are enormous structures by molecular standards with an estimated mass of 60 MDa in yeast (Rout *et al.*, 2000) and 125 MDa in vertebrates (Reichelt *et al.*, 1990; Cronshaw *et al.*, 2002). They are built in a modular fashion from only a limited number of molecular building blocks (Schwartz, 2005). NPCs are formed from ≈ 30 so-called nucleoporins (nups), many of which are organized in NPC subcomplexes. Nups are believed to exist in eight copies or multiples of eight per NPC, given its symmetry. Proteomic approaches aimed at providing an inventory of the NPC have yielded an extensive list of NPC proteins for the yeast (Rout *et al.*, 2000) and mammalian (Cronshaw *et al.*, 2002) NPC.

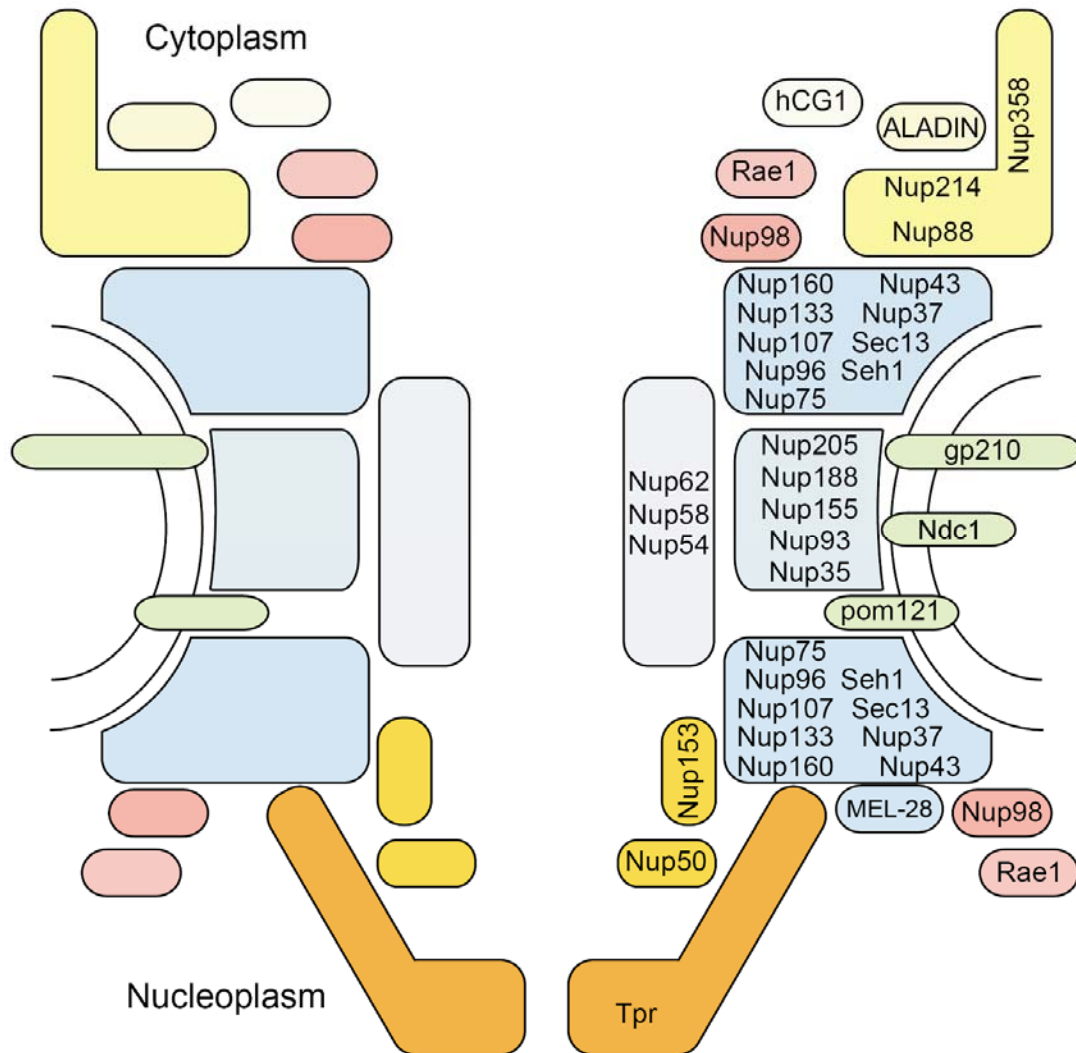


Figure 1-3. Nucleoporin organization within the metazoan NPC. The localization of nucleoporins in the NPC is indicated and nups in biochemically characterized subcomplexes are grouped. (Modified from Schwartz, 2005)

Nups can be divided into two groups based on the presence or absence of hydrophobic, natively unfolded FG repeat motifs (Denning *et al.*, 2003). FG repeat containing nups have been localized to the central channel of the nuclear pore and are assumed to constitute the permeability barrier of the NPC (Rout *et al.*, 2000; Denning *et al.*, 2003). Nups without FG repeats are thought to be structured and to form the backbone of NPC architecture (Rout *et al.*, 2000). The NPC is stably associated with

the NE membranes at sites where the INM and ONM join. Vertebrate and yeast NPCs each contain three transmembrane nups, Pom121, Ndc1 and gp210 in vertebrates and pom34, Ndc1 and pom152 in yeast (Mans *et al.*, 2004). Integral membrane nups are believed to anchor the NPC to the NE membrane.

Nups form evolutionarily conserved, biochemically stable NPC subcomplexes, which behave as an entity throughout the cell cycle and are believed to function as building blocks of the NPC. The largest of these complexes is the Nup107-160 complex in vertebrates or Nup84 complex in yeast (Belgareh *et al.*, 2001; Vasu *et al.*, 2001; Siniosoglou *et al.*, 1996), which is considered a key element of NPC structure. Alber *et al.* (2007) placed the Nup84 complex in the vicinity of the pore membrane (POM) in their yeast NPC model. Drin *et al.* (2007) identified an amphipathic α -helical motif, which senses membrane curvature as compared to flat membranes. Human Nup133 also contains this motif, suggesting that it might contribute to the so far poorly understood interaction between the NPC and the NE membranes. The Nup84 complex has a Y-shaped structure as judged by electron microscopy (Siniosoglou *et al.*, 2000; Lutzmann *et al.*, 2002), but so far no uniform model has emerged for the distribution of nups within the complex based on crystal structures (Hsia *et al.*, 2007; Browhan *et al.*, 2008). Nup205 and Nup93 reside in a distinct NPC subcomplex and are essential for NPC function and cell viability in *C. elegans* (Galy *et al.*, 2003). The Nup58 complex lines the central channel in the inner pore (Guan *et al.*, 1995) and is involved in gating transport cargoes through the NPC. Nup358/RanBP2 constitutes the cytoplasmic filaments of the NPC and attaches to the pore via Nup214 and Nup88 (Bernad *et al.*, 2004), while TPR, which forms the nuclear basket (Cordes *et al.*, 1997), is bound to the NPC via Nup153 (Walther *et al.*, 2001).

A computational and biochemical analysis assigned folds to the yeast and vertebrate nuclear pore proteins (Devos *et al.*, 2006). Interestingly, disordered FG repeats and two additional fold types, α -solenoids and β -propellers, accounted for >85% of all residues. This study also detected architectural similarities between NPCs and coated vesicles, suggesting that they might possess a common evolutionary origin. The authors had previously hypothesized that nups and vesicle coat proteins had evolved by duplication and divergence from very simple structural motifs (Devos *et al.*, 2004).

Two recently published crystal structures of parts of the yeast Nup84 complex provide additional evidence for a common ancestry of vesicle coat proteins and nups (Brohawn *et al.*, 2008; Debler *et al.*, 2008). A systematic analysis determined the dynamic organization of vertebrate nuclear pore proteins (Rabut *et al.*, 2004). Based on their dissociation rates from the NPC, which ranged from minutes to hours, nups were grouped into three categories: components of a stable central scaffold, more peripheral adapter nups and highly mobile proteins, which only transiently bind to NPCs. Interestingly, many additional proteins have been reported to localize to nuclear pores, although many of them have not been considered *bona fide* nups. Among them are the mitotic checkpoint proteins Mad1 and Mad2 (Campbell *et al.*, 2001; Iouk *et al.*, 2002) and RanGAP, which requires sumoylation for its localization to NPCs (Matunis *et al.*, 1996; Mahajan *et al.*, 1997).

1.3 Nucleocytoplasmic transport

The exchange of molecules between the nuclear interior and cytoplasm is mediated by NPCs and is an essential prerequisite for cell survival. Small molecules up to 20-40 kDa can pass the nuclear pore uninhibited by passive diffusion, whereas larger molecules have to be actively transported through the NPC. In this manner, cargoes up to several MDa, such as ribosomal subunits or viral particles, can traverse the pore. Active transport of cargo is a selective process and requires specific transport signals. These in turn are recognized by transport receptors, which mediate cargo passage through the nuclear pore (Mattaj and Englmeier, 1998; Görlich and Kutay, 1999). The largest group of transport receptors is constituted by members of the importin β superfamily (a.k.a. karyopherins), which interact directly with NPCs and possess an N-terminal RanGTP-binding motif. Based on the direction in which they carry their cargo these receptors can be classified as importins or exportins. In simple cases, the transport substrates are recognized directly by their respective receptor, in other scenarios, cargo recognition is mediated by adaptor molecules, such as importin α (Goldfarb *et al.*, 2004). Crm1 acts as an export receptor for leucine-rich nuclear export signals (NESs) (Fornerod *et al.*, 1997). mRNA export from the nucleus utilizes a different set of transport receptors, Mex67p-Mtr2p in yeast (Strässer and Hurt, 2000) and TAP-Nxt1 in humans (Katahira *et al.*, 1999; Guzik *et al.*, 2001).

The events of nucleocytoplasmic transport are controlled by the Ran GTPase system, which is conserved in all eukaryotes. Ran is an abundant, Ras-like small GTPase vital for nuclear organization that exists in GTP- and GDP-bound states. Conversion between these states requires additional proteins as Ran possesses low intrinsic activity for GTP hydrolysis or nucleotide exchange. Ran's active, GTP-bound form is generated by its chromatin-bound guanine-nucleotide exchange factor (GEF) RCC1 (Bischoff and Ponstingl, 1991; Klebe *et al.*, 1995). Hydrolysis of Ran-bound GTP to GDP is mediated by a cytosolic protein, the GTPase-activating protein RanGAP, which acts in concert with either RanBP1 or RanBP2 (Coutavas *et al.*, 1993; Yokoyama *et al.*, 1995). Consequently, interphase cells possess a high nuclear and low cytoplasmic RanGTP concentration and the reciprocal for RanGDP. The unequal distribution of RanGTP across the NE is instrumental in imposing directionality on nucleocytoplasmic transport, as RanGTP differentially influences cargo-receptor complex formation and cargo dissociation from their cognate transport receptor. Import cargo and receptor complexes form in the cytoplasm in the absence of RanGTP and enter the nucleus through nuclear pores. Binding of nuclear RanGTP to importins destabilizes the cargo-receptor complex, thereby liberating the import substrate in the nucleus. In contrast, the interaction of exportins with their cargoes is stabilized by RanGTP via cooperative binding and formation of a trimeric complex, which can then exit the nucleus. Once in the cytoplasm, this complex is dissociated by hydrolysis of Ran-bound GTP and the export cargo is delivered to its destination. Recycling of RanGDP to the nucleus is accomplished by NTF2 (Ribbeck *et al.*, 1998). In recent years, the structures of many components of the nucleocytoplasmic transport pathway have been solved and have helped further our understanding of this fascinating process (for a review see Cook *et al.*, 2007). Interestingly, the direction of transport can be inverted under certain experimental conditions (Nachury and Weis, 1999) and the actual passage of molecules through the pore is independent of Ran and energy (Englmeier *et al.*, 1999; Ribbeck *et al.*, 1999). Nevertheless, Ran is the key organizer and the driving force for all transport events, as GTP hydrolysis by Ran in the cytoplasm is the irreversible step, which confers directionality to nucleocytoplasmic transport.

Besides its well understood role in nucleocytoplasmic transport in interphase, Ran has also proven to be a key regulator of mitotic events (Hetzer *et al.*, 2002; Weis, 2003). Formation of RanGTP by RCC1 on chromatin persists throughout the cell cycle and leads to the formation of a RanGTP gradient ranging away from the condensed chromosomes in mitosis (Kalab *et al.*, 2002; Kalab *et al.*, 2006). In this manner, RanGTP acts as a universal spatial clue for cells to signal the position of chromatin and contributes to functions such as formation of the mitotic spindle (Clarke and Zhang, 2008) and postmitotic NPC assembly, as discussed in greater detail below.

NPCs are remarkable transport machines, which can mediate hundreds of transport events per second in both directions (Ribbeck and Görlich, 2001; Smith *et al.*, 2002). It has been a long standing question how such high transport rates can be reconciled with the simultaneously observed exquisite selectivity of NPCs. Translocation of cargo-receptor complexes through the pore crucially depends on interactions of FG nups with transport receptors (Rexach and Blobel, 1995; Shah *et al.*, 1998). A systematic deletion approach has defined the FG repeat nups essential for transport and viability in yeast (Strawn *et al.*, 2004). The structures of FG repeats in complex with importin β or NTF2 demonstrate that the FG repeat binding sites on the transport receptors are distinct from the sites for Ran or cargo molecule interaction and explain how transport receptors can bind to nups, while simultaneously interacting with a wide range of transport substrates (Bayliss *et al.*, 2000; Bayliss *et al.*, 2002). However, these structural snapshots cannot reveal the dynamics of translocation through the pore. Three models for the NPC transport mechanism have been proposed: The affinity gradient model predicts that cargo receptor complexes, while driven by Brownian motion, encounter stepwise increasing binding affinities upon passage through the pore (Ben-Efraim and Gerace, 2001). The Brownian affinity gating model is based on restricted diffusion through the pore and suggests that the probability for cargo entry into and passage through the NPC is significantly increased upon binding to transport receptors (Rout *et al.*, 2000). According to the selective phase model, FG repeat nucleoporins in the NPC form a meshwork through weak hydrophobic interactions, which acts as a physical barrier for molecules above a certain size (Ribbeck and Görlich, 2001). In order to enter and traverse the NPC, molecules have to become "dissolved" in the mesh, which requires a sufficiently hydrophobic surface

for interaction with FG repeats and competitive disruption of the inter-repeat contacts. Two recent publications have shown that the purified FG repeat domain of yeast Nsp1, which is required for viability in yeast, can form an elastic reversible hydrogel (Frey *et al.*, 2006) and that a saturated hydrogel has permeability properties similar in some respects to those of the nuclear pore (Frey *et al.*, 2007). An independent publication provided additional evidence that the FG domains of nups cooperate to establish the permeability barrier of the NPC (Patel *et al.*, 2007). Many transmembrane proteins are believed to pass from the ONM to the INM by passive diffusion through channels in NPCs (Soullam and Worman, 1993). Interestingly, a recent publication provided evidence that at least some integral membrane proteins are targeted to the INM by the same mechanism as soluble proteins (King *et al.*, 2006). This utilization of the Ran system could also explain the energy dependence of INM protein transport observed by Ohba *et al.* (2004). Having passed the NPC, INM proteins are prevented from diffusing back to the ER by stable interactions with underlying nuclear interaction partners, such as chromatin or the nuclear lamina ("diffusion-retention model"). The NPC accommodates a wide range of different transport pathways and nucleocytoplasmic transport is connected to many other cellular processes (see following paragraph). We can therefore expect interesting new findings, especially concerning the regulation of transport through the nuclear pore.

1.4 Functions of the NE and NPCs other than transport

The hypothesis that the nuclear periphery crucially contributes to nuclear organization was already stated more than two decades ago (Blobel, 1985). In recent years, it has become increasingly evident that the NE and NPCs not only serve as a passive barrier between the nucleus and cytoplasm and as transport devices, but actively participate in several other cellular functions, one of which is gene expression (for a review see Akhtar and Gasser, 2007). The general picture is that actively transcribed genes localize to the nuclear pore (Casolari *et al.*, 2004; Taddei *et al.*, 2006), while relocation of genes to the nuclear lamina and non-pore NE sites silences their expression (Pickersgill *et al.*, 2006; Reddy *et al.*, 2008). Other emerging areas of NPC function are modulating the activity of sumoylating and desumoylating enzymes (Palancade and Doye, 2008), DNA damage repair (Palancade *et al.*, 2007) or chromatin boundary

activity (Ishii *et al.*, 2002). Mice heterozygous for Nup96 exhibit specific defects in the immune system and are highly susceptible to viral infection (Faria *et al.*, 2006). Mutation of Nup155 causes atrial fibrillation in mice, thereby linking the NPC to cardiovascular disease (Zhang *et al.*, 2008). The expression levels of the Nup107-160 complex proteins are regulated during the cell cycle and ubiquitin-mediated degradation of Nup96 appears to control the expression of several cell cycle regulators (Chakraborty *et al.*, 2008). In *Drosophila melanogaster* Nup153 and the Tpr homologue Mtor critically contribute to dosage compensation of X-chromosomal genes in male flies (Mendjan *et al.*, 2006). In yeast, Ndc1 has essential functions both at the NPC and spindle pole bodies (Chial *et al.*, 1998).

1.5 The nuclear lamina

An essential element of the metazoan NE is the nuclear lamina, a network of type-V intermediate filaments which lines the INM. Lamins can be divided into A- and B-types based on their biochemical properties and behavior in mitosis. While B-type lamins are expressed in all cells and are essential for viability, A-type lamins (lamin A and C) arise by alternative splicing from a single gene, are expressed in a tissue-specific manner and are dispensable for cell survival. Lamins are elongated molecules and form coiled-coil dimers with their extended central domain, which polymerize head to head or head to tail into a two-dimensional lattice. The nuclear lamina confers physical stability on the nucleus, but is also involved in a variety of other cellular processes, such as chromatin organization, gene expression and signaling (for a review see Gruenbaum *et al.*, 2005). In mitosis, lamins are phosphorylated and the nuclear lamina is reversibly depolymerized (Gerace and Blobel, 1980). The nuclear lamina has become an intense focus of research, since mutations in lamins or lamin-associated proteins cause a wide range of heritable human diseases commonly referred to as "laminopathies" (Burke and Stewart, 2002). Among these clinical disorders are Emery-Dreyfuss muscular dystrophy and Hutchinson-Gilford progeria syndrome, which causes premature ageing. The study of lamins therefore links NE research to medical applications.

1.6 Dynamics of the nuclear envelope during the cell cycle

As cells divide chromatin condenses and the chromatids are segregated by the mitotic spindle. Yeast, filamentous fungi and certain protists undergo closed mitosis, in which the mitotic spindle forms inside the nucleus or spindle microtubules can penetrate the intact NE. In contrast, the NE of higher eukaryotes exhibits a highly dynamic behavior in M-phase. Metazoan cells undergo open mitosis, in which the NE breaks down in pro-metaphase and reforms in late anaphase/telophase. The nuclear membranes retract from chromatin and INM proteins diffuse freely throughout the ER, while soluble nups or NPC-subcomplexes become dispersed in the cytoplasm. These events are tightly coordinated in space and time with the formation of the mitotic spindle and the segregation of chromosomes to the two daughter cells. At the end of mitosis, new NPCs begin to assemble on chromatin and an intact NE reforms around the decondensing chromosomes.

1.6.1 Nuclear envelope breakdown

Upon entry into mitosis, metazoan cells disassemble their NE. The first step of nuclear envelope breakdown (NEBD) at the transition from prophase to prometaphase is marked by an increase in permeability of the NE and the release of certain nups from the NPC (Lénárt *et al.*, 2003). In mammalian somatic cells, NPC disassembly proceeds within minutes and begins with the dissociation of Nup98 from the pore, followed by a simultaneous release of several other nups (Dultz *et al.*, 2008). In subsequent steps, the nuclear lamina is disassembled (Gerace and Blobel, 1980) and the nuclear membranes retract from chromatin in a microtubule-dependent manner (Beaudouin *et al.*, 2002; Salina *et al.*, 2002). Interestingly, RanGTP has been shown to affect NEBD (Mühlhäusser and Kutay, 2007). Among the molecules involved in NEBD are the transmembrane nup gp210 (Galy *et al.*, 2008), the GTPase Rab5 and reticulons (Audhya *et al.*, 2007).

While soluble nups become dispersed throughout the cytoplasm in mitosis, integral membrane proteins of the nuclear membranes diffuse freely in the mitotic ER, which remains a continuous tubular network in living cells (Ellenberg *et al.*, 1997; Yang *et al.*,

1997; Puhka *et al.*, 2007). The hypothesis that NEBD would lead to vesiculation of the nuclear membrane derived from observations in *Xenopus laevis* egg extracts (Newport and Dunphy, 1992), probably stems from the fact that the ER is physically disrupted during the preparation of the extract and does not reflect the situation in living cells. The regulation of NEBD is believed to be carried out by mitotic kinases, which phosphorylate NE components, including nups, lamins and INM proteins. Cdk1 appears to be a universal mitotic kinase, which might phosphorylate nups and directly trigger lamina depolymerization. However, also Aurora A (Hachet *et al.*, 2007; Portier *et al.*, 2007) and a cyclin A2/Cdk complex (Gong *et al.*, 2007) play important roles in NEBD. The semi-open mitosis of *A.nidulans* is controlled by the NIMA kinase, which localizes to NPCs at the entry of mitosis and promotes dispersal of certain nups, including Nup98, which is phosphorylated by NIMA (De Souza *et al.*, 2004).

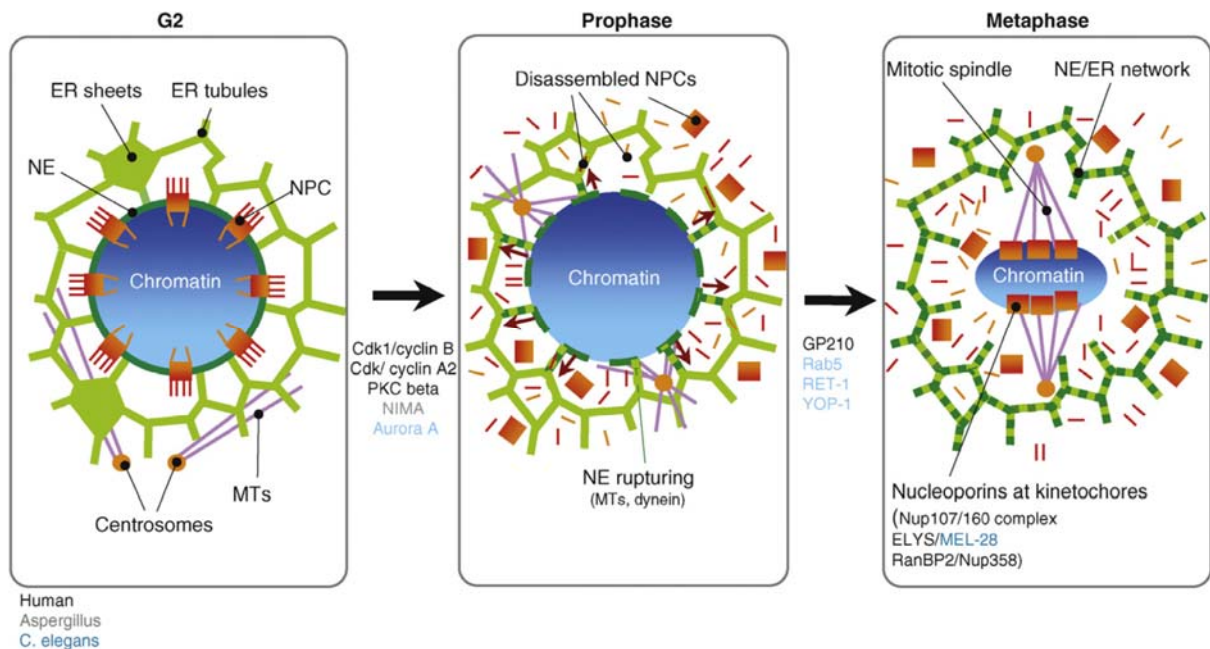


Figure 1-4. The events of nuclear envelope breakdown (NEBD). NE: nuclear envelope, dark green; ER: endoplasmic reticulum, light green; NPC: nuclear pore complex; MTs: microtubules. (Modified from Kutay and Hetzer, 2008)

1.6.2 Functions of NE and NPC components during mitosis

Several NE and NPC components have been reported to carry out important functions during mitosis. Nup358, a component of the cytoplasmic NPC filaments in interphase, possesses SUMO E3 ligase activity and anchors sumoylated RanGAP to the NPC. Following NPC disassembly, a fraction of Nup358 binds to spindle microtubules and MT-bound kinetochores and contributes to proper chromosome alignment and bipolar spindle formation (Salina *et al.*, 2003; Joseph *et al.*, 2004). Low Nup358 expression levels lead to aneuploidy and tumorigenesis in mice, suggesting that the function of Nup358 in mitosis is an important one (Dawlaty *et al.*, 2008). A number of nups, including the Nup107-160 complex, and MEL-28/ELYS, partly localize to kinetochores during mitosis (Loiodice *et al.*, 2004; Rasala *et al.*, 2006). Kinetochores targeting of the Nup107-160 complex depends on the Ndc80 complex and CENP-F, but is upstream of Nup358/RanGAP recruitment (Zuccolo *et al.*, 2007). In this way, the Nup107-160 complex has been shown to contribute to mitotic spindle formation *in vitro* (Orjalo *et al.*, 2006). The nup Rae1, which participates in mRNA export during interphase, contributes to spindle formation in mitosis (Blower *et al.*, 2005). In addition, Rae 1 expression is required for preventing aneuploidy and premature sister chromatid separation as a consequence of uncontrolled securin degradation (Jeganathan *et al.*, 2005), thus establishing a connection between nups and the spindle assembly checkpoint. In summary, many nups influence the progression or control of mitosis and an intimate connection between the NPC and mitotic spindle is emerging.

1.6.3 Nuclear envelope and nuclear pore complex formation

At the end of mitosis, the two daughter cells reform NEs around the segregated chromatids. From late anaphase onwards, the NE membranes enclose the decondensing chromatin and nuclear pores assemble in the newly forming NE. The observation that the ER remains an intact tubular network and that INM proteins are distributed in the ER during mitosis suggests that the tubular ER is the precursor of the NE membranes. In fact, live imaging demonstrated that nuclear assembly requires an intact ER and that ER targeting to chromosomes is accomplished by tubule-end binding and subsequent tethering to the chromatin surface (Anderson and Hetzer,

2007). These initial membrane-chromatin contacts might be mediated by direct binding of integral NE proteins to DNA. NE transmembrane proteins as a group are enriched in large cytosolic, positively charged domains and their interaction with DNA is critical for early steps in NE assembly (Ulbert *et al.*, 2006b). The hypothesis has been put forward that ER membrane subdomains, containing a specific set of proteins, might mediate chromosome attachment and be critically required for postmitotic NE formation (Mattaj, 2004). Once bound to chromatin, the tubules flatten and spread out to form a closed NE. It has been hypothesized that the spreading NE membranes might encircle sites where nuclear pores are formed, so that NPCs would occupy the holes between the merging NE membranes (Anderson and Hetzer, 2007). Interestingly, NE expansion also requires an intact ER which is in contact with the NE, suggesting that the increase in membrane surface is accomplished by lipid transfer from the ER to the growing NE. Based on the study by Anderson and Hetzer (2007), NE formation is independent of ATP or GTP hydrolysis when performed from a pre-formed ER. This contradicts previous publications, which implied that membrane fusion was required for NE formation (Vigers and Lohka, 1991; Boman *et al.*, 1992; Wiese *et al.*, 1997; Hetzer *et al.*, 2000; Baur *et al.*, 2007). Both results can be reconciled by considering the different experimental setups: In previous *in vitro* experiments, the NE precursor vesicles were added directly to chromatin and the soluble fraction of the extracts, so that ER formation occurred concomitantly with NE assembly. The observed inhibition of NE formation by interfering with membrane fusion events therefore may have resulted from a preceding block in ER fusion. In light of this result, the involvement of the AAA ATPase p97, which has been proposed to mediate homotypic fusion events in NE assembly (Hetzer *et al.*, 2001) has to be re-evaluated. p97 was later demonstrated to participate in NE formation by an alternative mechanism (Ramadan *et al.*, 2007), which can explain its importance without invoking membrane fusion. Based on this report, p97 is required for extracting ubiquitylated aurora B kinase from chromatin, thereby inactivating it and allowing chromatin decondensation and NE formation to proceed. It is nevertheless unclear how p97 would be able to exert its membrane fusion-independent role in NE formation in the presence of non-hydrolyzable NTP analogues.

ER tubules are formed by virtue of proteins from the reticulon family (Voeltz *et al.*, 2006) and the shape of the ER is indeed relevant for accurate timing of NE formation *in vivo* (Anderson and Hetzer, 2008). Overexpression of reticulons delays NE formation and inhibits NE expansion, whereas depleting them by RNAi accelerates nuclear assembly. This result suggests that restructuring the ER by transforming chromatin-bound membrane tubules into flat sheets is the rate-limiting step in NE formation.

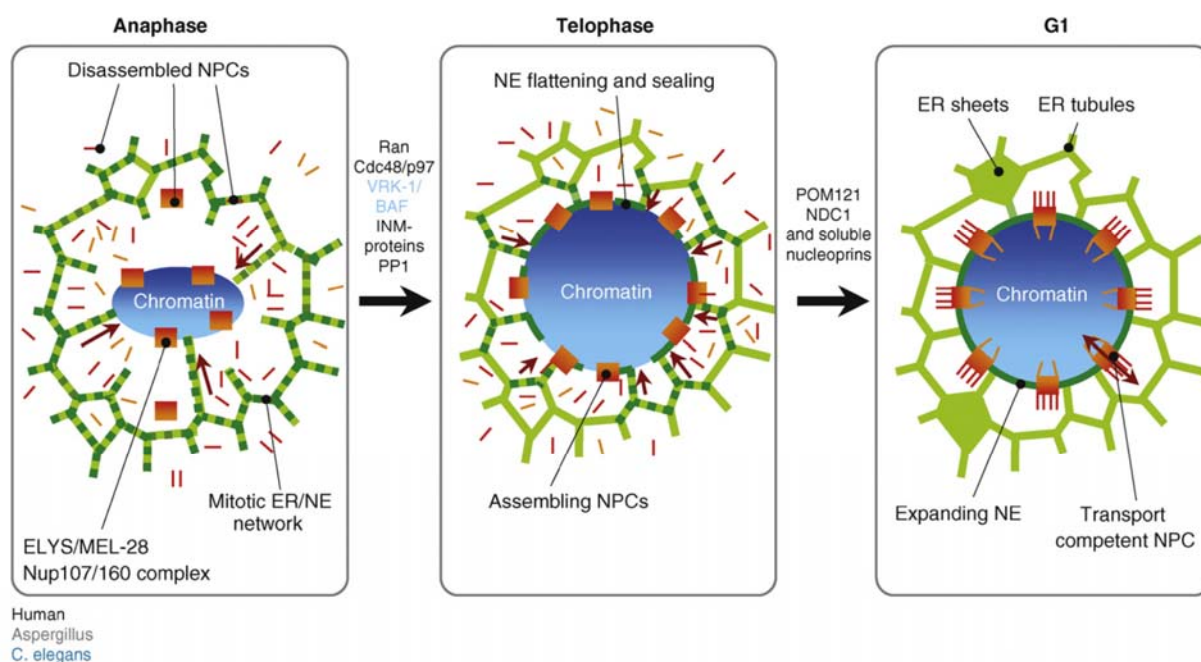


Figure 1-5. Schematic illustration of postmitotic NE and NPC formation. NE: nuclear envelope, dark green; ER: endoplasmic reticulum, light green; NPC: nuclear pore complex; MTs: microtubules. (Modified from Kutay and Hetzer, 2008)

The enclosure of chromatin by the NE membranes is closely coordinated in space and time with NPC formation. Contrary to their rather simultaneous dissociation from NPCs during NEBD, nups assemble into the forming NPC in a well-defined sequential order. In mammalian cells, the Nup107-160 complex and Nup153 are the first nups to accumulate at the chromatin periphery, followed by recruitment of the transmembrane nup pom121. The centrally located Nup205-93 and Nup58 complexes bind later to the forming NPC, but are incorporated clearly before the cytoplasmically orientated

Nup214 complex and the integral membrane nup gp210 (Bodoor *et al.*, 1999; Dultz *et al.*, 2008). Based on NPC structures observed in electron microscopy studies, the existence of NPC assembly intermediates has been proposed (Goldberg *et al.*, 1997; Kiseleva *et al.*, 2001).

Much of our mechanistic understanding of NE and NPC formation has been obtained with the help of an *in vitro* nuclear assembly assay derived from amphibian egg extract (Lohka and Masui, 1983; see also Materials and methods). With the help of this system, the contribution of several individual nuclear pore components to NPC assembly has been studied.

One of the largest and most important building blocks of the NPC is the Nup107-160 complex (or the homologous Nup84 complex in yeast). Deletion of proteins of the Nup84 complex led to defects in nuclear membrane and NPC organization and mRNA export in yeast (Siniosoglou *et al.*, 1996). The vertebrate Nup107-160 complex is the first complex of soluble nups to bind to chromatin early in NPC assembly (Walther *et al.*, 2003a). RNAi knockdown of Nup107-160 complex members in human cells resulted in reduced nuclear pore numbers, whereas employing *Xenopus laevis* egg extract immunodepleted of this complex in nuclear assembly gave rise to nuclei devoid of pores (Walther *et al.*, 2003a; Harel *et al.*, 2003a). These two publications establish Nup107-160 binding to chromatin as a key event for early NPC formation, as the presence of the Nup107-160 complex on chromatin was required for recruitment of all other soluble components of the NPC. Interestingly, addition of the Ca²⁺ chelator BAPTA to extracts caused the same phenotype as Nup107-160 depletion, but the BAPTA mechanism remains unclear (Macaulay and Forbes, 1996). The Nup58 complex (Finlay *et al.*, 1991) and the soluble nup Nup93 (Zabel *et al.*, 1996; Grandi *et al.*, 1997) are also required for assembly of functional NPCs, although at later stages than the Nup107-160 complex. Nup155 is essential for NE and NPC assembly in *C. elegans* and *in vitro* (Franz *et al.*, 2005), as is Nup53, which is a member of the Nup205-93 complex that interacts with the transmembrane nup Ndc1 (Hawryluk-Gara *et al.*, 2005; Mansfeld *et al.*, 2006; Hawryluk-Gara *et al.*, 2008). The nucleoplasmically orientated Nup153 is essential for incorporating several nups into the nascent NPC, notably nuclear basket components, affects NPC distribution in the NE and plays a

role in importin α/β -mediated protein import (Walther *et al.*, 2001). Depletion of Nup358, but not Nup214, from extracts resulted in loss of cytoplasmic filaments from *in vitro* assembled nuclei. However, both nups from the cytoplasmic face of the NPC were largely dispensable for importin α/β -mediated protein import (Walther *et al.*, 2002).

Of the three vertebrate transmembrane nups, only Ndc1 is essential for NPC formation (Mansfeld *et al.*, 2006; Stavru *et al.*, 2006b). pom121 plays a crucial role in NPC assembly *in vitro*, but the effect on NPC formation of its depletion from cultured human cells is variable (Antonin *et al.*, 2005; Mansfeld *et al.*, 2006; Stavru *et al.*, 2006a). Interestingly, the block in NE membrane closure *in vitro* caused by depletion of pom121 can be prevented by simultaneous removal of the Nup107-160 complex, suggesting that disruption of NE formation requires simultaneous NPC formation on chromatin. In contrast to Ndc1 and pom121, gp210 associates late with the assembling pore and is dispensable for NPC formation (Antonin *et al.*, 2005; Stavru *et al.*, 2006a). This is also reflected in the fact that certain cell types do not express gp210 (Eriksson *et al.*, 2004). It is unclear how these cells accomplish NEBD. In yeast, Ndc1 and pom152 contribute to nuclear pore biogenesis, whereas pom34 does not (Madrid *et al.*, 2006). *A.nidulans* cells lacking all three fungal transmembrane nups are viable, but a combined deletion of Nup84-120 complex members with Ndc1 is lethal or destabilizes the nuclear membranes, indicating that these nups have redundant functions (Liu *et al.*, 2009).

The Ran GTPase and other components of the Ran system have essential functions in NE and NPC assembly *in vivo* in yeast and *C. elegans* (Ryan *et al.*, 2003; Bamba *et al.*, 2002; Askjaer *et al.*, 2002). Importin α associates with membranes and too high or too low importin α concentrations in *Xenopus laevis* egg extract inhibit NE formation *in vitro* (Hachet *et al.*, 2004). Likewise, importin β plays a role in NE and NPC formation, *in vitro* (Harel *et al.*, 2003b), in yeast (Ryan *et al.*, 2007) and in *C. elegans* embryos (Askjaer *et al.*, 2002). Ran and importin β presumably impact NPC assembly by the same mechanism with which they act in mitotic spindle formation. The local generation of RanGTP by RCC1 dissociates certain nups from importin β , thereby allowing them

to bind to chromatin, assemble into larger complexes and to become inserted into membranes and ultimately promoting NPC assembly (Walther *et al.*, 2003b). In this manner, the local production of RanGTP could contribute to the proper spatial coordination of NPC assembly in postmitotic mitotic cells.

Chromosome segregation requires the activation of the anaphase promoting complex (APC) and securin degradation at the transition from metaphase to anaphase. The APC also inactivates the mitotic kinase Cdk1 by degrading its corresponding cyclin. Consequently, with declining kinase activity, phosphatases can remove mitosis-specific phosphorylation from NE and NPC components. Mitotic phosphorylation has been reported for several nups (Favreau *et al.*, 1996; Glavy *et al.*, 2007) and, although clear data on its functional relevance is missing, it is tempting to speculate that their dephosphorylation might contribute to the temporal coordination of NPC assembly.

Like the NE membranes and NPCs, the nuclear lamina reforms at the end of mitosis. Interestingly, A- and B-type lamins differ spatially and temporally with respect to their targeting to the assembling NE (Moir *et al.*, 2000). While lamin B is recruited to the NE in telophase and may actively participate in NE and NPC formation (Lopez-Soler *et al.*, 2001), lamins A and C are imported into nuclei after completion of NE assembly (Moir *et al.*, 2000). The contribution of lamins to nuclear assembly was reviewed by Holaska *et al.* (2002).

In cells undergoing open mitosis two principally different NPC assembly events can be distinguished, NPC formation into the intact interphase NE and NPC assembly at the end of mitosis. While postmitotic NPC assembly has been investigated in quite some detail, comparably little is known about interphase NPC assembly. NPC biogenesis in yeast can only occur by insertion of nuclear pores into an intact NE and the number of NPCs per yeast nucleus doubles during the cell cycle (Winey *et al.*, 1997). A typical mammalian nucleus contains in the order of 2000 nuclear pores and the NPC number doubles during interphase (Maul *et al.*, 1972). Recently, d'Angelo and Hetzer (2006) published evidence that NPCs are formed by a *de novo* mechanism in interphase, i.e. without using existing pores as a template. They showed that interphase NPC assembly occurs from both sides of the NE and requires RanGTP.

1.7 MEL-28 and NET5

1.7.1 MEL-28

In a systematic search for novel factors essential for postmitotic NE formation, Vincent Galy and Peter Askjaer, former Mattaj lab post-docs, identified a locus in *C. elegans* whose deletion resulted in pronuclear appearance defects. The gene, later termed mel-28, encodes a 200 kDa AT-hook-containing protein and has orthologues of similar size in most higher eukaryotes (de Jong-Curtain *et al.*, 2008). Filamentous fungi and *S.pombe* possess significantly smaller MEL-28 orthologues around 35 kDa (Liu *et al.*, 2009). Interestingly, mel-28 was found independently in an effort to functionally group *C. elegans* genes based on RNAi phenotypes of early embryos (Gunsalus *et al.*, 2005). This study also reported phenotypic similarities between mel-28 depletion and that of certain nups and the Ran GTPase.

Vincent Galy and Peter Askjaer extensively characterized the role of mel-28 in NE assembly using *C. elegans* as a model system (Galy *et al.*, 2006). They found that MEL-28 localizes to the NE in interphase and is recruited to kinetochores in mitosis, a behavior that it shares with its *Xenopus laevis* and human orthologues (see below). RNAi depletion or genetic mutation of mel-28 severely impaired nuclear morphology and led to abnormal distribution of both integral NE proteins and NPCs. The structural NE defects could be confirmed by transmission electron microscopy and were associated with functional defects and a lack of nuclear exclusion of cytoplasmic proteins. Vincent Galy's and Peter Askjaer's work suggests that MEL-28 is an early assembling, stable NE component essential for all aspects of NE formation. A parallel study by Fernandez and Piano (2006) reported additional roles for MEL-28 in mitosis and confirmed the involvement of MEL-28 in NE assembly, suggesting that it would act therein in a Ran-dependent manner.

Three earlier publications had dealt with the mouse MEL-28 orthologue, named ELYS by the authors for embryonic large molecule derived from yolk sac (Kimura *et al.*, 2002; Okita *et al.*, 2003; Okita *et al.*, 2004). Kimura *et al.* (2002) initially proposed a function for MEL-28 in haematopoiesis and suggested it might act as a transcription

factor. The observation that MEL-28 homozygous mutant embryos died 3-5 days after implantation, significantly earlier than onset of mouse haematopoiesis, indicated that MEL-28 was required for survival for other reasons (Okita *et al.*, 2004). The role of MEL-28 in nuclear organization was not addressed in any of these reports.

Cerstin Franz initiated the work on *Xenopus laevis* MEL-28, which opened up the possibility to study its role in nuclear assembly *in vitro*. My work has extended her results and addressed novel aspects of MEL-28 function, as explained in subsequent parts of this thesis. Since I began working on MEL-28, five studies from other research groups dealing with MEL-28/ELYS have been published (Rasala *et al.*, 2006; Gillespie *et al.*, 2007; Rasala *et al.*, 2008; Davuluri *et al.*, 2008; de Jong-Curtain *et al.*, 2008). These reports characterized the function of MEL-28 in nuclear assembly and obtained data very similar to ours (see Results), but also uncovered a previously unexpected functional link of MEL-28 to DNA replication (Gillespie *et al.*, 2007; Davuluri *et al.*, 2008).

MEL-28/ELYS is essential for nuclear integrity in invertebrates (Galy *et al.*, 2006; Fernandez and Piano, 2006) and vertebrates (Davuluri *et al.*, 2008; de Jong-Curtain *et al.*, 2008). A point mutation in the zebrafish ELYS gene, leading to a stop codon within the coding region, gives rise to the *flotte lotte* (*flo*) mutant phenotype. *flo* mutant fish exhibit widespread apoptosis in the intestine, pancreas, liver and eye, suggesting that these tissues are particularly vulnerable to loss of ELYS. Cells in these tissues display strongly disrupted nuclear pores and dissociation of nups from the NE into the cytoplasm (Davuluri *et al.*, 2008). At the ultrastructural level, *flo* mutant nuclei possess few if any well defined pores. Interestingly, *flo* mutant animals are more sensitive to treatment with DNA replication inhibitors than wild type fish (Davuluri *et al.*, 2008), an observation which is in line with *in vitro* data that MEL-28 interacts with the replication licensing system (Gillespie *et al.*, 2007). In the latter study, MEL-28 was shown to associate with the minichromosome maintenance (Mcm) proteins 2-7 on chromatin. Mcm2-7 are loaded onto chromosomes at the end of mitosis and are required for licensing origins of replication for use in the subsequent S phase. Preventing the loading of Mcm2-7 onto chromatin delayed chromatin recruitment of MEL-28 and nups

and as a consequence NPC assembly, suggesting that these two important cellular events are coordinated with each other.

Our work (Franz *et al.*, 2007 and results presented in this thesis) and that of others (Gillespie *et al.*, 2007; Rasala *et al.*, 2008) has demonstrated that MEL-28 plays a crucial role in postmitotic NPC formation. Since our findings and those of Gillespie *et al.* (2007) and Rasala *et al.* (2008) are highly redundant, they will be referred to and discussed in more detail in part 3 (Discussion) of this thesis.

1.7.2 NET5

NET5 was identified as an integral membrane protein of the NE in a subtractive proteomic approach (Schirmer *et al.*, 2003). An independent study linked its *C. elegans* orthologue T24F1.2 to several nups by phenotypic similarity and to the Ran GTPase by correlating their expression (Gunsalus *et al.*, 2005). These findings together with the observation by Matyas Gorjanacz that T24F1.2 caused synthetic lethality in combination with a group of NPC proteins specifically required for pore formation (personal communication), prompted me to clone and begin characterizing the human NET5 protein.

NET5/T24F1.2 is a comparably recently discovered protein and so far, only one study, describing its *S.pombe* orthologue Ima1, has been published (King *et al.*, 2008). In fission yeast, Ima1 is an NE protein enriched at sites where the microtubule organizing center (MTOC) is attached to the nucleus. Loss of Ima1 resulted in pronounced NE deformations and loss of spherical nuclear shape. In addition, *ima1* Δ cells became increasingly sensitive to microtubule-dependent forces exerted on the nucleus. Ima1 was required for proper localization of the *S.pombe* SUN and KASH proteins Sad1 and Kms2 and *ima1* deletion led to more frequent separation of centromeres from the normally unique MTOC attachment site, indicating that the MTOC attachment site was fragmented in *ima1* Δ cells. Based on the result that chromatin immunoprecipitation against GFP-Ima1 enriched the central centromeric region, the authors suggest that Ima1 specifically tethers centromeric heterochromatin to the NE.

Our approach has been to study the function of NET5/T24F1.2 in nuclear organization in human cells and *C. elegans* (see below).

1.8 Aim of the thesis

NE and NPC formation at the end of mitosis are two elaborate processes essential for cell survival. MEL-28 had been identified as an essential factor for postmitotic NE assembly *in vivo* and *in vitro*, but its mode of action remained unclear. The aim of this thesis was to closely investigate the role of MEL-28 in nuclear organization and to dissect the mechanism by which it acts in nuclear assembly. Accordingly, the primary objectives were: characterizing the MEL-28 RNAi and *in vitro* depletion phenotypes, clarifying the relation between MEL-28 and previously identified players in NE assembly and addressing the regulation of MEL-28 function, e.g. by the Ran system. To achieve this, I employed a wide range of techniques, from RNAi experiments in cultured cells to *in vitro* nuclear assembly and from molecular biology to biochemical methods and confocal microscopy.

Our understanding of NE dynamics is far from complete. While global approaches can help to identify novel genes involved in a process of interest, they do not reveal the mechanism by which the corresponding proteins function in that process. Based on the available information, NET5/T24F1.2 was a promising new candidate protein, implicated in NE and NPC organization. Together with Matyas Gorjanacz, I decided to carry out a thorough characterization on this interesting protein. While he focused on investigating T24F1.2 in *C. elegans*, I generated reagents for studying the human NET5 protein.

2 Results

2.1 MEL-28

The work on MEL-28 presented here is the continuation of a project initiated by three previous members of the Mattaj group. Peter Askjaer and Vincent Galy mapped the maternal-effect embryonic-lethal mutation *mel-28* to the C38D4.3 gene in *C. elegans*. They conducted a thorough characterization of its gene product MEL-28 demonstrating that MEL-28 is essential for many aspects of nuclear assembly in *C. elegans* (Galy *et al.* 2006). Cerstin Franz began working on the vertebrate orthologue of *C. elegans* MEL-28 by cloning the *Xenopus laevis* MEL-28 gene and generating antibodies against the *Xenopus laevis* MEL-28 protein. She carried out an initial characterization of its role in nuclear assembly *in vitro*. Her results demonstrated that the function of MEL-28 is conserved in metazoa, however, many open questions remained about the mechanism by which MEL-28 would act in nuclear assembly. Consequently, some of my experiments followed up on previous experimental avenues, while others addressed entirely new aspects of MEL-28 function in NE formation.

2.1.1 Generation of specific reagents against human MEL-28

Among the most important goals at the beginning of my PhD work was to generate reagents for studying the human MEL-28 protein. Such reagents were not available in the laboratory at the time, but promised to be very valuable tools and to open up several new experimental directions.

In order to produce polyclonal antibodies against human MEL-28, several fragments of the human MEL-28 cDNA were cloned into vectors for expression as His₆- or GST-tagged proteins in *E. coli*. In addition to the antigen previously published by Kimura *et al.* (2003), residues 1208-1582, four fragments of roughly equal size were chosen based on their predicted high hydrophilicity: residues 141-365, 1572-1800, 1801-2016 and 2017-2266. A full length cDNA clone of human MEL-28 previously generated by Peter Askjaer served as a template for the corresponding PCR reactions. All fragments were expressed in BL21 (DE5) Rosetta cells according to standard protocols (see Materials and methods) and evaluated for high expression and

solubility. Based on the results the fragment sizes were extended, finally yielding two large fragments of human MEL-28, amino acid residues 1208-1800 and 1572-2266, which were expressed and purified as His₆-tagged proteins and used for immunizing rabbits (Figure 2-1 A).

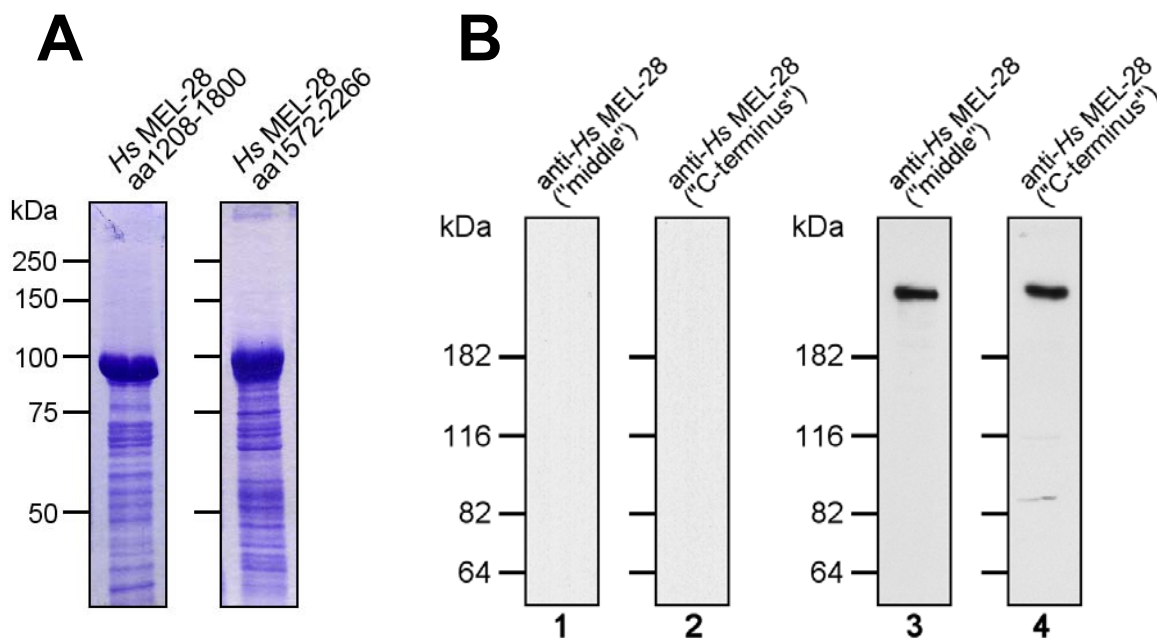


Figure 2-1. Generation of specific antibodies against human MEL-28. (A) Coomassie-stained SDS-PAGE gels with *Hs* MEL-28 fragments expressed in and purified from *E. coli*, which were used to immunize rabbits. (B) Western blot using the corresponding pre-immune sera (lanes 1+2) or affinity purified antibodies against *Hs* MEL-28 (lanes 3+4) on a HeLa cell lysate. Both antibodies recognize a single band at 250 kDa.

Western blotting using the corresponding rabbit sera revealed a major band at 250 kDa in HeLa cell total lysate (Figure 2-1 B), but not in *Xenopus laevis* or *C. elegans* (data not shown). The antibodies against human MEL-28 were affinity purified using the soluble fragments cross-linked to Sepharose and were used in all subsequent experiments.

2.1.2 Human MEL-28 is a nuclear envelope and kinetochore protein

In order to establish the subcellular localization of MEL-28 in human cells, cultured HeLa cells and U2OS cells were fixed with PFA and immunostained with anti-Hs MEL-28 antibodies (Figure 2-2). Co-staining was performed with mAb414, an NPC marker which recognizes the four FG repeat-containing nups Nup358, Nup214, Nup153 and p62 (Davis and Blobel, 1986). For both cell types very similar results were obtained (U2OS data not shown). MEL-28 localized to the NE of interphase cells, giving a strong rim staining around the nucleus. A weaker nucleoplasmic staining was also detectable. This staining was absent from cells labeled with the corresponding pre-immune sera (data not shown).

Mitotic cells displayed a loss of the MEL-28 nuclear rim staining indicative of NE breakdown, but showed bright MEL-28 foci on the condensed chromosomes from early prophase through late anaphase and a weaker diffuse overall chromosome staining. These foci were highly reminiscent of kinetochores. Rasala *et al.* (2006) demonstrated by performing co-staining for the kinetochore protein CENP-B that they indeed correspond to kinetochores. Human MEL-28 thus exhibits a similar behavior to its *C. elegans* and *Xenopus laevis* orthologues (Galy *et al.*, 2006; Franz *et al.*, 2007) changing localization between the NE and kinetochores during the cell cycle. Interestingly, cells in late anaphase could be observed with a relatively strong MEL-28 staining already evenly distributed on the decondensing chromatids, but low mAb414 signal, suggesting that MEL-28 might be generally distributed on chromatin before the FG repeat-containing nups began to assemble into NPCs at the end of mitosis.

2.1.3 MEL-28 localizes to nuclear pores and the INM

We wished to determine the localization of MEL-28 at the NE at higher resolution. Magnified confocal sections through the nuclear surface of human cells showed that MEL-28 was not evenly distributed in the plane of the NE, but displayed a dot-like pattern that bore resemblance to NPC staining. Upon co-labeling with mAb414, the MEL-28 staining largely coincided with the mAb414 signal in the NE, suggesting that MEL-28 resides at nuclear pores (Figure 2-3 A). In order to reliably

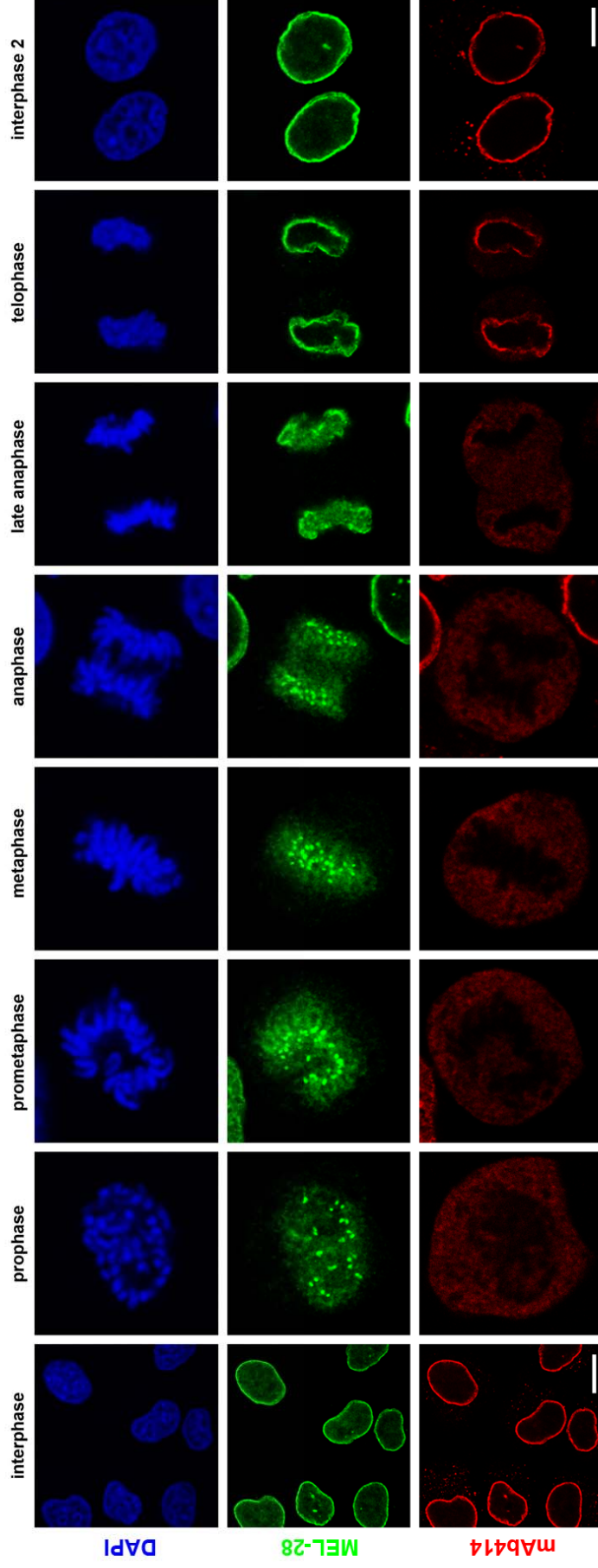


Figure 2-2. Human MEL-28 is a nuclear envelope and kinetochore protein. HeLa cells were fixed with 4% PFA and immunostained for MEL-28 or nuclear pores (mAb414). The gallery shows representative images from different stages of mitosis. Rasala et al. (2006) demonstrate that the MEL-28 foci visible from prophase to anaphase coincide with the kinetochore marker CENP-B. Scale bars, 15 μm (left column) and 5 μm (all others).

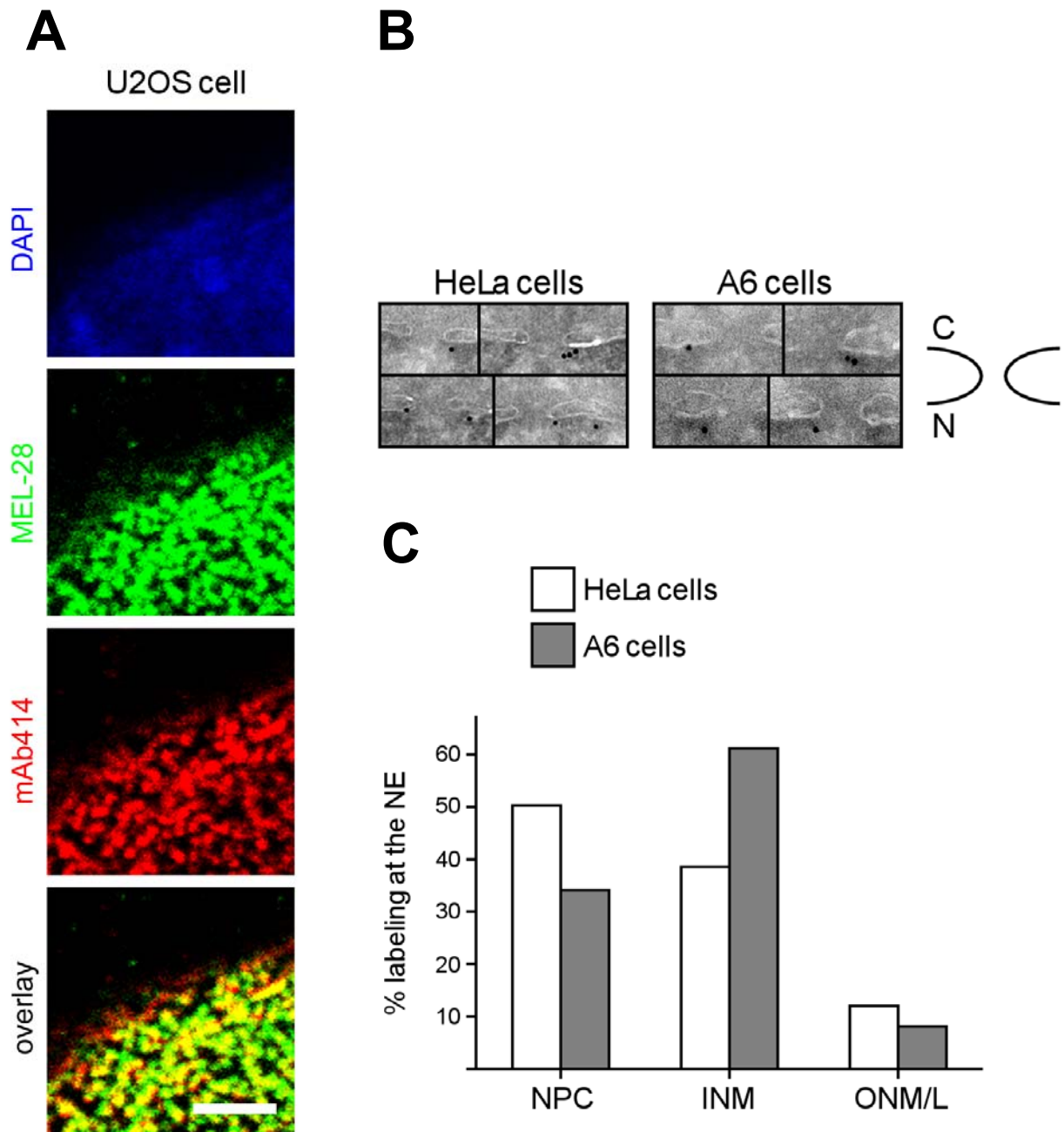


Figure 2-3. MEL-28 localizes to nuclear pores and the INM. (A) Confocal section through the nuclear surface of a fixed U2OS cell stained for MEL-28 and NPCs (mAb414). Scale bar, 1 μ m. (B) Examples of MEL-28 labeling at the NE. HeLa cells or *Xenopus laevis* A6 cells were fixed and processed for immunogold labeling according to the Tokuyasu technique. Labeling was performed with affinity purified antibodies against human or *Xenopus* MEL-28 and 10 nm protein A gold. The scheme illustrates the orientation of the NE: C-cytoplasm, N-nucleoplasm. (C) Quantitation of gold particles at the NE. NPC- nuclear pore complex, INM- inner nuclear membrane, ONM- outer nuclear membrane, L- lumen. Processing and labeling of cells for EM + counting of gold particles were carried out by Rachel Mellwig.

determine the precise localization of MEL-28 in the cell, electron microscopy (EM) was used. Rachel Mellwig processed HeLa and *Xenopus laevis* A6 cells for immunogold labeling with anti-human MEL-28 or anti-*Xl* MEL-28 antibodies according to the Tokoyasu technique (see Materials and methods). Gold particles could be detected primarily at nuclear pores and at the INM with very little labeling at the ONM. Figure 2-3 B shows examples of gold particles at nuclear pores in human or *Xenopus* cells. Rachel Mellwig quantified the labeling by counting 209 particles for HeLa cells and 215 particles for A6 cells. These results are summarized in Figure 2-3 C. Note that NPCs correspond to only a small fraction of the NE surface, so most MEL-28 is at NPCs.

Another clue about the orientation of MEL-28 in the NE could be obtained from an additional experiment in which HeLa cells were selectively permeabilized with different detergents (Figure 2-4). Treatment of cells with Triton X-100 leads to unspecific perforation of all cellular membranes, while treatment with digitonin selectively permeabilizes the plasma membrane and leaves the NE intact. While Nup358, a component of the cytoplasmic filaments of the NPC, was detectable under all conditions, the nuclear interior was only accessible after incubation with Triton X-100 as assessed by detection of the Cajal body marker coilin (Platani *et al.*, 2000). Likewise, MEL-28 immunolabeling was only detectable after Triton X-100 permeabilization, a result obtained with both antibodies, directed against the two different regions of human MEL-28.

Given that *Hs* MEL-28 is a very large protein consisting of 2266 amino acids it could potentially span the entire NE. Since no structural data on MEL-28 is currently available complete interpretation of this experiment is difficult. Attempts to affinity purify the antibodies directed against the extreme N-terminus (aa 1-195) of *Xl* MEL-28, which were produced by Cerstin Franz (Cerstin Franz PhD thesis figure 2.18), for comparative immunogold labeling were unsuccessful. We can nevertheless conclude that the C-terminal half of MEL-28 is orientated toward the inner face of the NE.

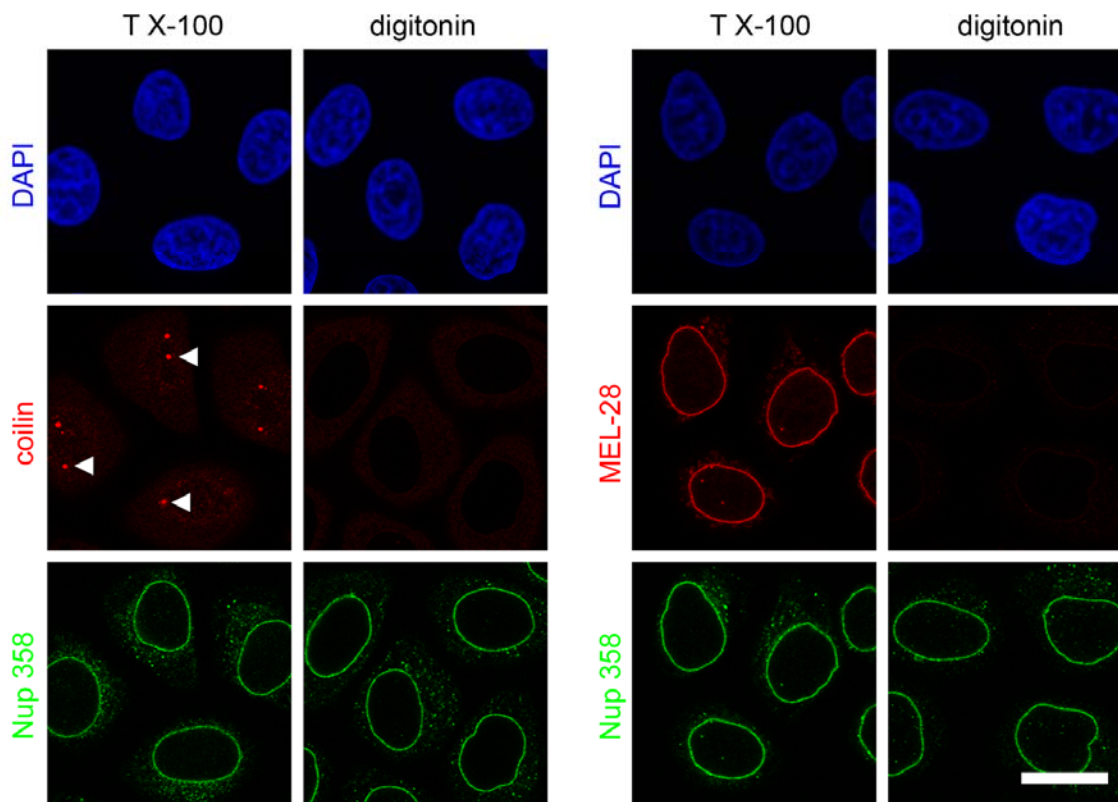


Figure 2-4. The C-terminus of MEL-28 faces the inner side of the NE. HeLa cells were fixed with PFA and permeabilized with 0.25% Triton X-100 (T X-100) or 0.025% digitonin. Triton X-100 treatment largely removes the NE membranes, while digitonin selectively permeabilizes the plasma membrane leaving the NE intact. Thus intranuclear antigens are only accessible after Triton X-100 treatment. Cells were immunostained with antibodies against coilin, MEL-28 and Nup358. The Cajal body protein coilin (arrowheads) served as an intranuclear marker, Nup358 as a marker for the outer face of the NE. Scale bar, 20 μ m.

2.1.4 MEL-28 is required for NPC maintenance in human cells

One of the most important open questions of the project was to address the function of MEL-28 in living vertebrate cells. RNA interference (RNAi) is a convenient and well-established method to examine the phenotypic consequences of depleting a specific protein from cells *in vivo*. Cerstin Franz had carried out an RNAi experiment in HeLa cells which suggested that the loss of human MEL-28 might affect the organization of nuclear pores. This result could, however, not be interpreted conclusively due to the unavailability of a useful antibody against human MEL-28 to monitor the depletion efficiency. With specific antibodies in hand we repeated the RNAi experiment. HeLa cells were transfected with control siRNA oligos directed against firefly luciferase, a gene not present in human cells, or two different oligos targeting two distinct regions within the MEL-28 mRNA. Similar results were obtained upon treatment with both MEL-28 oligos: analysis of HeLa cell lysates by Western blotting showed that MEL-28 levels were significantly reduced after 48 h of RNAi (Figure 2-5 A) while the levels of nups, α tubulin or Histone H2B were unaffected. The gradual loss of MEL-28 from HeLa cells upon RNAi treatment was confirmed by confocal microscopy. Cells fixed at different timepoints after transfection with MEL-28 siRNA oligos were immunostained for MEL-28, nups or INM proteins (Figure 2-5 B and C). After 2 days of RNAi treatment the MEL-28 signal in many cells was below detection limit. As they became depleted of MEL-28, the cells displayed a progressive loss of nups from the NE until after 3 days many had lost their mAb414 rim staining entirely. This was observed for all nups tested, suggesting that the entire NPC was lost from the NE. At the same time, the cells began to accumulate large nucleoporin-containing cytoplasmic aggregates, a phenotype already observed after depletion of Nup107-160 complex members (Walther *et al.*, 2003a). Such annulate lamellae (AL) can also be observed at low levels in wild type HeLa cells (Kessel, 1992). Both HeLa and U2OS cells displayed the same MEL-28 RNAi phenotype, although the effect was more pronounced in U2OS cells.

Interestingly, while MEL-28 depletion significantly altered the distribution of nups in the cells, the nuclear membranes appeared to be unaffected, as judged by immunostaining for the INM markers LEM2 and Emerin (Figure 2-5 C and

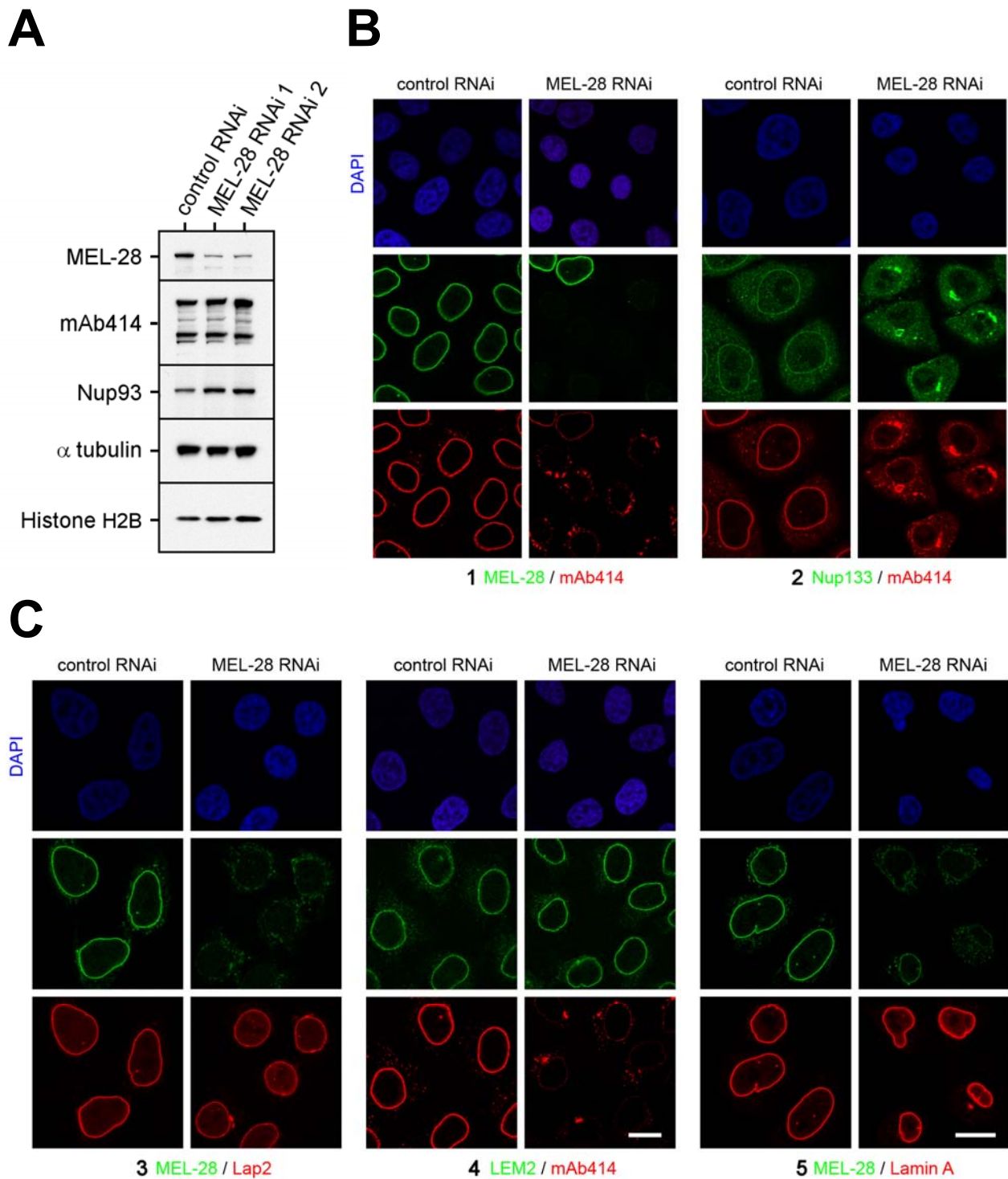


Figure 2-5. MEL-28 is required for NPC maintenance in human cells. (A) HeLa cells were treated for 48 h with two different siRNA oligos against MEL-28 and total cell lysates analyzed by Western blotting. (B+C) Phenotypic characterization of MEL-28 RNAi in HeLa cells fixed after 48 h (panels 2, 3 and 5) or 72 h (panels 1+4) of MEL-28 RNAi treatment with nuclear pore (B) and NE membrane (C) markers. Scale bar, 15 μ m. The RNAi experiments, labeling and recording of cells for panels 1 and 4 were performed by Sevil Yavuz.

data not shown), suggesting that MEL-28 was required specifically for proper NPC assembly, but not formation of the NE membranes. Cells that had lost MEL-28 possessed smaller nuclei than control cells, a phenotype consistent with defects in nucleocytoplasmic transport. Interestingly, Lap2 and Lamin A staining also remained largely unaltered after 48 h of MEL-28 RNAi (Figure 2-5 C), indicating that the nuclear lamina remained unaffected. This result, which was independently reported by Rasala *et al.* (2006), is very surprising as lamins A and C are thought to be imported into the nucleus after completion of NE and NPC assembly at the end of mitosis. Either the nuclear import of A-type lamins is more resistant to reduced NPC numbers compared to other transport events or MEL-28 affects interphase NPC formation. After 3 days of RNAi treatment many cells appeared apoptotic emphasizing that MEL-28 is required for cell survival. These results establish MEL-28 as an essential factor for NPC maintenance in human cells, however they do not resolve whether interphase NPC assembly or postmitotic NPC formation is impaired upon MEL-28 downregulation.

In order to confirm that the cytoplasmic aggregates observed upon MEL-28 RNAi were indeed annulate lamellae, we examined them by electron microscopy. Rachel Mellwig prepared RNAi-treated HeLa cells following two different protocols. Staining with osmium tetroxide and uranyl acetate permitted morphological characterization of the MEL-28 RNAi phenotype by EM (Figure 2-6 A). A significant increase in the number of cytoplasmic membrane stacks was observed following MEL-28 RNAi. The stacks were filled with frequent membrane gaps and constrictions resembling nuclear pores. In addition, the NE of the RNAi cells possessed very few nuclear pores compared to control cells. In a second experiment, Rachel Mellwig labeled the cells with mAb414 and Protein A gold (Figure 2-6 B). The membrane stacks stained strongly for FG repeat-containing nups proving that they were indeed AL. RNAi depletion of MEL-28 therefore results in the same phenotype as removal of the Nup107-160 complex (Walther *et al.*, 2003a).

2.1.5 Annulate lamellae can form independently of MEL-28

An interesting question that arose from the above experiments was whether AL formation was an immediate consequence of MEL-28 depletion. While MEL-28 co-

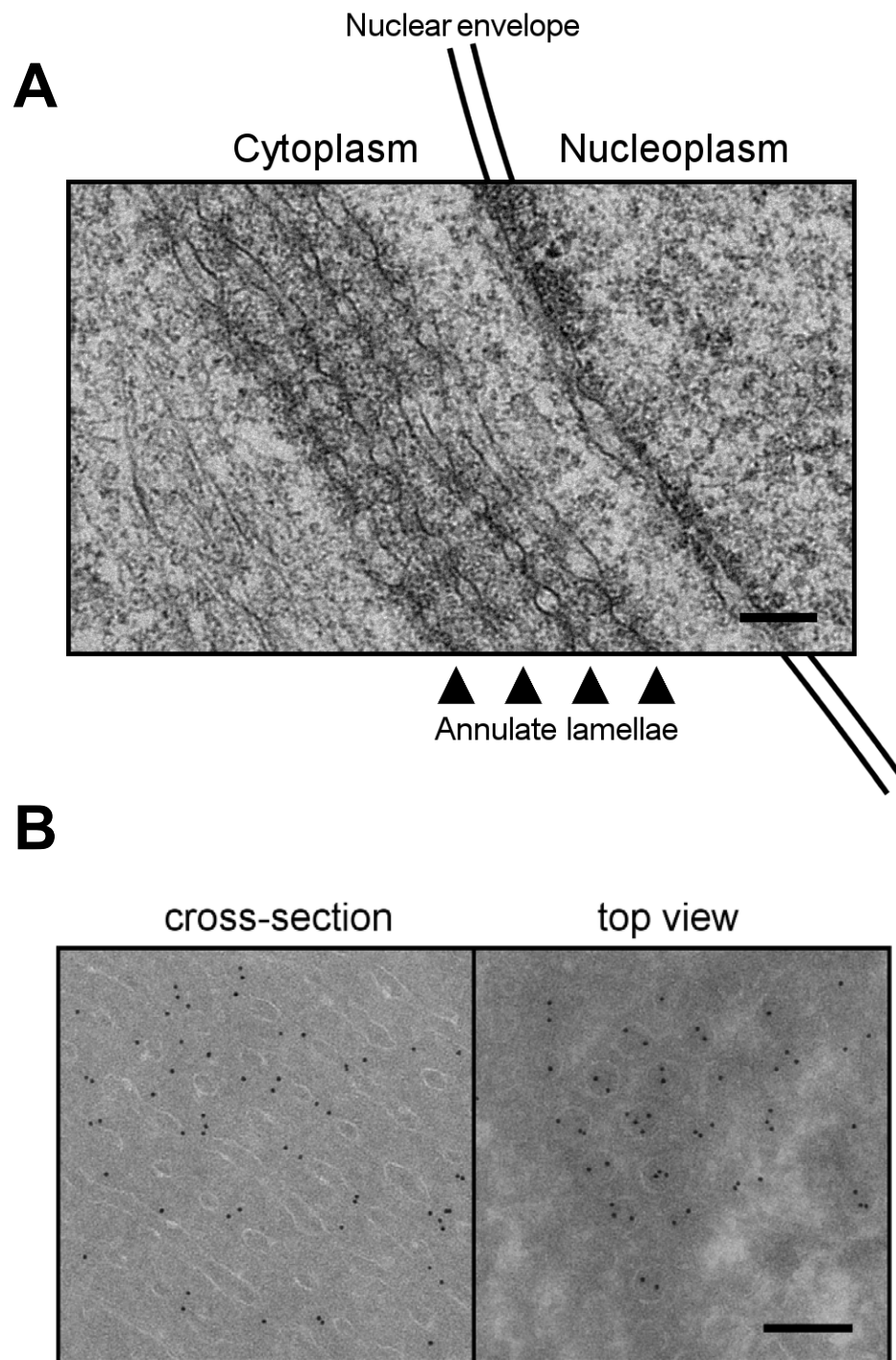


Figure 2-6. RNAi depletion of MEL-28 leads to annulate lamellae formation. HeLa cells were fixed after 72 h of MEL-28 RNAi treatment and stained with osmium tetroxide / uranyl acetate for morphological studies (**A**) or processed for immunogold labeling with mAb414 according to the Tokuyasu technique (**B**). (**B**) depicts the observed AL in cross-section or top view. Scale bars, 200 nm. Processing and labeling of cells were performed by Rachel Mellwig.

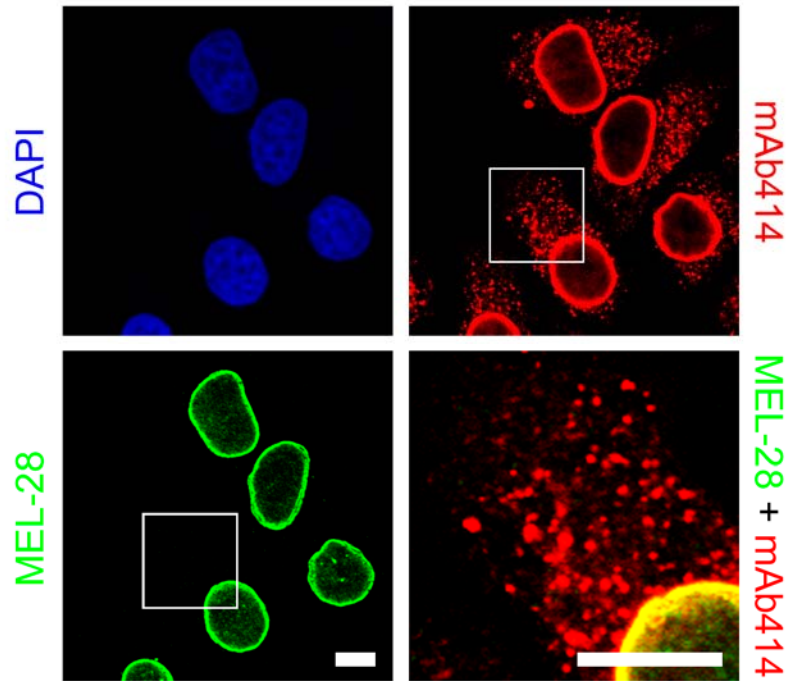
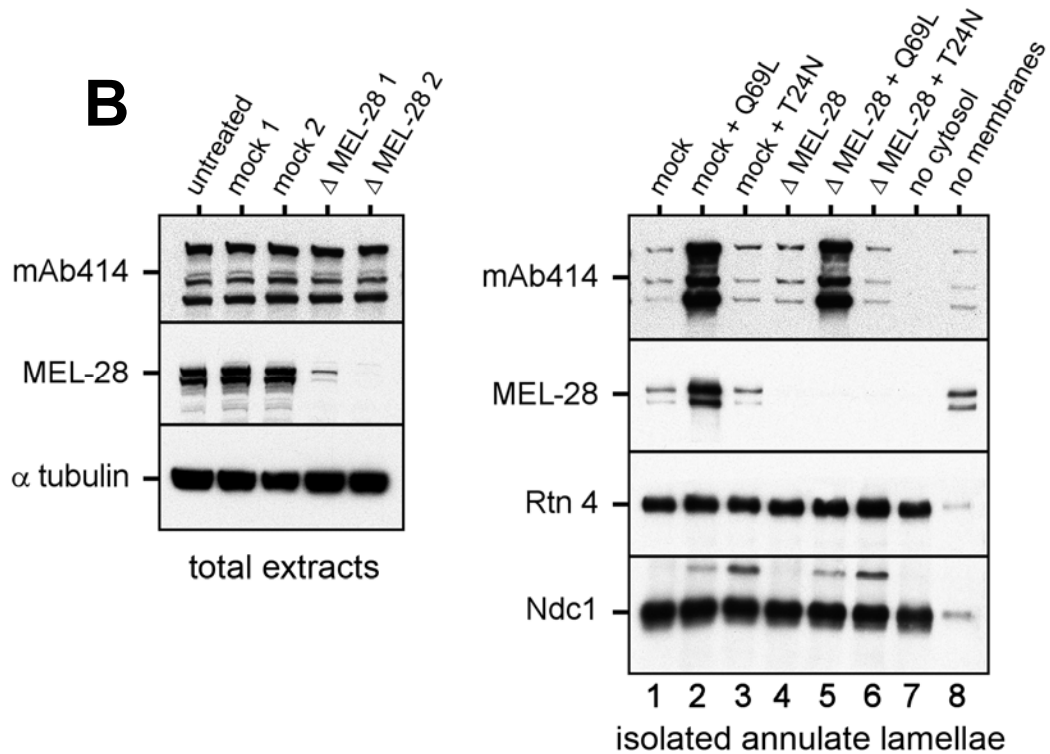
A**B**

Figure 2-7. MEL-28 is neither part of annulate lamellae nor required for AL formation. (A) HeLa cells were fixed and immunostained for MEL-28 or nuclear pores (mAb414). Scale bars, 10 μm. (B). Annulate lamellae form independent of MEL-28 in *Xenopus* egg extract. Mock or MEL-28-depleted *Xenopus laevis* egg extract was supplemented with Ran mutants (10μM final concentration) and incubated with membranes for 60 min. Annulate lamellae were purified through a sucrose cushion and analyzed by Western blotting.

localized with nups at the NE, it was never detected in the cytoplasmic mAb414-positive foci of wild type cells demonstrating that MEL-28 is not part of AL *in vivo* (Figure 2-7 A). In order to test, whether MEL-28 depletion *per se* would result in AL formation, we utilized the *Xenopus laevis* egg extract system in which AL can be readily formed by combining membranes with a cytosolic fraction (Meier *et al.*, 1995). Supplementing the extract with the constitutively GTP-bound Ran GTPase mutant Q69L leads to liberation of importins from nups and triggers assembly of nuclear pores in the membranes (Walther *et al.*, 2003b).

AL were formed for 60 min in mock or MEL-28-depleted extracts with or without addition of Ran mutants, isolated through a sucrose cushion and analyzed by Western blotting (Figure 2-7 B). Immunodepletion of MEL-28 did not significantly reduce mAb414 levels in the extract. When mock depleted extracts were supplemented with RanQ69L the levels of nups co-purified with the membranes were significantly elevated (Figure 2-7 B, right panel, lane 2). Addition of the nucleotide-free inactive form of Ran, T24N, did not induce this effect (lane 3). Interestingly, the MEL-28-depleted extracts behaved like the mock extracts in this assay. Removal of MEL-28 did not alter the amounts of nups in the purified membranes, but RanQ69L-mediated induction of AL formation was as efficient in the absence of MEL-28 as in the control. Thus, removal of MEL-28 *per se* does not induce AL formation or render it independent of RanGTP.

2.1.6 MEL-28 is required for postmitotic NPC assembly

It was therefore unclear how MEL-28 depletion would lead to AL formation in living cells. The main difference between the *in vivo* situation in the RNAi experiment and the *in vitro* AL formation assay was that annulate lamellae were formed in the absence of chromatin. The *Xl* egg extract system is, however, also suitable to recapitulate postmitotic nuclear assembly (see Introduction or Materials and methods). Using mock or MEL-28-depleted extracts in the *in vitro* nuclear assembly assay, Cerstin Franz showed that nuclei formed from MEL-28-free extract contain no detectable nups, suggesting that MEL-28 has an essential function early in postmitotic nuclear pore formation. However many important aspects of the MEL-28 depletion phenotype

remained unresolved. We repeated the experiment and investigated the MEL-28 depletion phenotype in detail. Immunodepletion of MEL-28 from cytosol did not significantly affect the levels of other nups (Figure 2-8 A). We confirmed that MEL-28-free extracts give rise to nuclei devoid of nups, but staining with the membrane dye DilC₁₈ suggested that they were surrounded by a membrane (Figure 2-8 B). Rachel Mellwig processed mock or MEL-28-free nuclei for close inspection by EM (Figure 2-8 C). Control nuclei contained decondensed chromatin and possessed a double membrane perforated with clearly visible nuclear pores. MEL-28-free nuclei were also encompassed by a double membrane, but lacked nuclear pores. Δ MEL-28 nuclei were also smaller than control nuclei and retained the rod-like shape which chromatin templates acquire after the phase I decondensation of nuclear assembly (Philpott *et al.*, 1991). At the same time the chromatin of Δ MEL-28 nuclei remained highly condensed demonstrating that the second nucleocytoplasmic transport-dependent phase of nuclear assembly did not occur.

The membrane phenotypes observed upon impairment of nuclear assembly *in vitro* fall into two distinct categories: Nuclei with a closed NE membrane devoid of pores as observed for removal of the Nup107-160 complex (Walther *et al.*, 2003a) or chromatin templates decorated with unfused vesicles characteristic for depletion of Nup53, Nup155 or the transmembrane nups pom121 or Ndc1 (Hawryluk-Gara *et al.*, 2008; Franz *et al.*, 2005; Antonin *et al.*, 2005; Mansfeld *et al.*, 2006). It was therefore important to assign the MEL-28 depletion phenotype to either group. In order to unambiguously determine whether MEL-28-free nuclei possess a closed NE, Wolfram Antonin carried out an exclusion assay (Figure 2-8 D). In this assay chromatin was decondensed with recombinant nucleoplasmin in the presence of biotinylated histones prior to addition of membranes. After completion of the nuclear assembly reaction fluorescently labeled streptavidin was added to the nuclei. Labeling of chromatin indicates the absence of a closed nuclear membrane. Supplementing the assembly reaction with high concentrations of RanQ69L inhibits formation of a closed nuclear membrane and served as negative control. MEL-28-free nuclei efficiently excluded fluorescently labeled streptavidin like mock nuclei. Δ MEL-28 nuclei thus acquire a closed NE membrane.

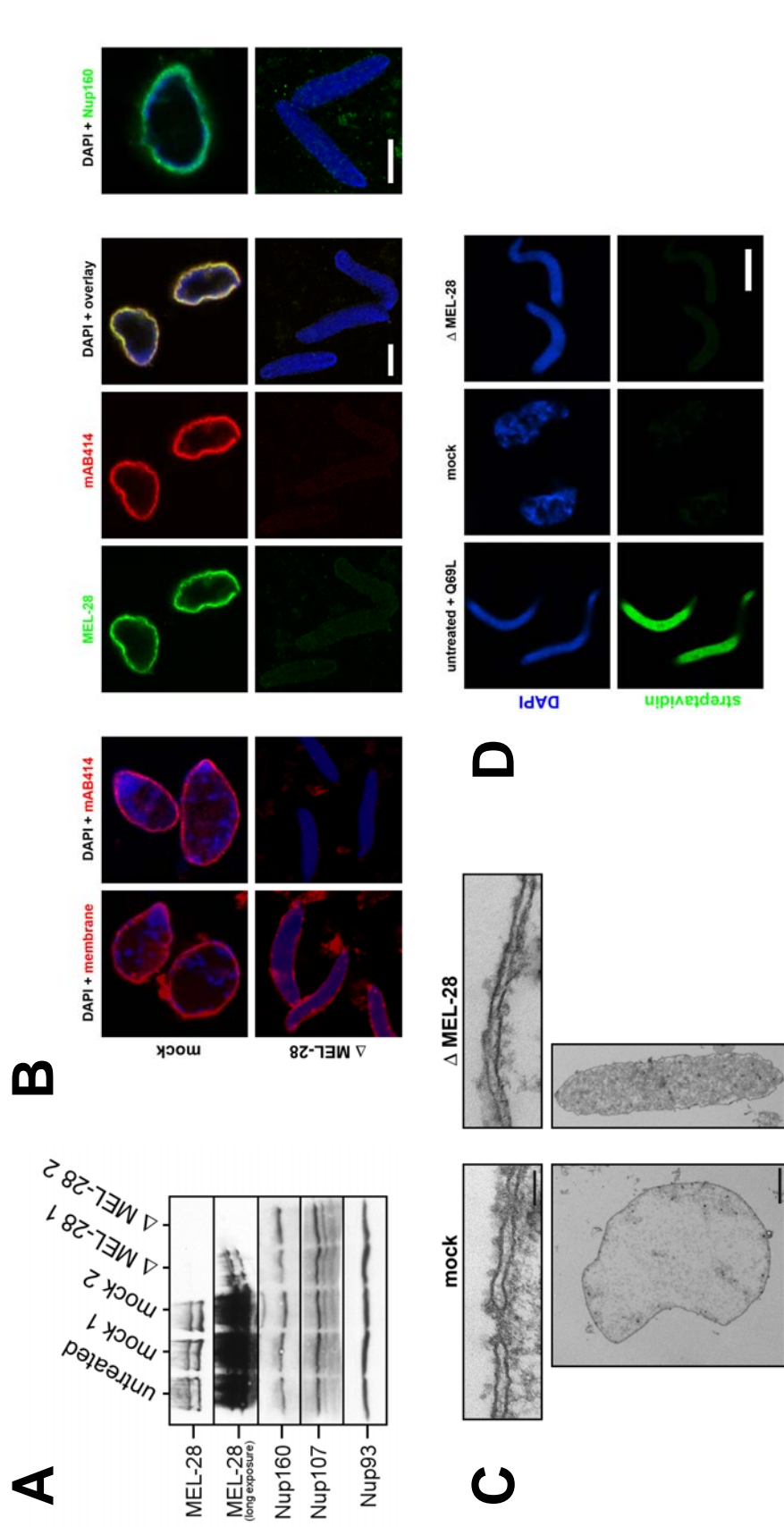


Figure 2-8. MEL-28 is required for postmitotic NPC formation. (A) Immunodepletion of MEL-28 from *Xenopus laevis* egg extract monitored by Western blotting. (B) MEL-28-depleted extracts form nuclei devoid of pores. Nuclei were formed in mock or MEL-28-depleted extracts, fixed, purified through a sucrose cushion and analyzed by immunostaining and confocal microscopy. Scale bars, 10 μ m. (C) Nuclei formed in mock or MEL-28-depleted extracts analyzed by electron microscopy. Scale bar, 100 nm (upper images) and 2 μ m (lower images). Processing of nuclei for EM was performed by Rachel Mellwig. (D) Nuclei assembled in MEL-28-depleted extracts have a closed nuclear envelope. An exclusion assay was carried out using biotinylated histones during the initial chromatin decondensation. Labeling of the chromatin with fluorescent streptavidin at the end of the nuclear assembly indicates the absence of a closed NE. Addition of RanQ69L to the extract yields chromatin templates without closed nuclear envelopes. Scale bar, 10 μ m. The exclusion assay was carried out by Wolfram Antonin.

Taken together, these results show that nuclei formed in the absence of MEL-28 possess a closed NE with inner and outer nuclear membranes, but lack nuclear pores. Thus, depletion of MEL-28 leads to the same nuclear assembly phenotype *in vitro* as depletion of the Nup107-160 complex.

2.1.7 MEL-28 interacts with the Nup107-160 complex

The finding that removal of MEL-28 from extract resulted in a phenotype previously observed for depletion of the Nup107-160 complex suggested an intimate functional relationship between MEL-28 and this complex. MEL-28 and Nup107 can be co-immunoprecipitated with each other from interphase egg extract (Cerstin Franz PhD thesis). In order to determine whether immunoprecipitation of MEL-28 would enrich the complete Nup107-160 complex, I repeated the experiment with affinity purified anti-XI MEL-28 antibodies cross-linked to protein A Sepharose beads and analyzed the IP eluates by Western blotting for additional nups (Figure 2-9 A). A control IP was performed with rabbit IgG. MEL-28, Nup107, Nup160 and Nup37 were precipitated in the MEL-28 IP, but not in the control IP. A weak p62 signal in the eluates was not considered a real interaction, since an IP with mAb414 did not co-precipitate MEL-28 and p62 was frequently found to generate a weak signal in control IPs (data not shown). In a separate unbiased approach to identify proteins bound to MEL-28 in *Xenopus* egg extract, MEL-28 IP eluates were separated on SDS-PAGE gels and stained with silver (Figure 2-10). Marc Gentzel analyzed prominent specific bands in the MEL-28 IP eluate by mass spectrometry and identified Nup133, Nup96 and Sec13 as additional interacting proteins. MEL-28 thus binds to the entire Nup107-160 complex in egg extract. The interaction was confirmed by mutual IP of MEL-28 or the Nup107-160 complex from membrane-free cytosol using serum against MEL-28 or nups (Figure 2-9 B). Nup93 and 205 are part of a separate nup complex and were precipitated as negative controls.

The availability of antibodies against human MEL-28 allowed me to ask whether the interaction between MEL-28 and the Nup107-160 complex also occurs in human cells. IPs from HeLa cell lysates were performed with affinity purified anti-human MEL-28 antibodies or an unrelated pre-immune serum as negative control and investigated by

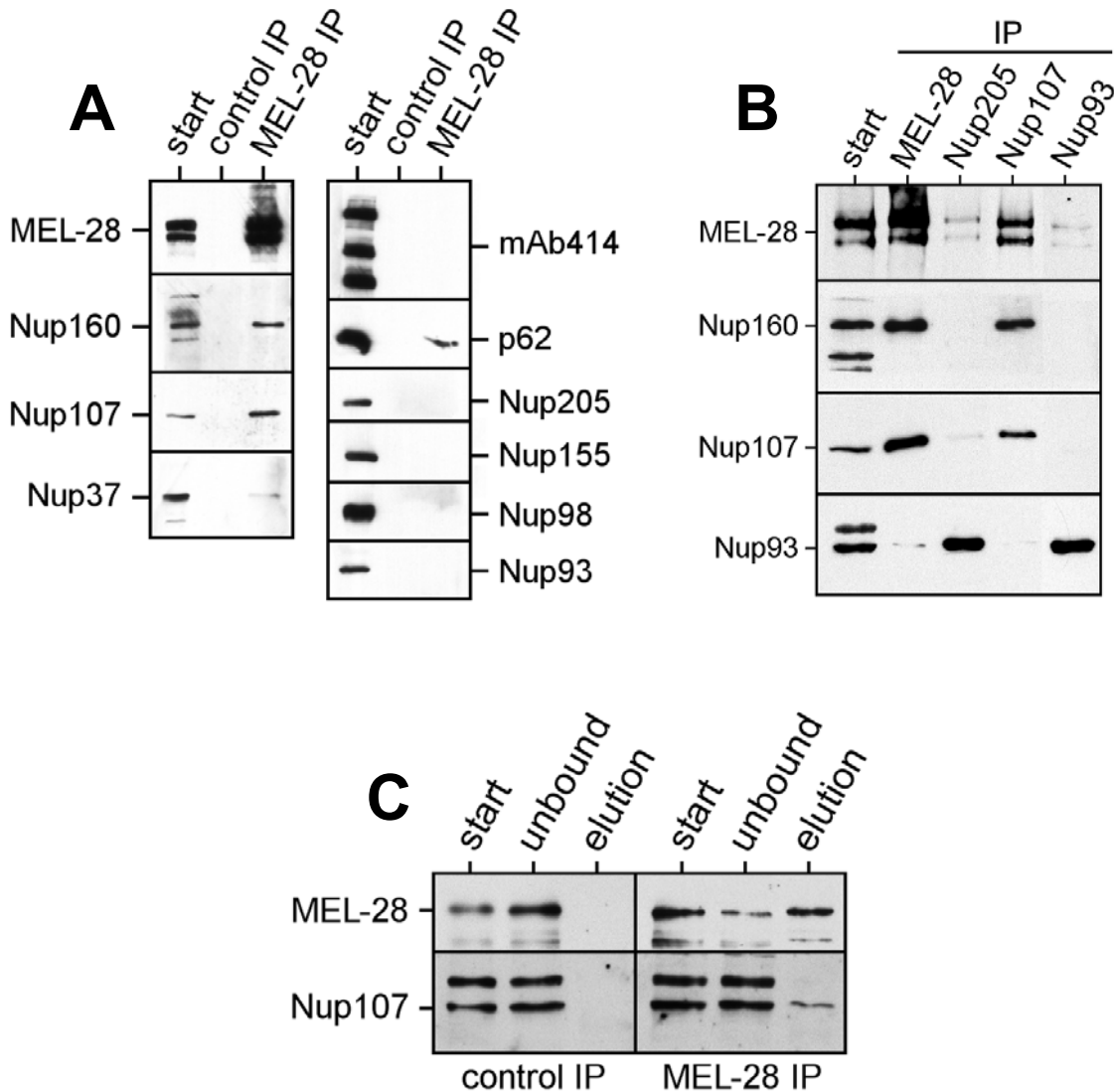


Figure 2-9. MEL-28 interacts with the Nup107-160 complex. (A) Immunoprecipitation of MEL-28 from membrane-free *Xenopus laevis* egg extract. The IP was performed with affinity purified anti-*Xl* MEL-28 antibodies cross-linked to Protein A Sepharose, the control IP with rabbit IgG. Eluates were analyzed by Western blotting. (B) Mutual IP of MEL-28 and the Nup107-160 complex from *Xl* egg extract. IPs were carried out with sera against the indicated proteins. The IPs against Nup205 and Nup93, which reside in a distinct Nup complex, served as negative control. (C) IP of human MEL-28 from a HeLa cell nuclear extract. The IP was performed with affinity purified anti-*Hs* MEL-28 antibodies ("C-terminus") cross-linked to Protein A Sepharose, the control IP with an unrelated pre-immune serum.

Western blotting (Figure 2-9 C). Interestingly, only antibodies against the C-terminus of *Hs* MEL-28 precipitated MEL-28, but not those directed against the middle fragment suggesting that only amino acids 1801-2266 of human MEL-28 are accessible in HeLa cell lysates. The MEL-28 IP eluate contained Nup107, which was not detected in the control IP, indicating that the interaction observed in the *Xenopus* system is conserved among vertebrates. Probing for other human nups was restricted by the available antibodies. Rasala *et al.* (2006) independently demonstrated that human MEL-28 interacts with the complete Nup107-160 complex.

2.1.8 Identification of proteins bound to MEL-28

As mentioned previously the MEL-28 IP eluates from interphase *Xenopus laevis* egg extract were analyzed by SDS-PAGE and silver staining to identify all proteins precipitated with MEL-28. Table 2-1 summarizes the candidate proteins for interaction with *Xenopus laevis* MEL-28 that were not Nup107-160 complex components.

Table 2-1 Unrelated proteins bound to MEL-28 in *Xenopus laevis* egg extract

No. in Fig. 2-10	Candidate protein	Gene ID
1	Homologous to dedicator of cytokinesis [<i>Mus musculus</i>]	gi 82915356
2	AND-1 protein	gi 2102674
3	T-complex protein 1 subunit gamma (TCP-1-gamma)	gi 1729875
4	Cyclase-associated protein 1b	gi 31747013
5	MGC81040 protein	gi 46249848
6	Homologous to BAE40130 unnamed protein product [<i>Mus musculus</i>]	gi 74207780
7	Centrin	gi 1017791

In addition to the above listed nups and candidate proteins, importin α and β were identified in the MEL-28 eluates. Importin β had previously been shown to bind to the Nup107-160 complex (Walther *et al.*, 2003b). AND-1 had been characterized in a previous publication (Köhler *et al.*, 1997) and we obtained a monoclonal antibody against this protein from the authors. AND-1, however, did not appear to interact with MEL-28, since an AND-1 IP did not co-precipitate MEL-28. The other candidates from the above list were not investigated in greater detail as part of this thesis.

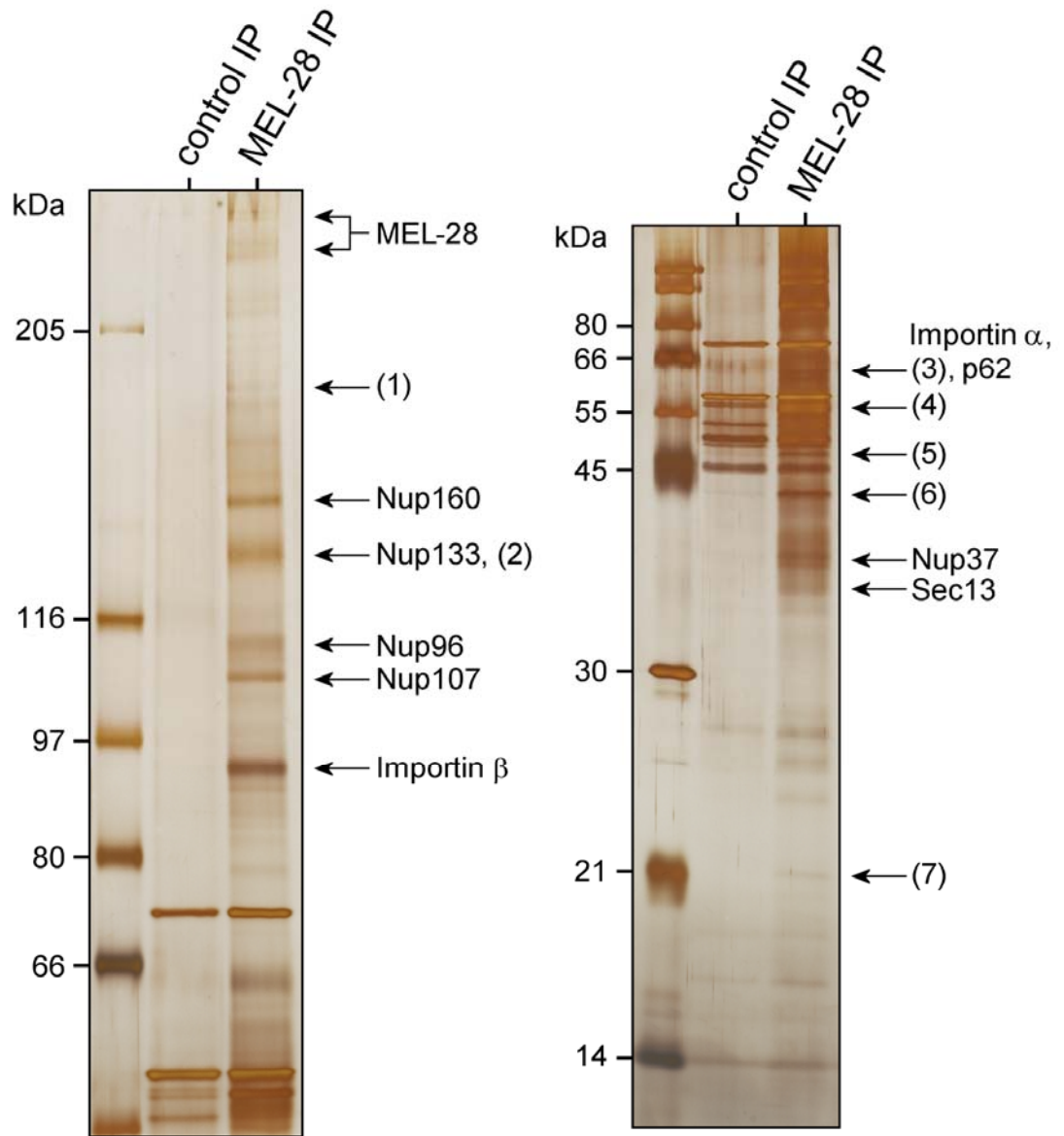


Figure 2-10. Proteins bound to MEL-28 in *Xenopus laevis* egg extract. MEL-28 was immunoprecipitated from membrane-free *Xenopus laevis* egg extract with affinity purified anti-XI MEL-28 antibodies cross-linked to Protein A Sepharose. The control IP was performed with rabbit IgG. Eluates were separated on 7% (left) or 15% (right) SDS-PAGE gels, analyzed by silver staining and specific bands were identified by mass spectrometry (MS). Nuclear pore proteins are marked. Unrelated proteins are numbered and listed in table 2-2. The identification of proteins by MS was carried by Marc Gentzel.

The above experiment was complemented with two additional IPs in which different starting material was employed and which intended to answer the following two questions. Firstly, do MEL-28 and the Nup107-160 complex bind to additional proteins from the membrane fraction of the egg extract? Secondly, does the composition of proteins bound to MEL-28 change during the cell cycle? To address the first question, MEL-28 was immunoprecipitated from membrane-free extract as above followed by a second incubation with detergent-solubilized total membranes. The second question was tackled by comparing silver-stained MEL-28 IP eluates from membrane-free interphase and mitotic extracts. *Xenopus laevis* eggs are arrested in metaphase of meiosis 2, and can be used to prepare mitotic extract when activation of the eggs is prevented. Neither approach, however, led to the identification of additional proteins.

In addition to IPs from egg extract, the antibodies against human MEL-28 were used to precipitate MEL-28 from HeLa nuclear extracts followed by SDS-PAGE and silver staining (data not shown). Although the eluates contained only a small number of bands suggesting the enrichment was specific, the experiment suffered from proteolytic degradation, despite the addition of protease inhibitors, and Nup160 was the only nup detectable. The proteins identified with the highest numbers of peptides besides MEL-28 are listed in table 2-2:

Table 2-2 Proteins enriched by the human MEL-28 IP from HeLa nuclear extract

Name	Gene ID
ubiquitin-conjugating BIR-domain enzyme APOLLON	gi 8489831
DNA-activated protein kinase, catalytic polypeptide	gi 13654237
I κ B kinase beta subunit; IKK beta	gi 3213217
Bruton's tyrosine kinase-associated protein-135; BAP-135	gi 1870688
Hydroxysteroid (17-beta) dehydrogenase 4	gi 13111861
kinesin family member 2C	gi 5803082

The above collection of candidate proteins suggests that the human MEL-28 IP might have enriched the nucleoplasmic pool of MEL-28, rather than the NE fraction. This is in line with the experimental conditions, since the nuclear extract was prepared without detergents.

2.1.9 MEL-28 acts upstream of the Nup107-160 complex in NPC assembly

Having identified the interaction between MEL-28 and the Nup107-160 complex, we wondered if MEL-28 and Nup107-160 formed a stoichiometric complex and what their functional relationship in nuclear assembly was. Wolfram Antonin had separated interphase egg extract by gel filtration and analyzed the migration behavior of nups and MEL-28 by Western blotting (Figure 2-11 A). In this experiment, a large fraction of MEL-28 co-migrated with Nup107 and Nup160 in a high molecular weight peak around 2 MDa indicating that this might be the complex previously purified in the MEL-28 IP. A smaller MEL-28 peak was observed at slightly lower molecular weight (fractions 8-10 in Figure 2-11 A), while a second Nup107/Nup160 peak followed significantly later (fractions 14-18 in Figure 2-11 A), suggesting that this was the MEL-28-free Nup107-160 complex which remained in extracts after MEL-28 immunodepletion (see e.g. Figure 2-8 A). The gel filtration experiment indicated that while a significant fraction of Nup107-160 complexes was MEL-28-free only a small proportion of MEL-28 was not bound to Nup107-160 complexes. This was indeed observed when the Nup107-160 complex was immunodepleted from egg extract: a significant part of MEL-28 was removed along with Nup107-160, but a small amount remained detectable in the extracts (Figure 2-11 B).

Removal of MEL-28 and the Nup107-160 complex caused the same phenotype in nuclear assembly, however, their hierarchy in this process was unclear. To address this issue we incubated chromatin templates with membrane-free Nup107-160 or MEL-28-depleted extract for 10 min, stopped the reactions by fixation and processed the samples for MEL-28 and Nup160 immunostaining followed by confocal microscopy (Figure 2-11 C). While MEL-28 could still bind to chromatin in the absence of the Nup107-160 complex, Nup107-160 complex recruitment to chromatin was abolished in MEL-28-depleted extracts. These results demonstrate that MEL-28 acts upstream of Nup107-160 and is required for the Nup107-160 complex to bind to chromatin in postmitotic NPC assembly.

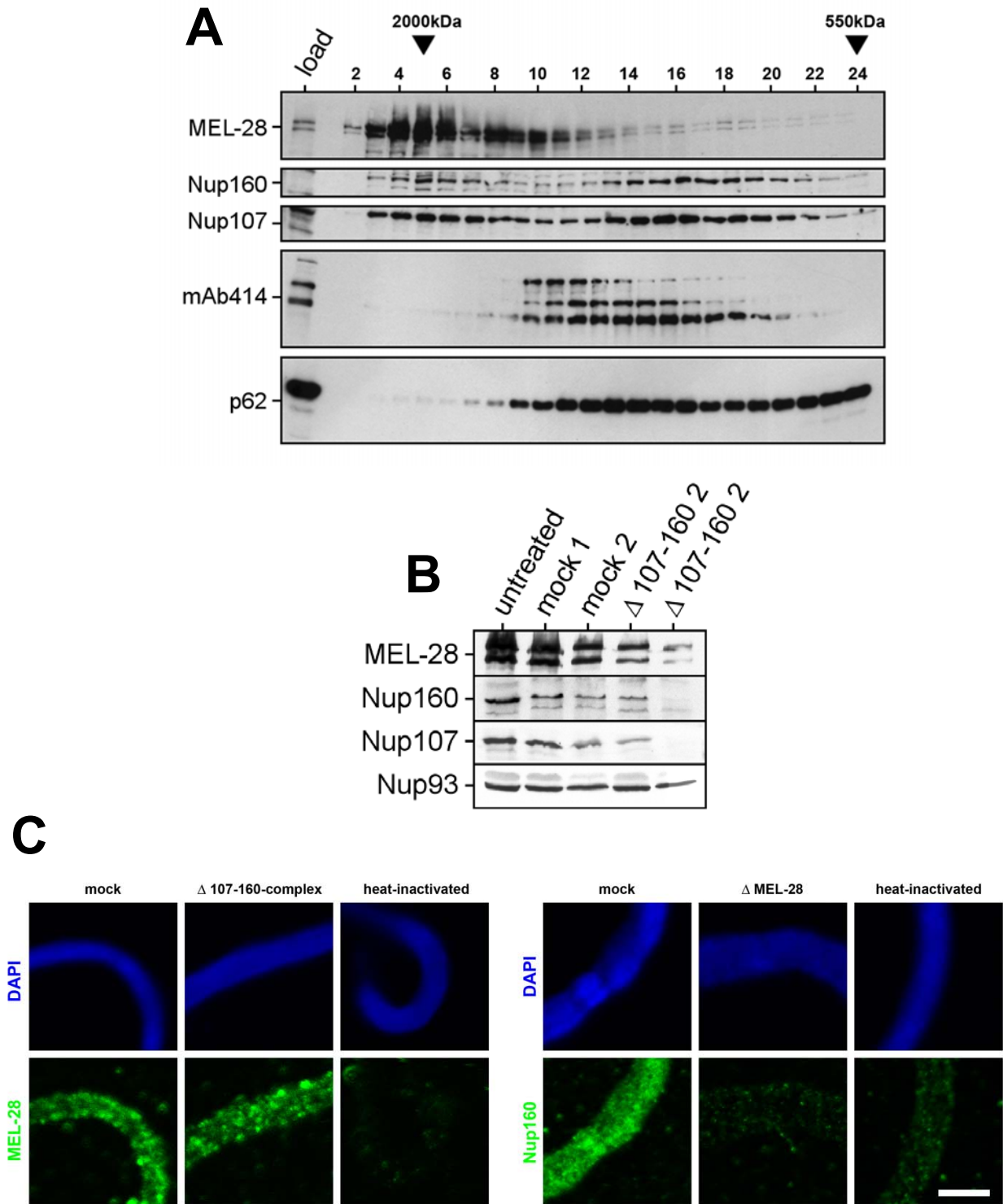


Figure 2-11. MEL-28 is required for recruitment of the Nup107-160 complex to chromatin but not vice versa. (A) *Xenopus laevis* egg extract separated on a Superose 6 gel filtration column. Fractions were analyzed by Western blotting. Fraction 1 corresponds to the void. Elution of dextran 2000 and ferritin (550 kDa) are indicated. The gel filtration experiment was performed by Wolfram Antonin. (B) Depletion of the Nup107-160 complex from cytosol with antibodies directed against Nup107. (C) Recruitment of MEL-28 or the Nup107-160 complex to chromatin. Extracts were depleted of MEL-28 or the Nup107-160 complex, centrifuged to remove membranes and the supernatants incubated with chromatin for 10 min. The chromatin templates were fixed, isolated through a sucrose cushion and analyzed by immunostaining and confocal microscopy. Scale bar, 10 μ m.

2.1.10 Mapping the NE-localization domain in MEL-28

We next wanted to define the region in MEL-28 which mediates interaction with the Nup107-160 complex. The starting point of this experiment was the observation that an N-terminally GFP-tagged full length *Xenopus* MEL-28 localized properly to the NE when expressed in HeLa cells (Figure 2-12 B). Western blotting of lysates from transfected cells indicated that the full length protein was expressed (Figure 2-12 A). Interestingly, this experiment showed that a new anti *Xenopus* MEL-28 antiserum, which I generated with the same antigen fragment that Cerstin Franz had used before, cross-reacted with the human protein (Figure 2-12 A).

Mapping followed the rationale to consecutively truncate the MEL-28 cDNA and check for localization of the GFP-tagged fragments in HeLa cells. At first I exploited the unique restriction sites in the MEL-28 sequence, releasing fragments of the cDNA and re-ligating the plasmid by blunt end ligation. This series of C-terminal truncations demonstrated that the C-terminal 800 amino acids of over-expressed *XI* MEL-28 are dispensable for NE localization (Figure 2-12 B). In a second round, additional N-terminal truncations were amplified by PCR, shortening the previously identified fragment by ≈ 200 amino acid increments. While most of the constructs did not display proper localization, amino acids 1007-1418 directed GFP to the NE in most transfected cells (Figure 2-12 C). These cells exhibited a slightly higher background GFP signal than cells transfected with the full length protein, but a strong enrichment at the NE was clearly visible. The fact that some longer fragments did not localize to the NE may indicate either a folding problem or shielding of the binding site. Although the experiment intended to narrow down the interaction domain in MEL-28 with the Nup107-160 complex, a possible interpretation of its result is that MEL-28 dimerizes via this region with human MEL-28 present in the HeLa cells and is thus brought to the NE. Figure 2-12 D schematically illustrates the minimal part of *XI* MEL-28 which was found to target GFP to the NE in HeLa cells. This fragment could be expressed in and purified from *E. coli* when expressed as a GST-tagged protein. Using it as bait in GST-pulldown experiments from *Xenopus* egg extract has not yet yielded a conclusive result, as the binding pattern of nups was not reproducible and the experimental conditions need to be optimized.

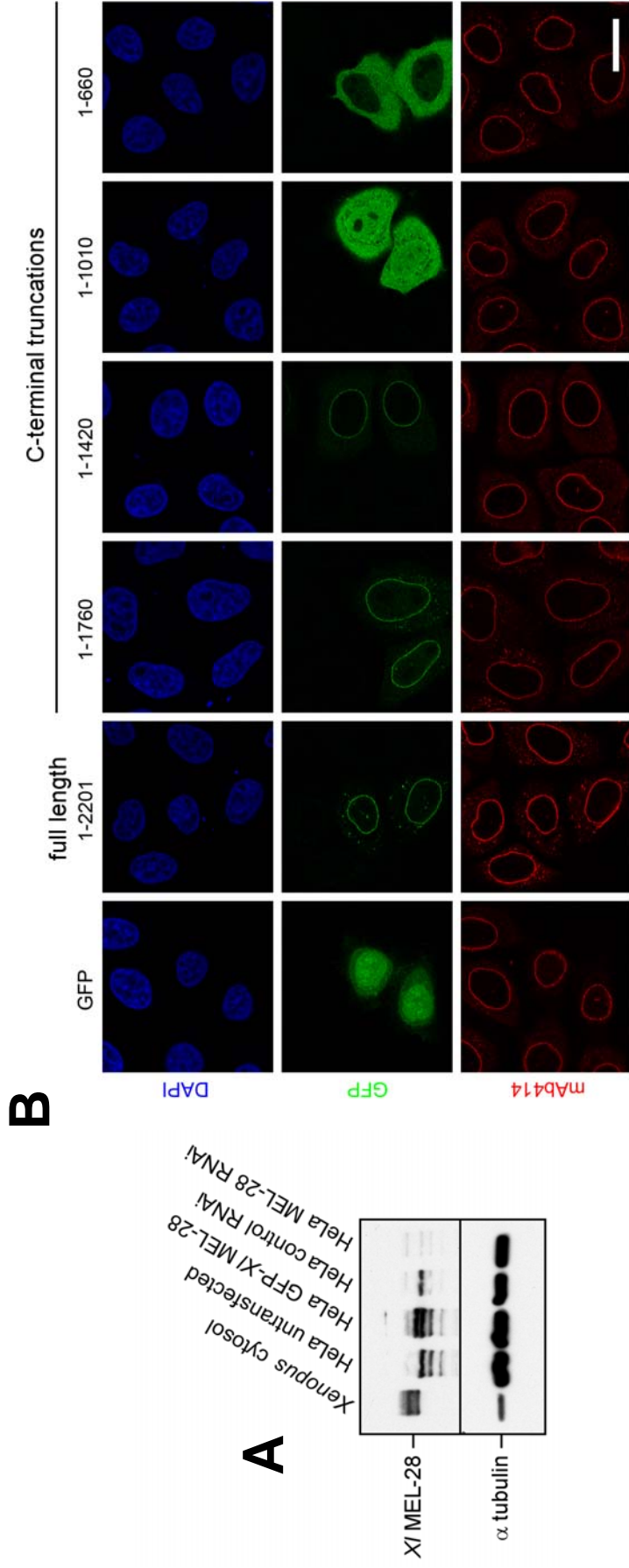


Figure 2-12. Mapping the minimal region for NE localization in MEL-28. (A) HeLa cells express full length *Xenopus laevis* MEL-28. Lysates from wildtype HeLa cells or cells expressing GFP-XI MEL-28 analyzed by Western blotting. The MEL-28 RNAi samples demonstrate that the antibody against XI MEL-28 cross-reacts with the human orthologue. (B+C) HeLa cells transiently expressing GFP, GFP-tagged full length XI MEL-28 or N- (B) and C-terminally (C) truncated fragments of XI MEL-28 were PFA-fixed and immunostained with mAb414. Scale bars, 20 μ m. (D) Schematic representation of the minimal region within the *Xenopus* MEL-28 protein sequence which mediates NE localization.

The difficulties to predict domains within MEL-28 by means of bioinformatics have significantly limited approaches to find soluble fragments useful for biochemical experiments. The lab of Darren Hart has developed a method, ESPRIT (Expression of Soluble Proteins by Random Incremental Truncation), which allows generation of a large library of randomly shortened cDNA fragments and subsequent screening of these constructs for expression and solubility with the aid of robotics (Tarendeau *et al.*, 2007). After initial attempts to generate the library in Heidelberg using a larger cDNA fragment failed, we decided to set up a collaboration with the Hart group. They used the minimal MEL-28 fragment, amino acids 1007-1418, as a template for a new library, which is currently being screened. Soluble fragments identified by this approach will be used for biochemical experiments in the future.

2.1.11 Interplay with the Ran GTPase system

Nuclear assembly has been shown to be regulated by the Ran GTPase system (Walther *et al.*, 2003b; Harel *et al.*, 2003b), but Ran's contribution to MEL-28 function had not been investigated. In order to examine the response of MEL-28 to manipulation of the Ran system, chromatin was incubated for 10 min with membrane-free cytosol supplemented with 5 μ M RanQ69L or RanT24N. The reactions were stopped by fixation, the chromatin templates purified through a sucrose cushion and MEL-28 was analyzed by immunostaining (Figure 2-13 A). Heat-inactivated extract, from which the heat-denatured nups and MEL-28 had been removed by centrifugation, but which supports decondensation of chromatin, was used as a negative control for non-specific binding of antibodies to chromatin. RanQ69L significantly enhanced the binding of MEL-28 to chromatin compared to the control reaction, while RanT24N did not (Figure 2-13 A). Interestingly, RanT24N did not reduce the chromatin recruitment of MEL-28, suggesting that a certain amount of MEL-28 can bind to chromatin independently of the Ran system. In a similar experiment, Ran mutants or importin β were added to cytosol at 20 μ M or 10 μ M, respectively, before incubation with sperm chromatin. After 10 min the chromatin templates were separated from the extract through a sucrose cushion, washed and analyzed by Western blotting (Figure 2-13 B). This experimental setup allowed simultaneous visualization of the recruitment of several nups to chromatin. RanQ69L triggered binding of MEL-28, Nup160 and

mAb414 antigens to chromatin. Importin β slightly diminished the amounts of these proteins on chromatin, an effect which could be reversed by addition of RanQ69L. At the same time, RanT24N had a particularly strong inhibitory effect on recruitment of the mAb414 antigens, while not affecting MEL-28 or Nup160. The binding of Nup358 and Nup214 to the chromatin templates, a comparably late event in NPC assembly *in vitro*, indicated that the extract contained residual amounts of membranes (see also Figure 2-13 C). The RanQ69L effect was more pronounced in the experiment shown in Figure 2-13 A as compared to Figure 2-13 B, possibly because the samples were fixed in A, thus allowing much better preservation of the chromatin templates. Longer incubation of chromatin with extracts led to a more substantial effect upon addition of RanQ69L, but the time was typically kept short to minimize the influence of mutual stabilization of proteins once bound on the chromatin surface at later time points.

In order to assess the contribution of MEL-28 to chromatin binding of nups in the presence of RanGTP, membrane-free mock or MEL-28-depleted cytosol was incubated with chromatin plus or minus 20 μ M RanQ69L or membranes. The absence of membranes was confirmed by probing for the transmembrane nup Ndc1. After 45 min the chromatin templates were purified through a sucrose cushion, washed and analyzed by Western blotting (Figure 2-13 C). Addition of RanQ69L increased the amount of nups bound to chromatin, particularly of Nup153 (the lowest of the three bands recognized by mAb414). Interestingly, Nup358 and Nup214 (the two upper mAb414 bands) could not be detected on chromatin in the absence of membranes demonstrating that membranes are required for completion of NPC assembly. It was striking that the levels of MEL-28, Nup160 and Nup153 on chromatin were higher with membranes compared to incubation with 20 μ M RanQ69L possibly reflecting the stabilization of NPCs on incorporation into membranes. Upon depletion of MEL-28, nup recruitment to chromatin was abolished. Not even high concentrations of Q69L could overcome the MEL-28 depletion, demonstrating that it is essential for nup binding to chromatin under all conditions.

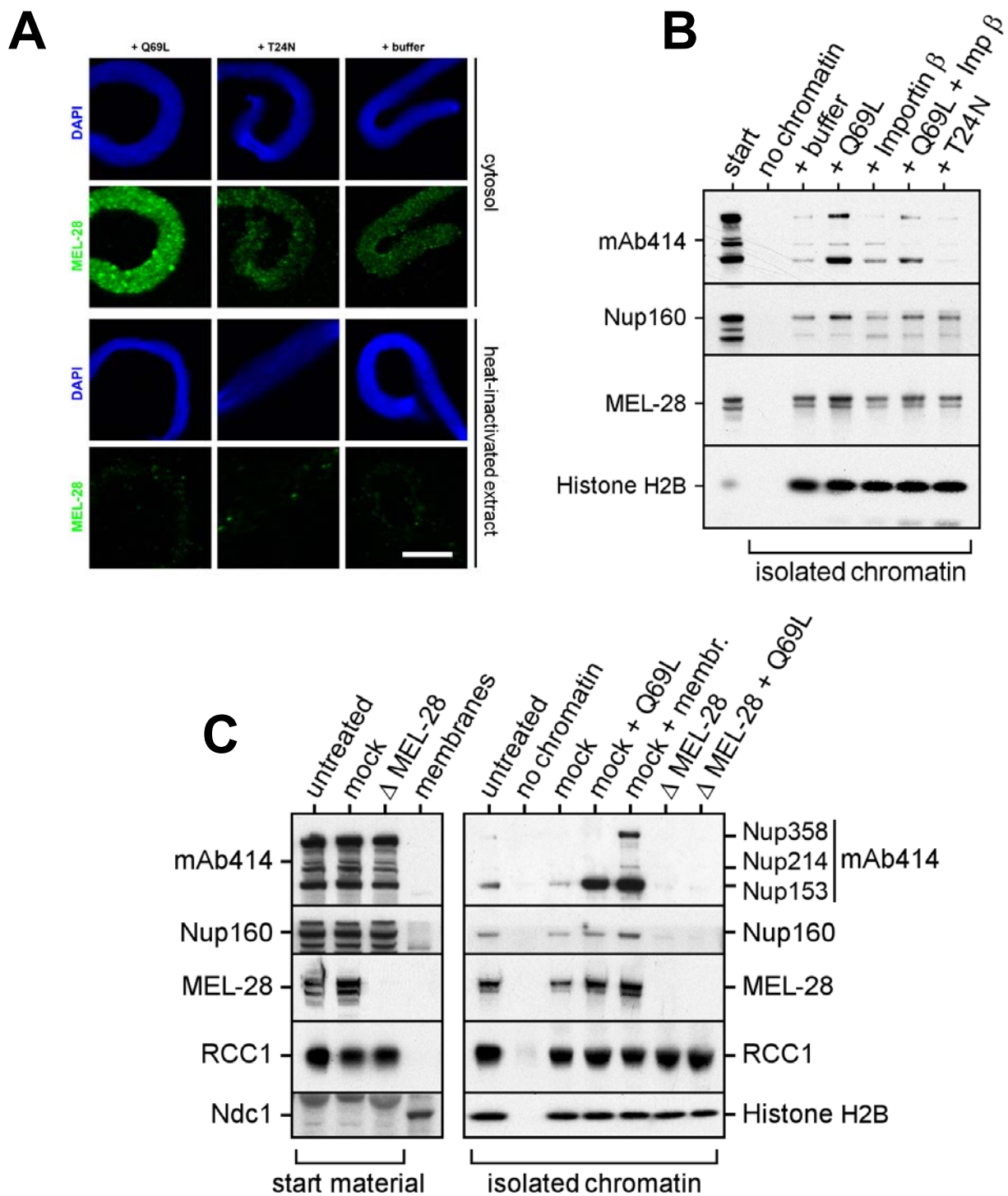


Figure 2-13. RanGTP-mediated recruitment of nucleoporins to chromatin is dependent on MEL-28. (A) MEL-28 binding to chromatin is enhanced by RanGTP. Membrane-free cytosol was supplemented with Ran mutants (5 μ M final conc.) and incubated with chromatin. The reactions were stopped by fixation after 10 min and processed for immunostaining with MEL-28 antibodies. Incubation with heat-inactivated extract served as control for unspecific antibody labeling of chromatin. Scale bar, 10 μ m. (B) The Ran system modulates nucleoporin binding to chromatin. Cytosol was supplemented with Ran mutants (20 μ M final conc.) or importin β (10 μ M final conc.) and incubated for 10 min with chromatin. The chromatin templates were purified through a sucrose cushion, washed and analyzed by Western blotting. (C) Recruitment reaction as in (B), but with mock or MEL-28-depleted membrane-free cytosol. Incubation time with extracts before purification of chromatin templates was 45 min.

In summary, nup recruitment to chromatin requires MEL-28 even in the presence of high RanQ69L concentrations. RanGTP positively modulates several early steps in NPC formation including MEL-28 binding to chromatin, but membranes are required for later steps and completion of nuclear assembly.

MEL-28 contains a predicted nuclear localization signal (NLS) between amino acids 1748-1758 and importin α and β were identified in the MEL-28 IPs from egg extract. However, since members of the Nup107-160 complex also bind importin β , it was unclear whether the interaction with MEL-28 was direct or indirect. Several NLS-containing *XI* MEL-28 fragments have been cloned, expressed and purified as GST-tagged proteins. Employing them as baits in GST-pulldowns from extract and testing for a direct interaction with purified importins is in progress.

2.1.12 Expression and purification of full length MEL-28

In order to fully demonstrate the specificity of any depletion phenotype it is necessary to perform a rescue experiment with recombinant protein. I have thus invested a significant part of my PhD work in expressing and purifying recombinant full length MEL-28 and optimizing the conditions of the "add-back" experiment. Attempts to express full length *Xenopus laevis* MEL-28 in *E. coli* were unsuccessful (data not shown). We therefore turned to the Baculovirus system for expression in insect cells. This work was carried out together with Ann-Marie Lawrence from the EMBL protein expression facility. I cloned constructs for expression of N- or C-terminally His₆-tagged or N-terminally FLAG- or HA-tagged *XI* MEL-28. Ann-Marie Lawrence prepared the corresponding viruses and performed the cell culture work and transfections. We tested four different insect cell lines, Sf9, TniHi5, High5 and Sf+, and analyzed cell lysates for maximal MEL-28 expression levels by Western blotting at different time points (0, 24, 40, 48 and 72h) (data not shown). Expression of both His₆-tagged proteins was strongest in Hi5 cells and peaked 24h post transfection for the N-terminal construct (Figure 2-14 A) while expression of the FLAG- and HA-tagged proteins was much lower (data not shown). Purification of FLAG- or HA-tagged MEL-28 was unsuccessful (data not shown). We therefore focused on the purification of the His₆-tagged proteins. Even under the best conditions the expression levels were too low to

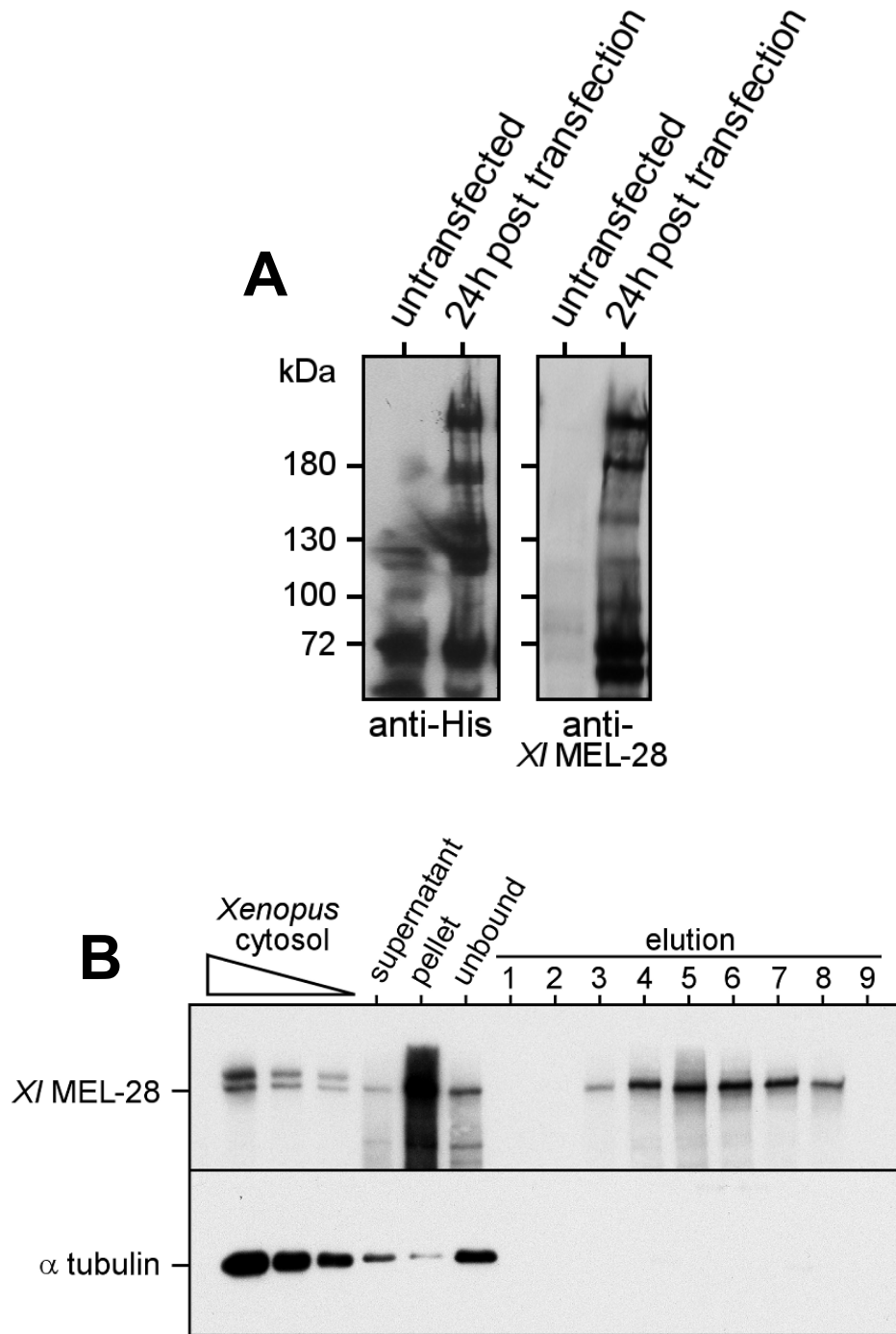


Figure 2-14. Expression and purification of full length MEL-28 from insect cells. (A) Total lysates of *Drosophila* Hi5 cells expressing XI MEL-28 analyzed by Western blotting. (B) Purification of recombinant MEL-28 from insect cells with Ni-NTA agarose monitored by Western blotting. Endogenous MEL-28 (0.5, 0.25 or 0.12 μ l cytosol per lane) is shown as a reference.

be monitored by Coomassie staining. We therefore followed the expression and purification of MEL-28 by Western blotting with anti-*Xl* MEL-28 antibodies. Ann-Marie Lawrence expressed the protein while I purified MEL-28 from the cell pellets. Figure 2-14 B depicts the purification of His₆-MEL-28. The purified protein corresponded to the lower of the two MEL-28 bands in *Xl* egg extract indicating that the full length protein had been expressed. Hi5 cells grow in adherent culture, which posed an inherent limitation on the amount of material that could be obtained. Four 175 cm² flasks typically yielded an amount of MEL-28 equivalent to 50-100 μl of cytosol. Also concentration of the purified protein proved to be very difficult.

2.1.13 Recombinant MEL-28 rescues the MEL-28 depletion phenotype in the first steps of NPC assembly

The recombinant MEL-28 was added back to MEL-28-depleted extracts in an attempt to restore the depletion phenotype. Addition of the C-terminally His₆-tagged purified protein inhibited nuclear assembly even in an undepleted reaction, possibly due to a dominant-negative effect of N-terminally truncated fragments, which had been purified along with the full length protein (data not shown). Therefore, only the N-terminally His₆-tagged MEL-28 was used in subsequent rescue experiments.

At first I tried to rescue the initial steps of NPC assembly with recombinant MEL-28 by performing a recruitment experiment similar to that performed in Figure 2-13 C. The purified recombinant MEL-28 did not contain nups as judged by Western blotting for Nup107 or with mAb414 (Figure 2-15 A, lane 2). RanQ69L and recombinant MEL-28 were added to the extracts on ice for 5 min and then incubated with chromatin at 20°C for 60 min. Such a long reaction time was required to reproducibly visualize nups by Western blotting after purifying and washing the chromatin templates. Recombinant MEL-28 could be added back to the depleted extracts to approximately endogenous concentrations and bound strongly to chromatin. Nup107 recruitment to chromatin was impaired in the absence of MEL-28, but was restored upon addition of the recombinant protein. The presence of 20 μM RanGTP did not significantly enhance or alter the rescue effect. Nup153 levels bound to chromatin displayed a significant increase in the rescue condition, even above the mock depleted samples. At the same

time Nup358 binding could be observed in these samples despite the absence of added membranes.

A more challenging experiment was the rescue of complete nuclear assembly, as it required higher concentrations of recombinant MEL-28 and higher activities of both extract and the purified protein. The rescue conditions were modified and optimized in several trials, but the restoration of full nuclear assembly was ultimately unsuccessful. Either the amounts of recombinant protein added to the depleted extract were insufficient to restore endogenous MEL-28 levels or the extracts suffered so severely from the combination of incubation with antibody beads and subsequent dilution, that even control reactions did not produce fully assembled nuclei. At the same time, low available amounts and problematic handling of the purified recombinant MEL-28 set a limit to further concentration of the protein and optimization of the rescue conditions. Figure 2-15 B depicts the outcome of a typical rescue experiment performed as in figure 2-8. MEL-28 staining and strong mAb414 foci were detectable on the chromatin surface of control samples. The majority of chromatin templates, however, had not acquired a continuous mAb414 rim staining, indicating that the assembly reaction stalled before completion (also see time course experiment in Franz *et al.* (2007) for comparison). Depletion of MEL-28 completely abrogated mAb414 binding to chromatin as observed in previous experiments. Upon addition of recombinant MEL-28 to depleted extract MEL-28 recruitment to chromatin was partially restored, albeit to significantly lower levels than in the control reaction. Formation of mAb414 foci was also clearly increased, but correspondingly did not reach control levels and nuclei in the rescue condition failed to acquire mAb414 rim staining. The failure to fully restore nuclear assembly with recombinant MEL-28 could be due to a number of reasons (see Discussion).

In conclusion, full length MEL-28 could be expressed and purified from insect cells. The recombinant protein restored MEL-28 binding and Nup107-160 complex recruitment to chromatin, but did not support later steps of NPC assembly. The observed rescue effect demonstrates that recruitment of nups such as the Nup107-160 complex can indeed be specifically attributed to MEL-28. At the same time it is evident that recombinant MEL-28 could not fully replace endogenous MEL-28 in NPC

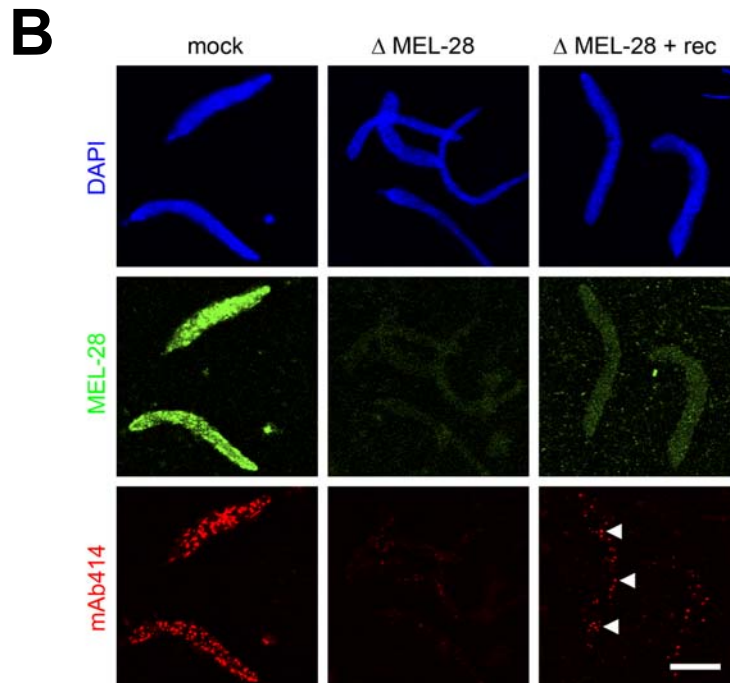
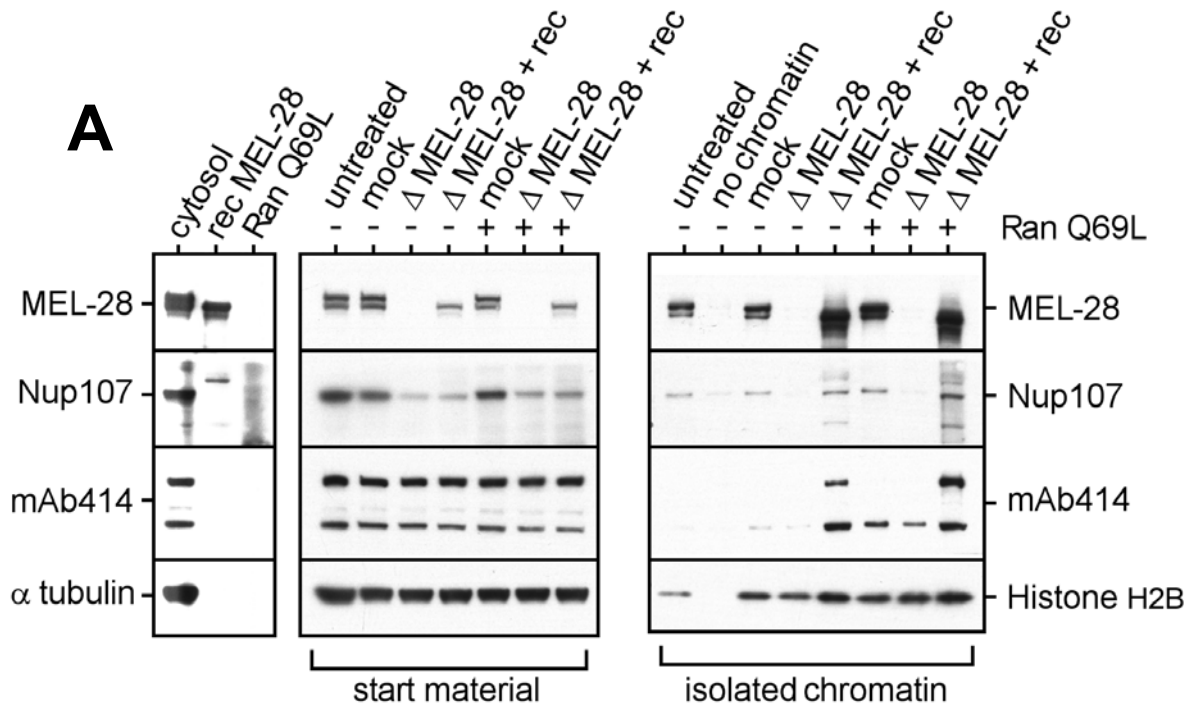


Figure 2-15. Recombinant MEL-28 partially rescues the MEL-28 depletion phenotype in NPC assembly. (A) Recruitment experiment with membrane-free extract. Mock or MEL-28-depleted cytosol was incubated with or without RanGTP (20 μ M final conc.) with chromatin for 60min. The chromatin templates were purified through a sucrose cushion, washed and analyzed by Western blotting. **(B)** Unsuccessful attempt to rescue complete nuclear assembly. Mock or MEL-28-depleted extracts were incubated with chromatin and membranes for 90 min, fixed and processed for immunofluorescence. mAb414 foci on chromatin are highlighted with arrowheads. Scale bar, 15 μ m.

assembly. It might therefore be rewarding to repeat the MEL-28 rescue experiment with recombinant protein from a different source.

2.1.14 Investigating the function of the MEL-28 AT hook

The rational design of experiments to investigate the function of MEL-28 in closer detail was hampered by difficulties predicting domains and motifs within the MEL-28 protein sequence. In addition, the lack of sufficient amounts of recombinant full length protein prevented the pursuit of certain biochemical experiments. We therefore chose an alternative, indirect approach to investigate early events in NPC assembly by inhibiting MEL-28 function with competitive protein fragments.

Besides its NLS sequence, the most prominent and in fact only other well predicted motif in the MEL-28 protein of most species is an AT hook which comprises amino acid residues 2122-2134 in *Xenopus laevis* MEL-28. AT hooks are small DNA-binding motifs found in chromatin- or DNA-binding proteins from a wide range of organisms (Aravind and Landsman, 1998). As their name implies AT hooks have a preference for AT-rich DNA sequences and are characterized by a central GRP (glycine-arginine-proline) signature surrounded by additional positive residues. The presence of the AT hook suggested that MEL-28 would bind directly to DNA and made MEL-28 a candidate for mediating chromatin anchorage of nups in nuclear assembly. This prediction is also supported by the previously described data in this thesis. The role of the MEL-28 AT hook in NPC assembly had, however, never been tested experimentally.

I addressed this issue by expressing the AT hook in a recombinant form fused to GST and investigating if this construct influenced nuclear assembly *in vitro*. The GST-tag facilitated both the purification of the AT hook and its convenient detection with antibodies against GST. Based on the published NMR structure of an AT hook bound to DNA (Huth *et al.*, 1997), which revealed the residues essential for DNA-binding, I prepared a mutated AT hook as a negative control. Two arginines and one lysine were mutated to glycine in the mutated AT hook, thus removing three positive charges (MEL-28_{MUT} in Figure 2-16 A). Two additional mutated MEL-28 AT hooks were

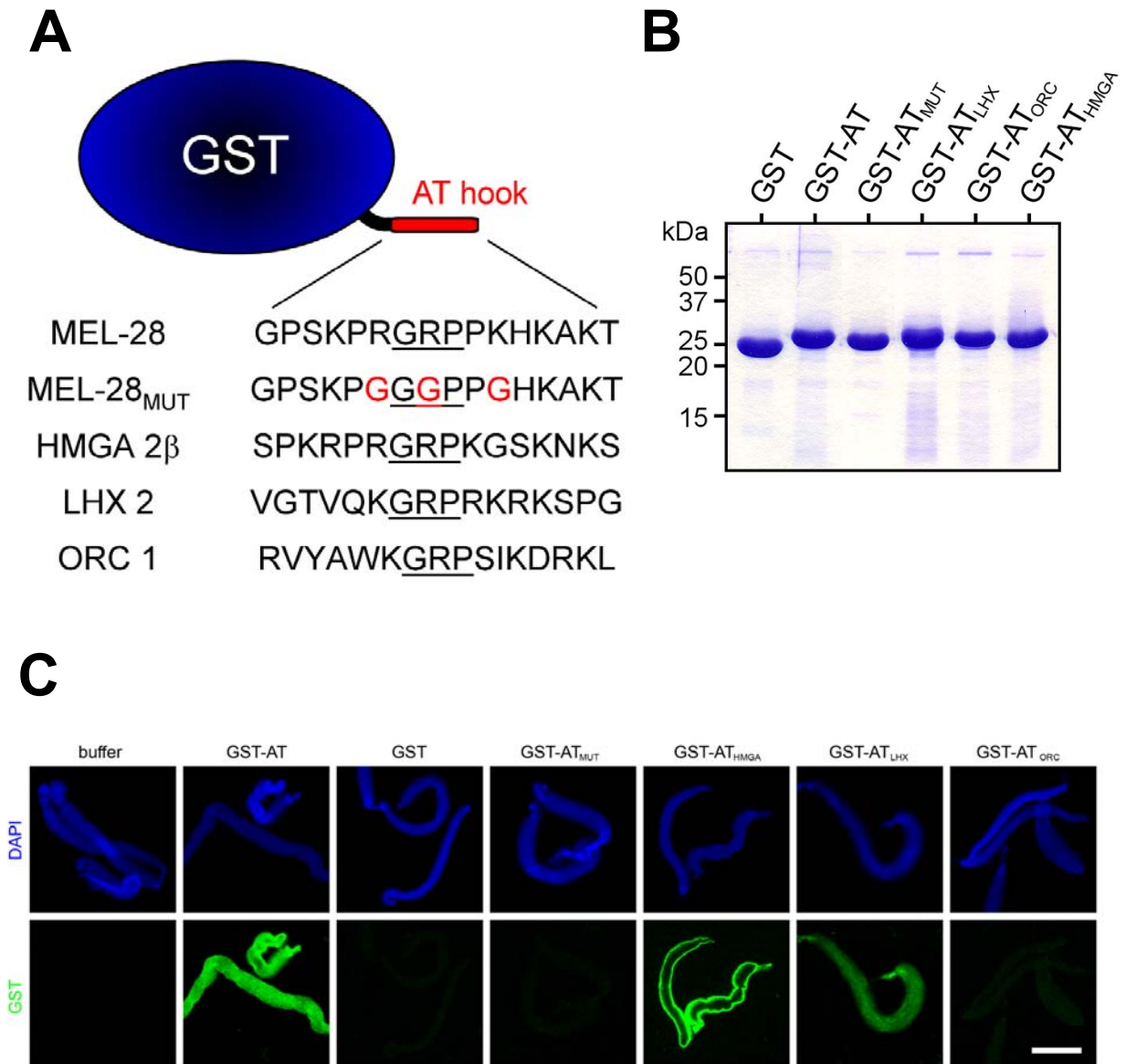


Figure 2-16. The AT hook in MEL-28 binds to chromatin. (A) Schematic representation of AT hooks fused to GST. Shown are the amino acid sequences of the MEL-28 AT hook, a mutated version predicted not to bind to DNA and the sequences of AT hooks from three unrelated proteins. (B) Coomassie-stained SDS-PAGE gel of purified AT hooks fused to GST expressed in *E. coli*. (C) DNA-binding properties of purified AT hooks. Membrane-free extract was supplemented with the purified GST or GST-AT hooks (1 μ M final conc.) and incubated with chromatin for 10 min. The reactions were stopped by fixation, chromatin templates purified through a sucrose cushion and processed for immunostaining. Scale bar, 15 μ m.

prepared, in which the same three residues were changed to alanine or serine, respectively. The 3x Ser mutated AT hook behaved like the 3x Gly mutant in all subsequent experiments, while the 3x Ala AT hook was degraded when expressed in bacteria (data not shown). All experiments shown as figures in this thesis made use of the 3x Gly mutant AT hook (MEL-28_{MUT}). In order to provide additional controls and to assess the specificity of the MEL-28 AT hook I prepared corresponding constructs with AT hooks from three unrelated *Xenopus laevis* proteins, HMGA 2 β , LHX2 and ORC 1. Figure 2-16 A illustrates the experimental strategy and lists the amino acid sequences of the AT hooks used.

The GST-AT hook constructs were expressed in *E. coli* and purified via Glutathione Sepharose. All proteins were obtained in high purity and concentration and the AT hook constructs displayed a lower electrophoretic mobility compared to GST alone (Figure 2-16 B).

To investigate whether the purified AT hook constructs could bind to chromatin membrane-free extracts were supplemented with 1 μ M GST-AT hooks or GST and incubated with chromatin for 10 min before fixation. The chromatin templates were purified through a sucrose cushion and analyzed by immunostaining for GST (Figure 2-16 C). No staining was detected after incubation of the chromatin with extract containing buffer or GST, demonstrating that GST alone cannot bind to chromatin. In contrast, the GST-MEL-28 AT hook bound strongly to chromatin while the mutated version behaved like GST. This result proves that the MEL-28 AT hook is an active chromatin binding motif under nuclear assembly conditions and that mutating the critical residues in the AT hook abolishes DNA-binding. The additional three control AT hooks from unrelated proteins exhibited a graded chromatin binding pattern. While the HMGA 2 β AT hook was highly enriched on chromatin, the LHX2 AT hook revealed intermediate binding and the ORC1 AT hook did not target GST to chromatin. These three constructs therefore allowed evaluating whether an effect on nuclear assembly generally correlated with the strength of chromatin binding of the respective AT hook.

2.1.15 Inhibition of nuclear assembly with an excess of AT hook recapitulates the MEL-28 depletion phenotype

After showing that GST-AT hook constructs can bind to sperm chromatin, we then wanted to assess whether excess recombinant AT hook could recapitulate the MEL-28 depletion phenotype, possibly by acting in a dominant negative manner against endogenous MEL-28. To do this, we performed nuclear assembly reactions in the presence and absence of purified GST-AT hooks. While nuclei with a strong mAb414 rim staining formed in control reactions, adding the GST-AT hook to extract at 36 μ M gave rise to nuclei devoid of pores (Figure 2-17). At the same time, identical concentrations of GST or the mutated MEL-28 AT hook had no inhibitory effect suggesting that DNA-binding of the GST-AT hook prevented NPC formation. Interestingly, addition of the HMGA 2 β AT hook to 36 μ M led to the same phenotype as for the MEL-28 AT hook. The additional two control AT hooks from LHX2 and ORC1 displayed a stepwise pattern for inhibition of nuclear assembly analogous to Figure 2-16 C, suggesting that the degree of inhibition of NPC formation correlates with the strength of DNA-binding (Figures 2-17 C and 2-16 C). A similar effect was observed when nuclei were assembled in extracts with decreasing MEL-28 AT hook concentrations. At 18 μ M a mixed population of nuclei with varying mAb414 labeling emerged, while with 4 μ M GST-AT hook practically all nuclei acquired a mAb414 rim staining (data not shown). The nuclei formed under all conditions possessed a closed nuclear membrane as judged by DilC₁₈ membrane staining.

Our immediate idea was that inhibition of NPC assembly by the AT hook might be a consequence of displacement of endogenous MEL-28 from chromatin. However, when we tested how much MEL-28 would bind to chromatin after 10 min incubation in extracts with 36 μ M GST-AT hook, the levels were not significantly reduced compared to extracts containing buffer or GST (Figure 2-18 A). Moreover, when we analyzed nuclei assembled in the presence of 36 μ M GST-AT hook, we found that they still possessed a clearly visible MEL-28 nuclear rim staining comparable to control nuclei (Figure 2-18 B). The anti-XI MEL-28 antibody was generated against a fragment of MEL-28 which did not contain the AT hook so that cross-reactivity could be ruled out. In order to inspect the effect of AT hook addition on MEL-28 chromatin binding more

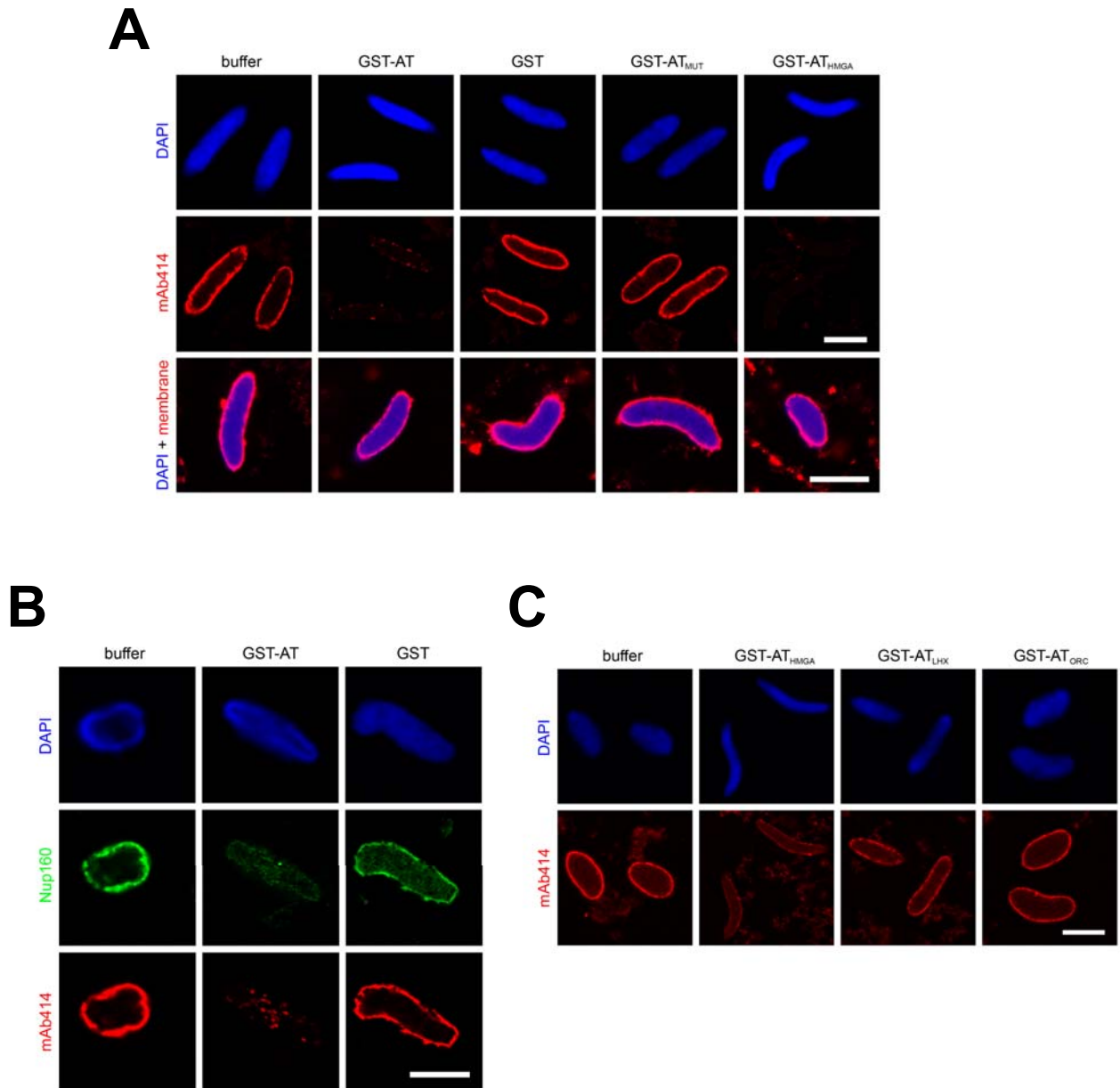


Figure 2-17. Inhibition of nuclear assembly with an excess of AT hook recapitulates the MEL-28 depletion phenotype. Cytosol was supplemented with GST or GST-AT hooks (36 μ M final conc.) and employed in a nuclear assembly reaction. The reactions were stopped by fixation after 90 min, nuclei purified through a sucrose cushion and analyzed by immunostaining and confocal microscopy. Pre-labeled floated membranes were used in the reactions illustrating the membrane staining. Nuclei shown in (A) and (C) were fixed with glutaraldehyde+PFA, those in (B) with PFA. Scale bars, 10 μ m.

closely, chromatin was incubated with membrane free cytosol with or without addition of GST or varying concentrations of GST-AT hook constructs. After 10 min the chromatin templates were purified through a sucrose cushion, washed and analyzed by Western blotting (Figure 2-18 C). In buffer-diluted extracts a significant amount of MEL-28 bound to chromatin. Upon addition of increasing GST-AT hook concentrations to the extract, more and more GST signal was detected on the isolated chromatin while the amount of MEL-28 became progressively reduced. Nevertheless, even in the presence of 36 μM GST-AT hook, conditions that prevent NPC assembly *in vitro*, a considerable amount of MEL-28 was detected on chromatin, which could account for the MEL-28 signal in Figure 2-18 A+B. High concentrations of AT hook therefore do not displace endogenous MEL-28 from chromatin, but reduce its local concentration on the chromatin templates. Interestingly, the HMGA 2 β AT hook bound more strongly to chromatin than the MEL-28 AT hook, caused a much stronger reduction of MEL-28 binding to chromatin and even led to a reduction of RCC1 levels on chromatin indicating that this particular AT hook changed the chromatin in a more fundamental way than the MEL-28 AT hook. At the same time the chromatinization of the sperm head DNA seemed unaffected by the HMGA 2 β AT hook as judged by Histone H2B levels. The notion that stronger chromatin binding by the HMGA 2 β AT hook caused more pronounced MEL-28 displacement is also in accord with the finding that this AT hook inhibited NPC assembly at concentrations lower than 36 μM (data not shown).

In summary, supplementing nuclear assembly reactions with the MEL-28 AT hook fused to GST strongly inhibited NPC assembly, thus recapitulating the MEL-28 depletion phenotype. MEL-28 levels on chromatin were reduced but not abolished, suggesting either that displacement of MEL-28 is not the only effect of AT hook addition or that NPC assembly requires a threshold concentration of MEL-28 on chromatin which is not reached in the presence of 36 μM AT hook. Interestingly, NPC formation could also be prevented with an unrelated AT hook, provided that it bound to chromatin with sufficient strength, demonstrating that the inhibition in nuclear assembly was not exclusive for or specific to the MEL-28 AT hook.

We were intrigued by the observation that a short 16 amino acid peptide could inhibit the function of a 2201 amino acid protein like MEL-28 and prevent the entire process

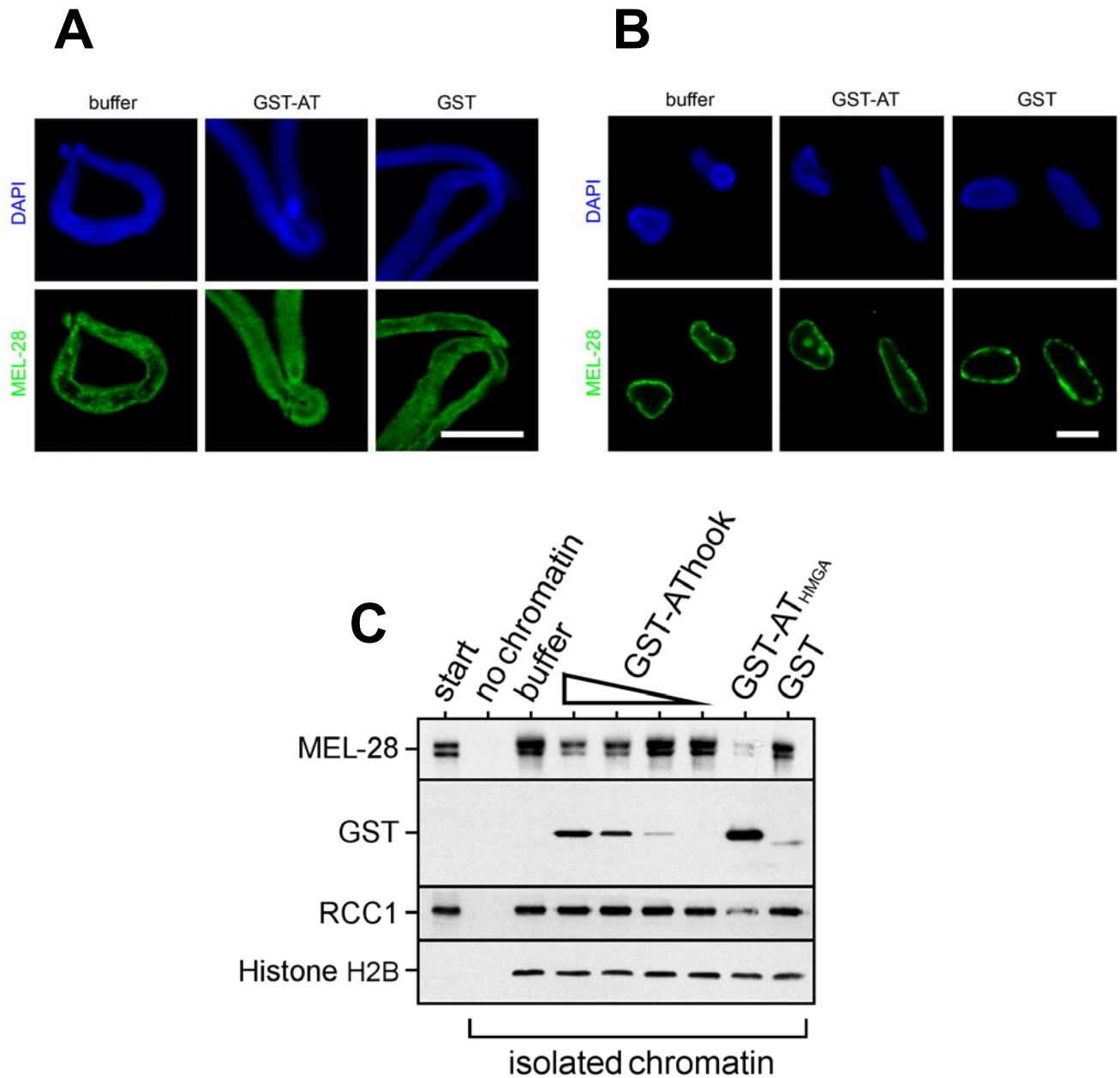


Figure 2-18. The MEL-28 AT hook does not displace endogenous MEL-28 from chromatin. (A) Recruitment reaction. Membrane-free cytosol was supplemented with GST or GST-AT hook (36 μ M final conc.) and incubated with chromatin for 10 min before the reaction was stopped by fixation. Chromatin templates were purified through a sucrose cushion and processed for immunofluorescence. (B) Complete assembly reaction in the presence of 36 μ M GST or GST-AT hook. Nuclei were prepared for confocal microscopy as chromatin templates in (A). Scale bars in A+B, 10 μ m. (C) Chromatin binding assay as in (A). The final GST-AT hook concentrations in the cytosol were 36, 15, 4 and 0.8 μ M, those of GST or GST-AT hook_{HMGA} were 36 μ M. After 10 min incubation the chromatin templates were purified through a sucrose cushion, washed and analyzed by Western blotting.

of NPC formation. However, high concentrations of AT hook constructs were required to bring about this phenotype. We therefore wondered how they related to the endogenous MEL-28 concentration in egg extract. Given the lack of sufficient amounts of recombinant MEL-28, the molar concentration of MEL-28 in extracts could only be determined indirectly by Western blotting with the help of the purified antigen XI MEL-28 aa1602-2120.

By comparison with a BSA gradient on a Coomassie-stained gel (Figure 2-19 A) and by performing a Bradford assay, the concentration of the antigen was estimated to be 0.6 mg/ml. In a second step, mixtures of decreasing quantities of extract and increasing amounts of MEL-28 aa1602-2120 were analyzed by Western blotting and probing for XI MEL-28. Considering the molar mass of the antigen fragment (58 kDa) and by matching signals of equivalent strength, the concentration of endogenous MEL-28 could be estimated (Figure 2-19 B). 0.063 μ l cytosol corresponded to 4.75 fmol of antigen, according to which $[\text{MEL-28}]_{\text{endogenous}}$ in egg extract is ≈ 75 nM. Inhibition of NPC assembly *in vitro* thus required a ≈ 500 fold excess of MEL-28 AT hook over the endogenous MEL-28.

2.1.16 The C-terminus of MEL-28 contains at least one chromatin binding motif besides the AT hook

Gillespie *et al.* (2007) also investigated the function of MEL-28 in nuclear assembly in a very similar way to us and drew analogous conclusions to those presented here. In one such experiment extract was supplemented with a larger MEL-28 fragment designated recombinant AT hook (rATh) which comprised the C-terminal 208 amino acids of MEL-28 and contained the AT hook. This construct blocked NPC assembly already at 2 μ M and prevented recruitment of endogenous MEL-28 to chromatin (Gillespie *et al.*, 2007), suggesting that the C-terminus of MEL-28 harbors additional chromatin binding sites, which allow larger fragments to compete more efficiently with full length MEL-28 for chromatin binding. We wished to repeat and expand on this experiment and evaluate the role of the AT hook in the context of the larger rATh fragment by introducing the same three mutations that previously abolished AT hook chromatin binding. Both rATh and the mutated form rATh_{MUT} were expressed as GST

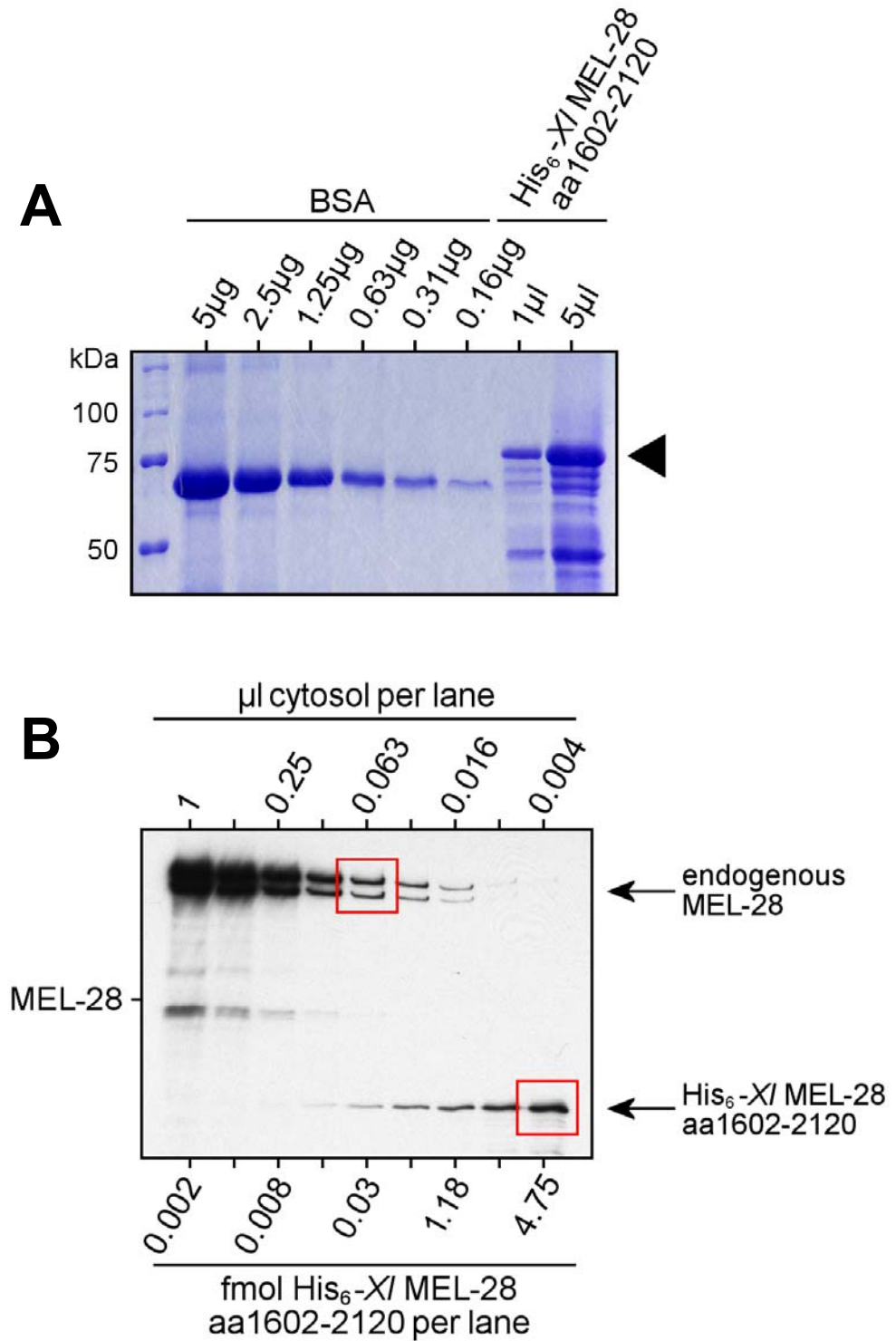


Figure 2-19. The endogenous MEL-28 concentration in *Xenopus laevis* egg extract is ≈ 75 nM. (A) With the help of a BSA gradient the concentration of purified MEL-28 fragment aa1602-2120 (arrowhead) was estimated to be ≈ 0.6 mg/ml. (B) Sample mixtures with decreasing amounts of cytosol and increasing concentrations of MEL-28 aa1602-2120 were analyzed by Western blotting. Taking the molar mass of the MEL-28 fragment into account and by matching signals of equivalent strength (red boxes) the concentration of MEL-28 in extracts could be estimated.

fusion proteins and purified using Glutathione Sepharose (Figure 2-20 A).

When employed in a chromatin-recruitment reaction with membrane-free extract an interesting picture emerged: Incubation with 9 μ M GST-AT hook or 2 μ M GST-rATH led to approximately equivalent amounts of GST moieties in the isolated chromatin pellets, indicating that the affinity of rATH for chromatin was higher than that of the AT hook alone. Moreover, the wild type GST-rATH and the mutated version bound to chromatin with equal intensity, establishing that the AT hook is not the only chromatin-targeting element in the C-terminus of MEL-28. Rasala *et al.* (2008) followed the same experimental strategy and drew the identical conclusion that the C-terminus of MEL-28 contains at least two chromatin binding motifs. This result could explain why the full length MEL-28 protein has a significantly higher affinity for chromatin than the AT hook alone and why a 50 fold excess of AT hook over the endogenous MEL-28 does not lead to inhibition of NPC assembly. Interestingly, these findings are in line with the more global conclusion by Aravind and Landsman (1997) that AT hooks appear to be an auxiliary protein motif that cooperates with other DNA-binding activities within a protein to achieve high binding activity, and may act as a versatile minor groove tether.

Strikingly, 2 μ M of our GST-rATH construct did not prevent chromatin binding of MEL-28, which is in contrast to the result by Gillespie *et al.* (2007). This difference can, however, be attributed to differences in the respective experimental setups. The rATH used by Gillespie *et al.* (2007) was prepared with a different *Xenopus laevis* MEL-28 clone (LOC397707) than the one we used for our experiments (see Cerstin Franz' thesis). The two resulting rATH constructs are 81% identical. In addition, the fragments carried different affinity tags (His₆ versus GST) and probing for MEL-28 was carried out with different antibodies against XI MEL-28. All of this variation could reconcile the differing results.

A basic method for assessing the features of proteins is to analyze the distribution of charges along their amino acid sequence. In cases such as MEL-28, with little or no structural information available, such analysis can serve as a guide to the protein's overall organization. Naturally, these results must be interpreted with care, however

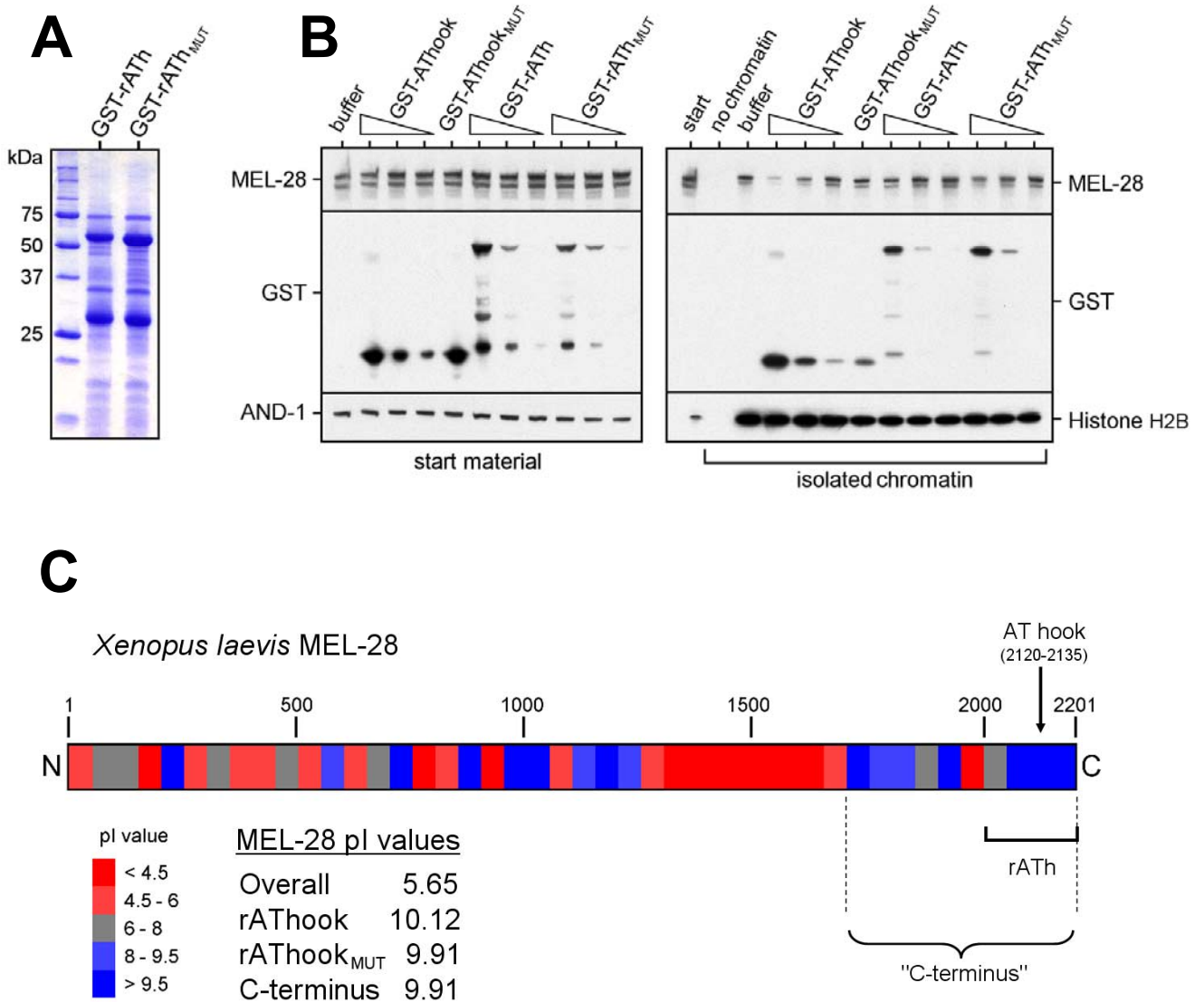


Figure 2-20. The C-terminus of MEL-28 contains at least one chromatin binding motif besides the AT hook. (A) Coomassie-stained SDS-PAGE gel of purified GST-rATh or GST-rATh_{MUT}. **(B)** Chromatin-recruitment assay from membrane-free extract. Cytosol was supplemented with GST-AT hook (36, 9 and 2 μ M final conc.), GST-AT hook_{MUT} (36 μ M final conc.), GST-rATh or GST-rATh_{MUT} (2, 0.5 and 0.12 μ M final conc. for both) and incubated with chromatin for 10 min. The chromatin templates were purified through a sucrose cushion, washed and analyzed by Western blotting. **(C)** Schematic representation of the XI MEL-28 protein showing the isoelectric point (pI) values of 50 amino acid increments along the entire protein sequence. The positions of the AT hook and the rATh fragment at the C-terminus are indicated.

analyzing the charge distribution along MEL-28 supports previous experimental results. Figure 2-20 C depicts a schematic plot of the isoelectric point (pI) values of 50 amino acid increments along the *Xenopus laevis* MEL-28 protein sequence. It is evident that positive charges cluster at the C-terminus of MEL-28. The average isoelectric point of the last 500 amino acids is 9.91. Similarly, the rATh possess a pI value of 10.12, while the average value for the full length protein is acidic (pI = 5.65). Interestingly, the mutated rATh also exhibits a highly basic pI value of 9.91, which could explain why it still strongly binds to chromatin. This argumentation is supported by structure prediction algorithms (see Materials and methods), all of which predict the entire C-terminal half of MEL-28 to be disordered. Based on this analysis MEL-28 possesses a positively charged 500 amino acid stretch at the C-terminus, which is likely accessible and could contain multiple chromatin binding sites.

2.1.17 MEL-28 binding to chromatin is regulated during the cell cycle

The NE undergoes dramatic changes during open mitosis. The discovery of MEL-28 as one of the key molecules for accurate postmitotic NPC formation in metazoa suggested that its function is regulated along with cell division. We began analyzing this important aspect by asking whether the two key functions of MEL-28, interaction with the Nup107-160 complex and chromatin binding, change during the cell cycle. Both questions can be readily addressed experimentally in the *Xenopus laevis* egg extract system by comparing MEL-28 activity in interphase and mitotic extracts.

In order to test for the stability of the MEL-28 and Nup107-160 complex interaction in interphase or mitosis, MEL-28 was immunoprecipitated from membrane-free extract of either cell cycle stage and the IP eluates were analyzed by Western blotting (Figure 2-21 A). In both cases similarly high amounts of Nup107 and Nup160 were detected along with precipitated MEL-28, suggesting that MEL-28 binding to the Nup107-160 complex is not altered and that both interact throughout the cell cycle. Interestingly, the amounts of Nup153 (lowest mAb414 band) detected by IP from interphase cytosol and presumably precipitated via the Nup107-160 complex (Vasu *et al.*, 2001), were significantly diminished upon IP from mitotic extract, indicating that this interaction might be regulated on progression from interphase to mitosis.

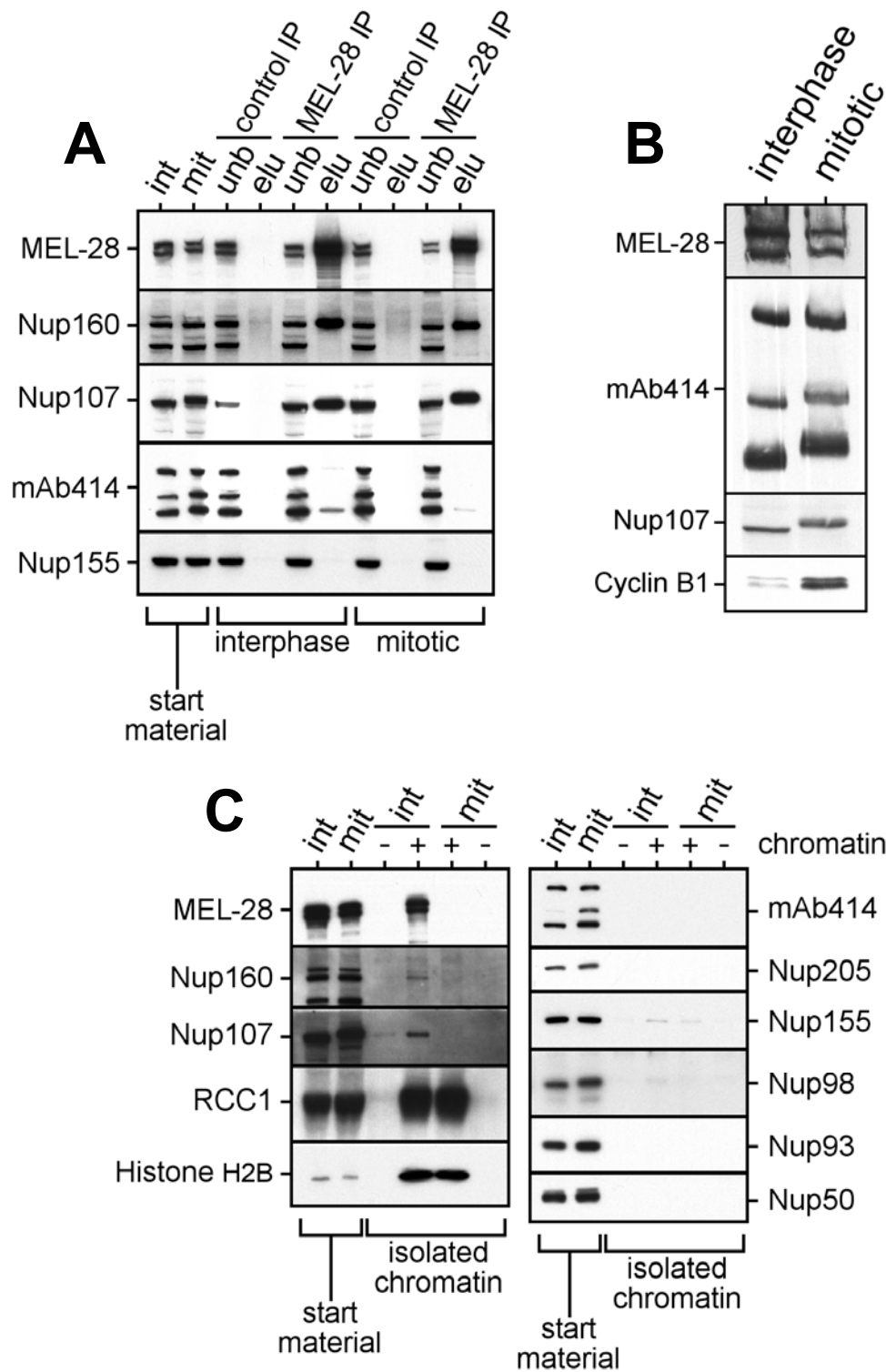


Figure 2-21. MEL-28 binding to chromatin is regulated during the cell cycle. (A) Immunoprecipitation of MEL-28 from membrane-free interphase (int) or mitotic (mit) *XI* egg extract. Eluates were analyzed by Western blotting. (B) The electrophoretic mobility of MEL-28 changes during the cell cycle. (See also (A).) Interphase and mitotic *XI* egg extract was separated by SDS-PAGE and analyzed by Western blotting. (C) Chromatin-recruitment experiment with membrane-free interphase (int) or mitotic (mit) cytosol. After 10 min of incubation with extract the chromatin templates were purified through a sucrose cushion, washed and analyzed by Western blotting.

A remarkably different picture emerged when we examined the regulation of MEL-28 binding to chromatin. Membrane-free interphase or mitotic cytosol was incubated with chromatin for 10 min. The chromatin templates were isolated through a sucrose cushion, washed and analyzed by Western blotting (Figure 2-21 C). MEL-28 and the Nup107-160 complex were recruited to chromatin from interphase extract but not from mitotic extract, indicating that NPC assembly is also regulated at the level of nup association with chromatin. This finding also supports the pre-pore hypothesis, which states that some nups begin to accumulate on chromatin during NPC assembly before the binding of ER membranes (Walther *et al.*, 2003b). At the same time, we did not detect other nups bound to chromatin in the absence of membranes either in interphase or mitotic extract. Differential chromatin binding of MEL-28 during the cell cycle was independently reported by Gillespie *et al.* (2007).

Mitotic phosphorylation has been demonstrated for many nups (Favreau *et al.*, 1996; Glavy *et al.*, 2007). A recent proteomic approach identified many previously unknown phosphorylation sites in proteins of the human mitotic spindle (Nousiainen *et al.*, 2006). Among them were sites in several nups and nine serine residues in human MEL-28, which are conserved in *Xenopus laevis* MEL-28. Comparing interphase and mitotic egg extract by Western blotting, we observed a shift in electrophoretic mobility for several nups including MEL-28 (Figure 2-21 B). It is therefore an attractive hypothesis that the mitotic regulation of MEL-28 binding to chromatin might be mediated by phosphorylation, which we will test in future experiments.

2.2 NET5 - a novel NE transmembrane protein

2.2.1 NET5 is a conserved transmembrane protein with a well defined domain organization

The *C. elegans* protein T24F1.2 and its human orthologue NET5 were identified as NE proteins in two independent studies (Gunsalus *et al.*, 2005; Schirmer *et al.*, 2003). Matyas Gorjanacz discovered that T24F1.2 genetically interacts with a specific subset of nups and we decided to analyze this molecule in greater detail. This project was performed in a collaboration with Matyas Gorjanacz, Nathalie Daigle and Rachel Mellwig.

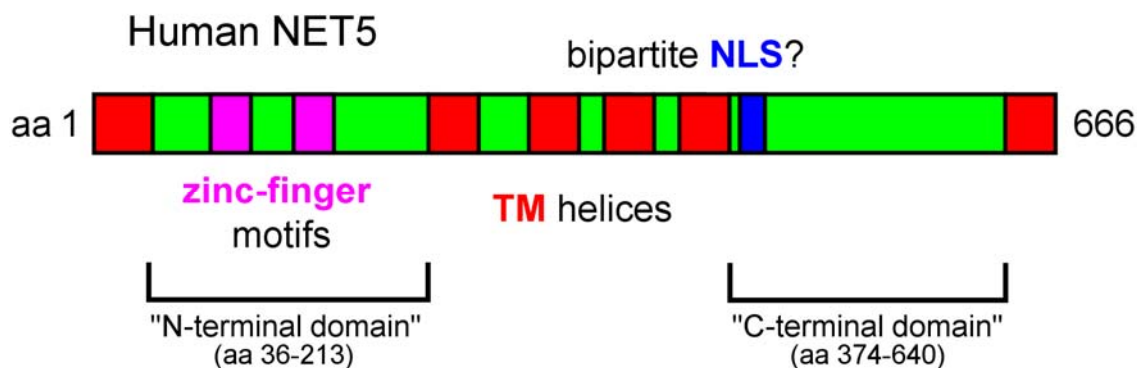


Figure 2-22. Topology of NET5. Predicted domains and motifs of human NET5 are highlighted.

T24F1.2/NET5 shows high conservation in metazoa, although a *Xenopus* orthologue has not yet been identified. According to computational prediction NET5 possesses six transmembrane helices and two larger luminal domains (Figure 2-22). Some prediction algorithms proposed that the first transmembrane helix might be a signal peptide, however our results (see Figure 2-27) and those of King *et al.* (2008) indicate that it is rather a membrane-adhering hydrophobic helix which is not removed during translation. The N- and C-terminal domains should therefore be exposed to the nucleoplasm or cytoplasm. The N-terminal domain is the most conserved part of NET5

and contains four pairs of highly conserved cysteines, which likely possess functional relevance. Bioinformatic predictions suggest they may form novel zinc finger motifs. The C-terminal domain contains a putative bipartite NLS. Human cells possess two additional predicted NET5 isoforms besides the full length 666 amino acid protein. The second isoform lacks the eighth exon, which results in a 23 amino acid deletion in the C-terminal domain, while a third shorter isoform lacks almost the entire C-terminal domain and differs from the full length protein in its last five amino acids (fragment aa 1-394 in Figure 2-27).

2.2.2 Human NET5 localizes to foci in the nuclear envelope

I cloned the full length human NET5 cDNA from isolated HeLa total RNA by means of RT-PCR. This construct served as a template for generating a GFP-tagged full length NET5 and fragments for expression in *E. coli* and raising polyclonal antibodies in rabbits. Despite significant efforts, attempts to generate antibodies against the N-terminal domain failed. The C-terminal domain suffered from severe degradation when expressed in *E. coli*, but could be purified as an N-terminally GST-tagged and C-terminally His₆-tagged protein in a two-step purification using first Ni-NTA agarose and second Glutathione Sepharose (Figure 2-23 A). The antibodies from two rabbits raised against the C-terminal domain were affinity purified using the antigen cross-linked to Sepharose. Both antibodies displayed a punctate staining in the plane of the NE when used for immunolabeling of HeLa cells and the same pattern was observed upon expressing the GFP-tagged full length NET5 protein (Figure 2-23 D). When followed through mitosis, NET5 exhibited dynamics typical of an NE membrane protein, becoming dispersed throughout the ER from prophase onwards and returning to the forming NE late in telophase (data not shown). The predicted molecular weight of human NET5 is 72 kDa. Interestingly, only one of the affinity purified anti-NET5 antibodies (number "2") recognized a band at the expected size when used for Western blotting on total HeLa cell lysate (Figure 2-23 B). Both antibodies detected a second lower band at 60 kDa, which does not correspond to any of the predicted isoforms and is thus considered an unspecific cross-reactivity. Antibody "2" detected an additional band at about 100 kDa in lysates of HeLa cells expressing GFP-tagged

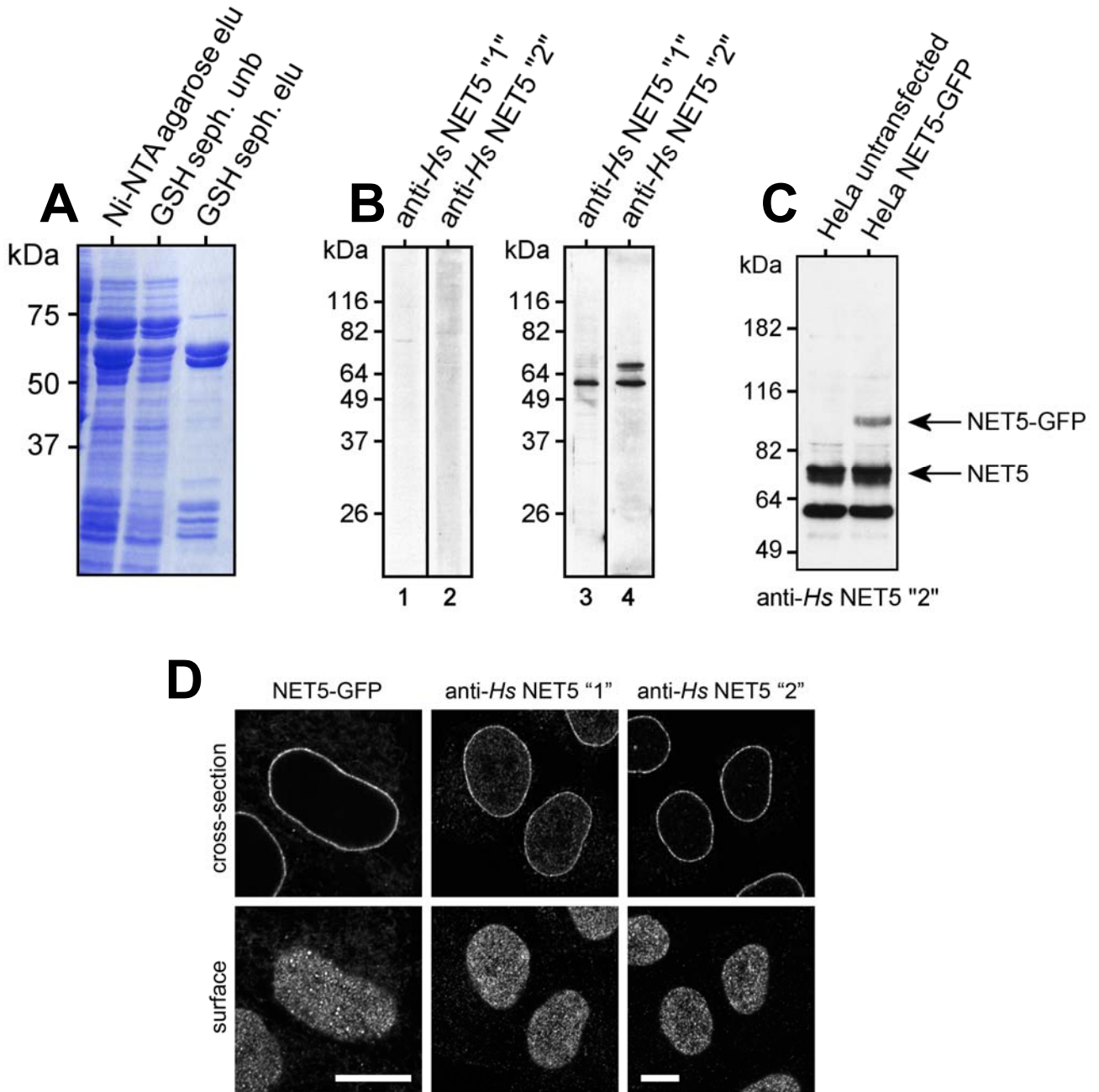


Figure 2-23. Human NET5 localizes to foci in the nuclear envelope. (A) Coomassie stained samples from the purification of the N-terminally GST- and C-terminally His₆-tagged C-terminal domain (aa 374-640) of human NET5. The protocol followed a 2-step purification using first Ni-NTA agarose and second Glutathione Sepharose. The final eluate was used to immunize rabbits. **(B)** Probing a HeLa cell lysate with pre-immune sera (lanes 1+2) or affinity purified antibodies (lanes 3+4) from two different rabbits corresponding to **(A)**. The predicted size of full length *Hs* NET5 is 72 kDa, which corresponds to the upper band in the anti-*Hs* NET5 "2" lane. **(C)** Western blot of untransfected HeLa cells or cells expressing a C-terminally GFP-tagged human NET5. Probing was with the second of the affinity purified anti-human NET5 antibodies from **(B)**. **(D)** Comparison of NET5-GFP localization in HeLa cells with antibody staining of endogenous NET5. All cells shown are fixed samples. Scale bars, 10 μ m. Staining and recording of the cells were performed by Nathalie Daigle.

full length NET5, demonstrating that it indeed recognizes NET5 in Western blotting (Figure 2-23 C). This additional band was not detected with antibodies against GFP, presumably because the amounts were very low. Additional proof that anti-NET5 antibody “2” recognizes the correct protein came from analyzing NET5 RNAi samples by Western blot (Figure 2-25 A).

The punctate localization pattern of NET5 was strongly reminiscent of nuclear pore staining. In order to test for co-localization we performed immunostaining with NET5 and NPC markers. Surprisingly, neither the anti-NET5 antibody staining with either antibody, nor the signal of NET5-GFP, co-localized with mAb414 labeling in the plane of the NE (Figure 2-24 A and data not shown) suggesting that the NET5 foci are structures distinct from nuclear pores. Figure 2-24 B depicts the qualitative assessment NET5 and mAb414 signal overlap along an arbitrarily chosen 10 μm path and illustrates that NET5 and mAb414 peaks rarely coincide.

Based on the light microscopy results, we decided to use both anti-NET5 antibodies after affinity purification for immunogold labeling of human cells. Rachel Mellwig labeled HeLa cells and confirmed that human NET5 localizes to the INM (data not shown). Interestingly, while staining with both antibodies gave identical results at the light microscopy levels, Rachel Mellwig found that gold particles were highly enriched at nuclear pores for the anti-NET5 antibody “1” (data not shown), the antibody which did not recognize full length NET5 in Western blotting. This finding is particularly intriguing because *C. elegans* T24F1.2 was also found at nuclear pores (Rachel Mellwig and Matyas Gorjanacz, personal communication).

In summary, NET5 localizes to foci in the NE which are distinct from nuclear pores at the light microscopy level. Immunogold labeling with an antibody against the C-terminus of NET5 suggests that a fraction of NET5 might specifically localize to nuclear pores. This interpretation, however, requires that this particular antibody recognizes only the native antigen and does not detect the denatured NET5 protein in Western blotting. We are currently examining the localization of NET5-GFP in HeLa cells with immunogold labeling and by probing for GFP in order to shed light on this interesting open question.

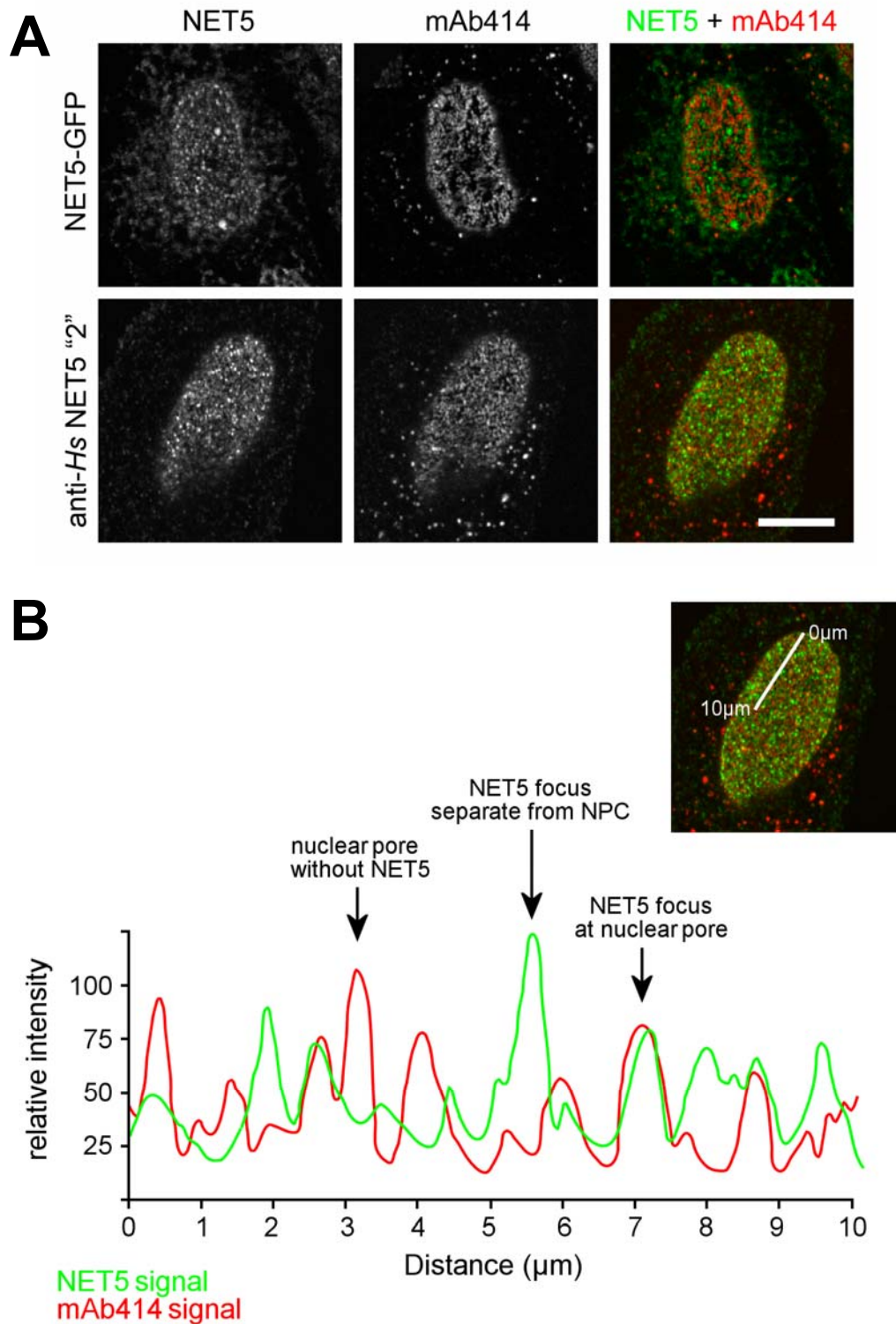


Figure 2-24. The NET5 foci are not identical to nuclear pores. (A) HeLa cells expressing NET5-GFP or wild type cells labeled with anti-NET5 antibodies were co-stained with mAb414. Scale bar, 10 μm . Staining and recording of the cells were carried out by Nathalie Daigle. **(B)** Qualitative assessment of NET5 and mAb414 colocalization along an arbitrarily chosen 10 μm path. The NET5 and mAb414 curves were recorded with the Carl Zeiss LSM software and smoothed manually. The white line in the insert illustrates the section of the NE along which the signals were recorded.

2.2.3 RNAi depletion of NET5 causes aberrant nuclear and cytoskeletal morphology and folding of the nuclear envelope

We wished to investigate the possible NE- and NPC-related role of NET5 by performing RNAi-mediated down-regulation of this novel NE protein. In total four different siRNA oligos against NET5 were used, two against sequences in the NET5 coding region and two against the 3'-UTR. Treatment with all four oligos reduced the amounts of NET5 in HeLa cell lysates after 48 h as judged by Western blotting with anti-NET5 antibody "2" (Figure 2-25 A). At the same time no significant loss of NET5 from RNAi-treated HeLa cells was detected by NET5 immunofluorescence (data not shown). This finding, together with the residual Western blotting signal, indicates that a fraction of NET5 persisted despite RNAi treatment. Initial difficulties to visualize the loss of NET5 at the protein level prompted us to perform qPCR to analyze whether the RNAi treatment reduced the amounts of NET5 mRNA. All four oligos caused a reduction in NET5 mRNA levels by 50-85% (data not shown), which is consistent with the decrease in NET5 observed in Western blotting. The qPCR analysis also suggested that NET5 mRNA levels in HeLa cells were orders of magnitude lower compared to the actin and GAPDH control mRNAs.

Loss of NET5 from human cells led to a complex phenotype. Nathalie Daigle investigated the NET5 RNAi phenotype induced with the oligos targeting the coding sequence by staining HeLa cells for NE markers (Figures 2-25 B and 2-26 A) and cytoskeletal proteins (Figure 2-26 B). Probing for the INM protein Emerin revealed that, in contrast to the spherical nuclei of control cells, NET5 RNAi-treated cells possessed a highly lobulated, irregular NE. The nuclear lamina appeared largely intact based on staining for Lap2 and Lamin B1, but displayed wide gaps through which chromatin seemed to bulge out of the nucleus. Taken together, these results demonstrate that NET5 is essential for nuclear integrity and that reduction of NET5 levels in HeLa cells affects nuclear organization at different levels. Besides these alterations in nuclear architecture, RNAi-treatment resulted in a dramatic rearrangement of the cytoskeleton (Figure 2-26 B). While the cytoplasm of control cells was filled with a fine interphase microtubule network, NET5 RNAi led to the formation of thick microtubule bundles which often surrounded the distorted nuclei.

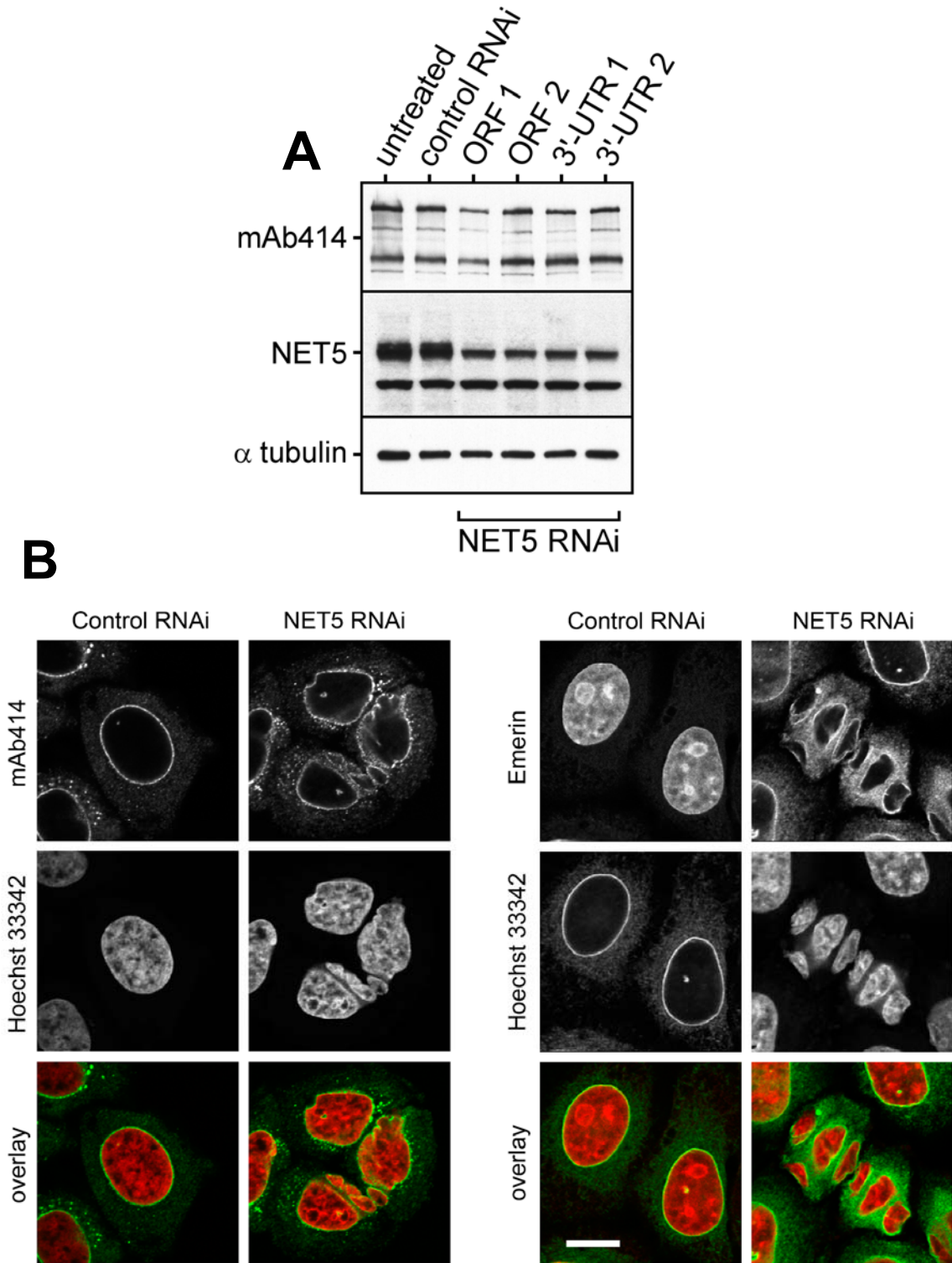


Figure 2-25. RNAi depletion of NET5 causes aberrant nuclear morphology and leads to invagination of the nuclear envelope. (A) Western blot analyzing total lysates of HeLa cells collected 48 h after transfection with different siRNA oligos. Two oligonucleotides target regions in the open reading frame of NET5, two are directed against the 3'UTR. Probing for NET5 was with anti-*Hs* NET5 "2". (B) Phenotypic characterization of the NET5 RNAi. HeLa cells were treated with a mixture of the two ORF siRNA oligos for 48 h, fixed and processed for immunostaining. Scale bar, 10 μ m. The RNAi experiment, labeling and recording of cells were carried out by Nathalie Daigle.

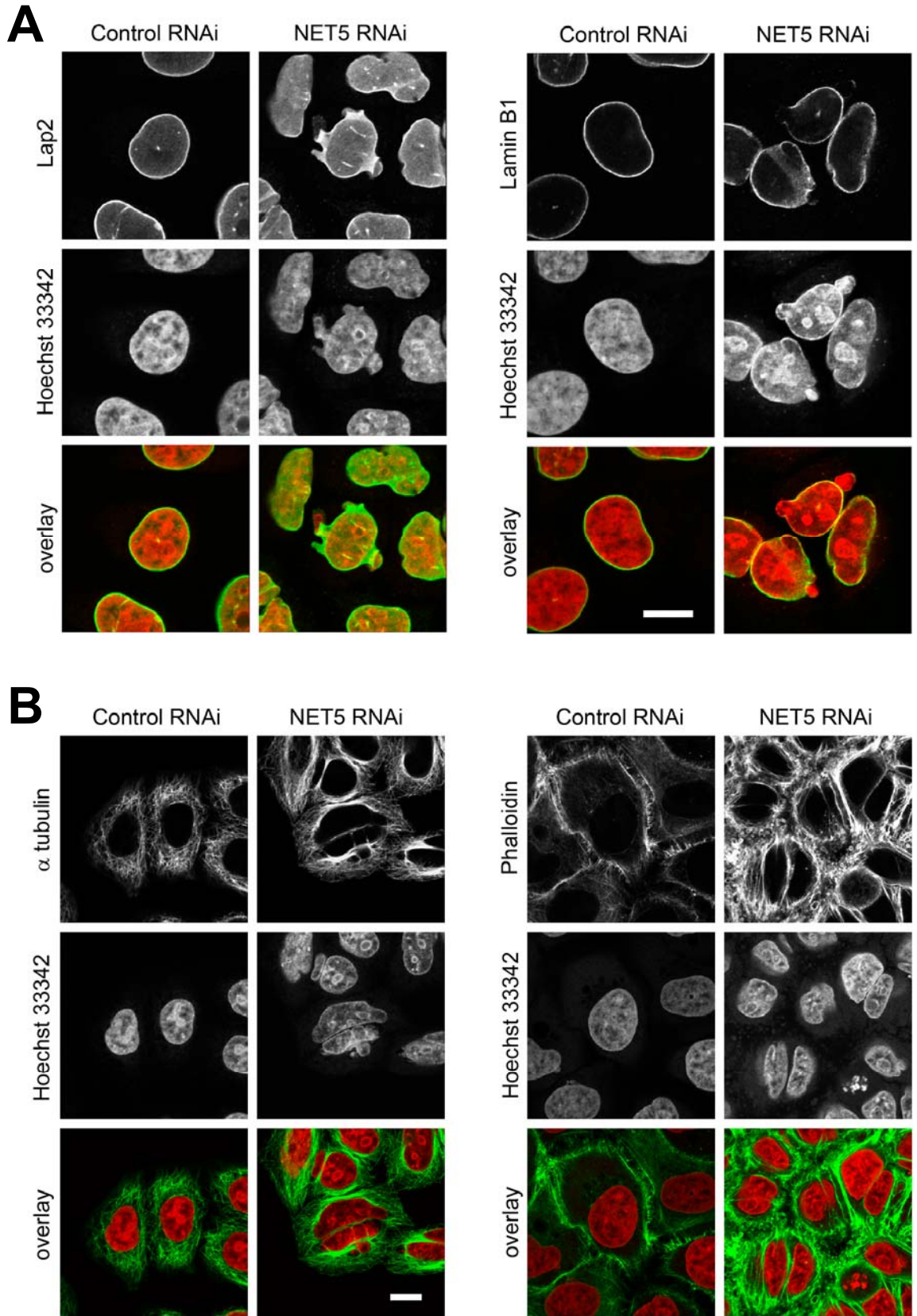


Figure 2-26. RNAi depletion of NET5 results in distortion of nuclear shape and perturbs cytoskeletal organization. (A+B) Characterization of the NET5 RNAi phenotype in HeLa cells. Cells were transfected with a mixture of the two ORF siRNA oligos for 48 h, fixed and stained for NE (A) or cytoskeleton markers (B). Scale bar, 10 μ m. The RNAi experiment, labeling and recording of cells were performed by Nathalie Daigle.

Labeling with phalloidin which binds to actin filaments revealed massive formation of actin cables upon NET5 RNAi treatment, which were reminiscent of stress fibers. Interestingly, the nuclei of NET5 RNAi-treated cells seemed to fall to the bottom of the cell (data not shown), suggesting that nuclear attachment to the microtubule cytoskeleton and nuclear positioning might be impaired. The oligos targeting the 3'-UTR induced a prometaphase arrest, eventually followed by cell death. We can hypothesize that the different phenotypes arise from the fact that the oligos against the 3'-UTR hit all three NET5 isoforms, whereas the ORF oligos should only affect isoforms including the C-terminal domain.

Taken together, RNAi knockdown of NET5 in HeLa cells leads to aberrant nuclear morphology indicative of a severe structural defect and to extensive disorganization of the cytoskeleton. The nuclear phenotype bears resemblance to the corresponding situation in *C. elegans*, where depletion of T24F1.2 results in NPC clustering and invagination of the NE membrane (Matyas Gorjanacz, personal communication). We are currently investigating the RNAi phenotypes in human cells and nematodes by transmission electron microscopy (TEM). It will be valuable for our understanding of NET5/T24F1.2 function to compare the observed defects in both systems at high resolution.

2.2.4 Mapping the sequence requirements for NET5 localization

NET5 possesses a well predicted topology. This allowed us to pursue a rational approach to map the requirements for NET5 localization and function in human cells. Based on the topology prediction displayed in Figure 2-22, I cloned several truncated NET5 protein fragments for expression with a C-terminal GFP-tag. Nathalie Daigle carried out the transfections into HeLa cells and recorded the localization patterns. Figure 2-27 schematically depicts the different fragments on the left side and shows corresponding typical localization on the right side.

Full length NET5 localized to foci in the NE and the first or last predicted transmembrane helices were dispensable for this localization (Figure 2-27, compare constructs 1-3). Removal of the C-terminal domain resulted in a smooth uniform

distribution of NET5 in the plane of the NE, which was not affected by the presence or absence of the putative NLS (constructs 4 and 5). The C-terminal domain is thus essential for targeting NET5 to the foci within the NE. Nathalie Daigle performed iFRAP experiments with full length NET5 and the aa 1-394 construct to determine the mobility of NET5 in the NE. While the half time for recovery was about 20 min for the full length protein, the shorter isoform was much more mobile with a half time roughly one order of magnitude lower (data not shown). We concluded that binding to foci renders NET5 largely immobile within the NE. Interestingly, the C-terminal domain was not sufficient for binding to NE foci, but localized throughout the cell (construct 6). This result also supports the notion that the putative NLS is not functional, since this construct should otherwise accumulate in the nucleus. Further shortening of NET5 defined amino acids 1-213 as the minimal construct for NE localization (construct 7). Interestingly, the first predicted transmembrane helix is required for NE targeting of the N-terminal domain alone (construct 8), although it is dispensable in the context of the full length protein. This finding suggests that the N-terminal domain bears binding sites for NE proteins, but requires the help of a hydrophobic membrane tether for NE targeting. To address the functional relevance of the conserved cysteine pairs in NET5, Nathalie Daigle mutated both residues of either the first or second cysteine pair to alanine (second pair shown as construct 9 in Figure 2-27). When expressed in HeLa cells, these constructs exhibited a strikingly different localization compared to wild type NET5. While a weak NE signal and some NE foci were still detectable, significant amounts of the mutated protein redistributed to the ER. This result establishes the importance of one of the cysteine pairs for NET5 localization and demonstrates that NET5 retention in the NE requires an intact N-terminal domain. Similar truncation constructs of T24F1.2 fused to GFP and expressed in *C. elegans* embryos showed analogous localization patterns, suggesting functional conservation of the NET5/T24F1.2 domains (Matyas Gorjanacz, personal communication).

In conclusion, we have dissected the basic requirements for NET5 localization by analyzing the expression of truncated or mutated variants in human cells. Targeting of NET5 to the NE mainly relies on the N-terminal domain, but requires an additional hydrophobic motif for adhesion to the NE membrane. Binding of NET5 to the NE foci is mediated by the C-terminal domain and leads to stable interaction of NET5 with

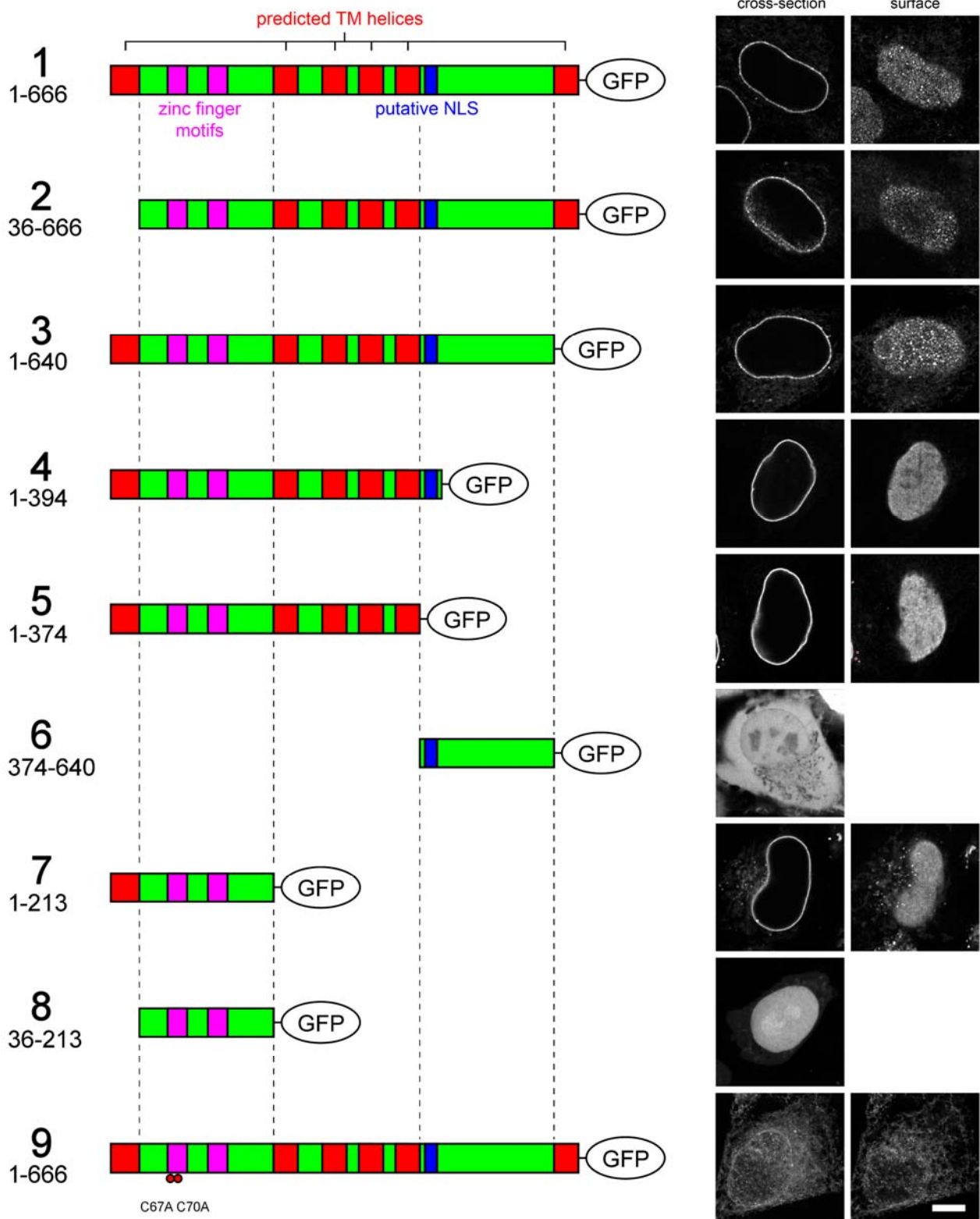


Figure 2-27. Mapping the requirements for NET5 localization. Truncated C-terminally GFP-tagged versions of human NET5 (schematically depicted on the left side) were transiently expressed in HeLa cells. The last construct is the full length protein, in which the first of the four conserved Cysteine pairs was mutated. The images on the right side show typical nuclei of live HeLa cells expressing the corresponding constructs from the left side. Scale bar, 10 μm. Transfection and recording of cells were performed by Nathalie Daigle.

these structures. Besides providing a solid foundation for the analysis of NET5 function at the NE, the truncated NET5-GFP constructs may serve as tools to perform rescue experiments following NET5 RNAi.

2.2.5 Additional approaches and experiments

In addition to the above experiments, we have pursued other experimental avenues to investigate the role of NET5 in nuclear organization. Biochemical approaches to affinity purify binding partners of NET5 have been hampered by difficulties in working with NET5 fragments in a recombinant form. I therefore prepared constructs of the N- and C-terminal domain for Yeast 2-Hybrid Screening, which was carried out by the group of Manfred Koegl at the German Cancer Research Center (DKFZ). While the C-terminal domain did not specifically interact with candidates upon raising the stringency of the Yeast 2-Hybrid assay, several candidate binding proteins were identified for the N-terminal domain. They are listed in Table 2-3.

Table 2-3 Candidate proteins for interaction with human NET5

Candidate protein	Gene ID
PDZ and LIM domain-containing protein 7 (enigma)	gi 33598968
nuclear factor of kappa light polypeptide gene enhancer in B-cells 1	gi 34577122
O-sialoglycoprotein endopeptidase;	gi 8923380
chromosome 10 open reading frame 30	gi 155029542 gi 155029544
centromere protein T	gi 126722969
polymerase (DNA directed) iota	gi 154350220
zinc finger protein 483	gi 190014620 gi 55741870
DEAD (Asp-Glu-Ala-Asp) box polypeptide 46	gi 41327773
ATP synthase, H ⁺ transporting, mitochondrial F0 complex, subunit B1	gi 21361565
bone morphogenetic protein 5	gi 10835091
kinectin 1 (kinesin receptor)	gi 33620775, gi 118498362, gi 118498368, gi 118498356
coiled-coil domain containing 57	gi 92091575, gi 25955524, gi 84040219
Ran GTPase, member RAS oncogene family	gi 5453555
RANBP2-like and GRIP domain containing 1	-
RAN binding protein 1	gi 4506407
RAN binding protein 2	gi 150418007

I will perform GST-pull down experiments from HeLa cell lysates with the purified C-terminal human NET5 domain. Analyzing the proteins bound to this bait might allow a better definition of the NE foci to which NET5 binds. IP experiments to identify NET5 binding partners are also planned, but might be complicated by the fact that NET5 is a transmembrane protein. We have received reagents for CenpT, one of the candidates from the Yeast 2-Hybrid list of NET5 interactors, from Manfred Koegl. Nathalie Daigle has examined the localization of human CenpT with the reagents, but could not establish an obvious connection to NET5, although the CenpT phenotype reported in the MitoCheck database is similar to the NET5 RNAi phenotype. Following up on some of the NET5 interacting candidate proteins and defining the mechanism of NET5 action promise to be interesting avenues of research in the future.

3 Discussion

The formation of NPCs in interphase and NE/NPC assembly at the end of mitosis are vital events in the life of a cell. This thesis represents a contribution to our understanding of nuclear assembly and provides a thorough investigation of the role of MEL-28 in this essential process. In addition, it contains an initial characterization of the novel NE transmembrane protein NET5.

3.1 MEL-28

3.1.1 MEL-28 is a conserved NPC/INM protein in metazoa

MEL-28 orthologues have been identified in a wide range of metazoa. MEL-28/ELYS is a large protein and its size is well conserved among organisms: *Homo sapiens* (2266 aa), *Mus musculus* (2243 aa), *Xenopus laevis* (2201 aa), *Danio rerio* (2527 aa), *Caenorhabditis elegans* (1784 aa). Human and mouse MEL-28 are 70% identical, the human and *Xenopus laevis* proteins 44% and human and *C. elegans* MEL-28 19%. The N-terminal halves of the proteins display a higher degree of sequence conservation and most analyzed MEL-28 proteins contain one or more AT hook motifs near their C-termini. Taken together, these results indicate that MEL-28 has an important conserved function in multicellular organisms, whose cells undergo open mitosis.

In *C. elegans*, *Xenopus laevis* and humans, MEL-28 is an NE protein in interphase and partly localizes to kinetochores during mitosis (Galy *et al.*, 2006; Franz *et al.*, 2007). Although comparable data from other organisms is not available, it is likely that this dynamic localization is conserved in all metazoa. Close investigation of MEL-28 localization by immunogold labeling and electron microscopy revealed that a significant proportion of MEL-28 is concentrated at nuclear pores in interphase in the three species listed above (Galy *et al.*, 2006 and Figure 2-3). In cultured vertebrate cells some MEL-28 localizes to the INM and a fraction of MEL-28 is nuclear in interphase. This data suggests that MEL-28 may function inside the nucleus, at the INM and at nuclear pores.

3.1.2 MEL-28 is essential for NPC formation

In vivo experiments from several model organisms and *in vitro* results using the *Xenopus laevis* egg extract nuclear assembly system have shown that MEL-28 has a role in NPC formation. The observation that homozygous MEL-28 knockout mice are not viable (Okita *et al.*, 2004) demonstrated that MEL-28 is required for an essential cellular process. RNAi-depletion or genetic mutation of MEL-28 led to severe structural nuclear defects in *C. elegans* (Galy *et al.*, 2006; Fernandez and Piano, 2006) and *Danio rerio* (Davuluri *et al.*, 2008 and de Jong-Curtain *et al.*, 2008). When examined by electron microscopy, MEL-28 deficient cells possessed fewer nuclear pores than control cells or no pores at all. RNAi-mediated MEL-28 knockdown in human cells resulted in loss of nups from the NE into the cytoplasm (Rasala *et al.*, 2006; Franz *et al.*, 2007), a result that is mirrored by the MEL-28 mutant zebrafish (Davuluri *et al.*, 2008). Interestingly, the NE membranes appeared intact in the RNAi-treated cells, suggesting that MEL-28 is specifically involved in NPC formation, but dispensable for organization of the nuclear membranes. This result is supported by TEM analysis of *in vitro* assembled MEL-28-free nuclei, which possessed an evenly spaced double NE membrane (Figure 2-8 C). MEL-28 RNAi *C. elegans* embryos displayed abnormal chromatin morphology and were deficient in several additional processes such as centrosome separation, kinetochore assembly and mitotic spindle formation (Fernandez and Piano, 2006). This finding, together with the observation that RNAi treatment in HeLa cells significantly increased the number of cells with cytokinesis defects (Rasala *et al.*, 2006), suggests that MEL-28 has additional functions in cell division.

3.1.3 MEL-28 interacts with the Nup107-160 complex

MEL-28 interacts with the Nup107-160 complex in *Xenopus laevis* egg extract and HeLa cells (Figure 2-9 and Rasala *et al.*, 2006). The intimate functional relationship between MEL-28 and this nup complex was already hinted at by the similar RNAi phenotypes in HeLa cells. In both cases, NPC assembly in the NE was impaired and annulate lamellae formed in the cytoplasm of the RNAi-treated cells (Figure 2-5 and Walther *et al.*, 2003a). In fact, MEL-28 and the Nup107-160 complex act together in

NPC formation, as discussed in more detail below. In order to better define the region in MEL-28 which mediates NE targeting, a series of GFP-tagged N- or C-terminally truncated MEL-28 fragments was generated. Examining their subcellular localization upon expression in HeLa cells revealed that amino acids 1007-1418 are sufficient to target MEL-28 to the NE (Figure 2-12). Whether this region directly binds to the Nup107-160 complex could not be assessed to date as I have not yet been successful in generating soluble recombinant MEL-28 sub-fragments, but we hope this issue can be addressed in future experiments with soluble MEL-28 fragments generated with the help of the ESPRIT method (Tarendeau *et al.*, 2007).

In addition to its role in NPC formation, the Nup107-160 complex has been reported to participate in mitotic spindle formation *in vitro* (Orjalo *et al.*, 2006) and to contribute to kinetochore function (Zuccolo *et al.*, 2007). MEL-28-Nup107-160 complex interaction persists during the cell cycle (Figure 2-21 A) and MEL-28 is required for targeting the Nup107-160 complex to kinetochores in human cells (Rasala *et al.*, 2006). Considering the mitotic phenotypes in *C. elegans* embryos depleted of MEL-28, it would be rewarding to examine whether depleting MEL-28 from mitotic *Xenopus laevis* egg extract affects mitotic spindle formation.

3.1.4 MEL-28 functions in postmitotic NPC formation by recruiting nucleoporins to chromatin

MEL-28 is essential for correct NPC formation in living cells. Studying the consequences of MEL-28 depletion on nuclear assembly in the *Xenopus laevis in vitro* system allowed us to specifically ask if MEL-28 has a role in postmitotic NPC formation. Since MEL-28-free extracts give rise to nuclei devoid of NPCs (Figure 2-8), MEL-28 is essential for NPC assembly at the end of mitosis. The Δ MEL-28 nuclei were surrounded by a closed NE membrane, but contained no nuclear pores (Figure 2-8). MEL-28 is therefore required for inserting nups into the NE in late anaphase/telophase. Interestingly, MEL-28 depletion causes the same *in vitro* nuclear assembly phenotype as depletion of the Nup107-160 complex (Walther *et al.*, 2003a), indicating that they act in the same pathway. Prior to my work, Nup107-160 complex binding to chromatin was the earliest described step in postmitotic NPC formation. The

result that MEL-28 is required for recruitment of the Nup107-160 complex to chromatin, but can bind to chromatin independently of this complex (Figure 2-11 C), places MEL-28 upstream of all previously studied nups, including the Nup107-160 complex. MEL-28 binding to chromatin is therefore the first identified event in NPC assembly at the end of mitosis. In addition, our data indicate that MEL-28 binds directly to chromatin (as discussed below). MEL-28 can be targeted to chromatin in the absence of membranes and recruit the Nup107-160 complex and Nup153 to chromatin under these conditions (Figure 2-13 C and Rasala *et al.*, 2008). This finding supports the pre-pore hypothesis, according to which a subset of NPC proteins initiates NPC assembly on chromatin independently of NE membrane targeting to the chromatin surface. Although both processes can be separated experimentally *in vitro*, they probably occur simultaneously *in vivo*. Our results specifically demonstrate that MEL-28 acts in postmitotic NPC assembly, but it is conceivable that it might carry out an analogous function in interphase. Interestingly, MEL-28 RNAi-treated human cells maintain a robust nuclear lamina staining (Figure 2-5 and Rasala *et al.*, 2006). We plan to investigate the potential involvement of MEL-28 in interphase NPC formation by performing additional experiments and with the help of a temperature-sensitive *C. elegans* mel-28 mutant strain now available in our lab.

Removal of MEL-28 from cells induces the formation of annulate lamellae (AL), cytoplasmic membrane stacks that contain NPCs (Figure 2-6). AL contain nups, but are free of MEL-28 (Figure 2-7 A and Rasala *et al.*, 2008). Interestingly, RanGTP-mediated AL formation was equally efficient in mock or MEL-28-depleted extract (Figure 2-7 B), demonstrating that MEL-28 is not required for NPC formation *per se*. This conclusion is also supported by the result that MEL-28 RNAi treatment in HeLa cells did not alter nup levels (Figure 2-5 A), but instead led to a significant redistribution of NPCs in the cell from the NE to AL. MEL-28 therefore appears to provide localization information and to direct NPC formation to the region of chromatin rather than to mediate the process of NPC assembly itself. Loss of MEL-28 nevertheless has severe consequences for cells, as they lose their ability to assemble NPCs in the right place, i.e. in the NE, which leads to cell death.

3.1.5 Recombinant MEL-28 rescues Nup107-160 complex binding to chromatin

In order to demonstrate that the observed depletion phenotype can be attributed specifically to MEL-28, *Xenopus laevis* MEL-28 was expressed in and purified from insect cells (Figure 2-14). Addition of the recombinant protein to depleted extracts rescued the recruitment of the Nup107-160 complex to chromatin, but did not support later steps of NPC assembly (Figure 2-15). The purified protein can therefore interact with the Nup107-160 complex and bind to chromatin, but does not allow completion of NPC formation. Either the recombinant MEL-28 is improperly folded when expressed in Hi5 cells, which might explain why it is degraded after 24h of expression, or it lacks a specific modification required for full activity. The rescue experiment generally suffered from the very low amounts of recombinant MEL-28 produced and the fact that the purified protein could not be concentrated without loss. MEL-28 is stable in egg extract, which suggests that it might need components in the extract and possibly binding partners, such as the Nup107-160 complex, for stability. The rescue of nup recruitment to chromatin in the absence of membranes can be performed with highly diluted extracts, whereas full nuclear assembly tolerates only very mild dilution. The purified material available for this work was not sufficiently active to support complete *in vitro* nuclear assembly following the harsh depletion procedure and dilution of the extract. Repeating the rescue experiments with more concentrated and possibly more active recombinant MEL-28 is highly desirable but could not be achieved.

3.1.6 The MEL-28 AT hook binds to chromatin and is important for NPC formation

Studying the detailed mechanism of MEL-28 function in NPC assembly was complicated by difficulties in predicting domains or motifs in the MEL-28 protein sequence and the unavailability of sufficient recombinant protein. The best experimental strategy, removing or mutating motifs, such as the predicted NLS or the AT hook, and testing their functional importance in the context of the full length protein was not feasible. We chose the next best approach by interfering with NPC formation with the aid of MEL-28 fragments. This series of experiments demonstrated that the MEL-28 AT hook binds to chromatin in nuclear assembly and that supplementing

extracts with high concentrations of purified GST-AT hook (36 μ M) leads to inhibition of NPC formation in a manner analogous to depletion of MEL-28. Binding of the AT hook to chromatin and inhibition of NPC formation were critically dependent on three basic residues in the AT hook which were previously shown to mediate DNA binding in other AT hooks (Figure 2-16 and 2-17 A and Aravind and Landsman, 1998). The inhibition of nuclear assembly with the help of an AT hook-containing MEL-28 fragment was independently reported by Gillespie *et al.* (2007) and Rasala *et al.*, (2008). Although these experiments do not directly prove the involvement of the MEL-28 AT hook in NPC assembly, they provide indirect evidence that it contributes to MEL-28 chromatin binding and thus probably participates in nuclear assembly. Interestingly, the AT hook is not the only chromatin binding motif in the positively charged C-terminus of MEL-28 (Figure 2-20 and Rasala *et al.*, 2008). It is therefore likely that two or more motifs cooperate in targeting MEL-28 to chromatin to achieve a higher binding affinity and thereby direct NPC formation to the chromatin surface. Identifying these additional chromatin binding motifs and assessing their relative contribution to the overall MEL-28 chromatin affinity are rewarding future experiments.

While Gillespie *et al.* (2007) and Rasala *et al.* (2008) observed displacement of endogenous MEL-28 from chromatin upon inhibition with C-terminal MEL-28 fragments at 2 μ M or 10 μ M, respectively, we found MEL-28 chromatin levels to be reduced in the presence of 36 μ M GST-AT hook. In addition to the different experimental conditions, MEL-28 clones and antibodies used, which might account for the differing results, the longer MEL-28 fragments employed by Gillespie *et al.*, (2007) and Rasala *et al.* (2008) may compete more efficiently with endogenous MEL-28 for chromatin binding. Our result demonstrates that reduction of MEL-28 amounts on chromatin below a certain threshold are sufficient to prevent NPC formation on chromatin. Interestingly, a significant amount of MEL-28 remained on chromatin in the presence of the AT hook and organized into an NE rim staining during the course of nuclear assembly. It is intriguing to ask what MEL-28 binds to in the NE membrane under these conditions.

In order to assess the specificity of NPC assembly inhibition by the AT hook construct, we conducted two additional experiments. First we estimated the concentration of

MEL-28 in egg extract and second evaluated the effect of AT hooks from unrelated proteins on nuclear assembly. We were astonished that a 16 amino acid fragment was able to interfere with the function of the 245 kDa protein MEL-28 and to inhibit the entire process of NPC formation (Figure 2-17). However, we estimated the concentration of MEL-28 in egg extract to be ≈ 75 nM (Figure 2-19). This made clear that an enormous (500-fold) excess over the endogenous MEL-28 was necessary for achieving the inhibition phenotype. Testing unrelated AT hooks for inhibition of nuclear assembly showed that the degree of inhibition correlates with the chromatin binding affinity of the AT hook (Figures 2-16 C and 2-17 C). In particular the HMGA 2 β AT hook bound strongly to chromatin and was more powerful in inhibiting NPC formation than the MEL-28 AT hook (Figures 2-17 A and 2-18 C). Therefore, inhibition of NPC assembly *in vitro* is not specific for the MEL-28 AT hook.

AT hooks are minor groove DNA binding motifs with a preference for AT-rich sequences. Rasala *et al.* (2008) carried out an elegant experiment, in which they sought to inhibit nuclear assembly with antibiotics that specifically bind to AT-rich or GC-rich DNA sequences. While the AT-binding Distamycin A phenocopied the AT hook inhibition, addition of the GC-binding Chromomycin A₃ did not affect nuclear assembly, indicating that MEL-28 indeed initiates NPC formation on chromatin by binding to AT-rich DNA sequences. Whether MEL-28 possesses DNA sequence specificity beyond AT-rich Vs GC-rich, is a question for future investigation.

In summary, supplementing nuclear assembly reactions with the MEL-28 AT hook fused to GST strongly inhibits NPC formation, thus recapitulating the MEL-28 depletion phenotype. AT hook construct binding to chromatin is essential for inhibiting NPC assembly, although a high excess of AT hook over endogenous MEL-28 is required and the inhibition is not specific for the MEL-28 AT hook. Direct MEL-28 binding to chromatin is therefore an essential step in postmitotic NPC assembly and NPC formation requires a certain minimal concentration of MEL-28 on chromatin.

3.1.7 Regulation of MEL-28 function by the GTPase Ran

Several important events of nuclear assembly have been shown to be regulated by the Ran GTPase system (Walther *et al.*, 2003b). Based on our experiments, we can add MEL-28 to the list of key factors whose activity is modulated by RanGTP. MEL-28 binding to chromatin was enhanced by RanGTP and slightly reduced by addition of importin β (Figure 2-13). Interestingly, the inactive Ran mutant T24N decreased mAb414 antigen binding to chromatin, but not MEL-28 recruitment, suggesting that MEL-28 can bind to chromatin independently of Ran (Figure 2-13B) even if inefficiently. Interestingly, the interaction of MEL-28 with the Nup107-160 complex was not affected by addition of RanQ69L (data not shown). Targeting of nups to chromatin critically depended on MEL-28, even in the presence of 20 μ M RanGTP (Figure 2-13 C). MEL-28 contains a predicted NLS motif and importins α and β were identified in the MEL-28 IP eluates (Figure 2-10). We are currently investigating whether MEL-28 binds directly to importins and whether such an interaction is relevant for nuclear assembly.

3.1.8 The function of MEL-28 is regulated during the cell cycle

The NE and NPCs undergo dramatic changes during the cell cycle, many of which arise as a consequence of posttranslational modification of NE and NPC components. We asked if the two main functions of MEL-28, interaction with a subset of nups and binding to chromatin, are regulated throughout the cell cycle by comparing the situations in interphase and mitotic *Xenopus laevis* egg extract. MEL-28 binding to the Nup107-160 complex was stable in both cell cycle stages (Figure 2-21 A). In contrast, recruitment of MEL-28 and the Nup107-160 complex to chromatin, which occurred readily in interphase extract, was abolished in mitotic extract (Figure 2-21 C). This result, combined with the observation that MEL-28 is phosphorylated in mitosis (Nousiainen *et al.*, 2006 and Figure 2-21 B), suggests that mitotic phosphorylation might regulate MEL-28 chromatin binding. It is conceivable that addition of phosphate residues might change the charge distribution in the C-terminus of MEL-28 and thereby alter its chromatin binding affinity. Whether additional proteins are involved in dissociating MEL-28 from chromatin is unknown. At the end of mitosis, phosphatases

could remove the phosphates and permit MEL-28 to bind to chromatin, thus initiating NPC formation on the segregated chromatids. It would be interesting to examine the consequences of MEL-28 dephosphorylation on chromatin binding and NPC assembly *in vitro* and to identify the kinases and phosphatases that modify MEL-28 in living cells.

In addition to its involvement in NPC formation, links between MEL-28 and other cellular processes are emerging. While MEL-28 at kinetochores might critically influence the assembly and function of the mitotic spindle, Gillespie *et al.* (2007) uncovered a functional connection between MEL-28 and the minichromosome maintenance (MCM) proteins. The Mcm protein complex, Mcm2-7, is the probable replicative helicase and is loaded onto chromatin in late mitosis and early G1 phase prior to NE formation and S phase entry. Loading of Mcm2-7 onto chromatin was required for timely MEL-28 targeting to chromatin and NPC formation, suggesting that the two important cellular events of licensing replication and NPC assembly are coordinated with one another. The fact that we did not identify Mcm proteins in our MEL-28 IP eluates suggests that MEL-28 does not bind directly to Mcm2-7 or that their interaction might only take place on chromatin, a conclusion supported by findings in Gillespie *et al.* (2007). In summary, MEL-28 is part of an emerging picture in which NPC formation is intimately connected to other cell cycle events.

3.1.9 Model for MEL-28 in postmitotic NPC formation

Based on the available information on MEL-28 function we can extend our model of postmitotic NPC assembly (Figure 3-1). In late anaphase/telophase mitotic kinase activity subsides and phosphatases can dephosphorylate cellular proteins, including NE and NPC components (step 1 in figure 3-1). Removal of phosphates from MEL-28 might render it competent for binding to chromatin. MEL-28 chromatin binding is mediated by the AT hook and additional motifs in the C-terminus. In the vicinity of decondensing chromatin, MEL-28 encounters a high local concentration of RanGTP, which might dissociate it from importin β , thereby enhancing its binding to chromatin (step 2). Our data suggest that MEL-28 binds to chromatin alone and then recruits the Nup107-160 complex (step 3) but we cannot exclude that MEL-28 and the Nup107-

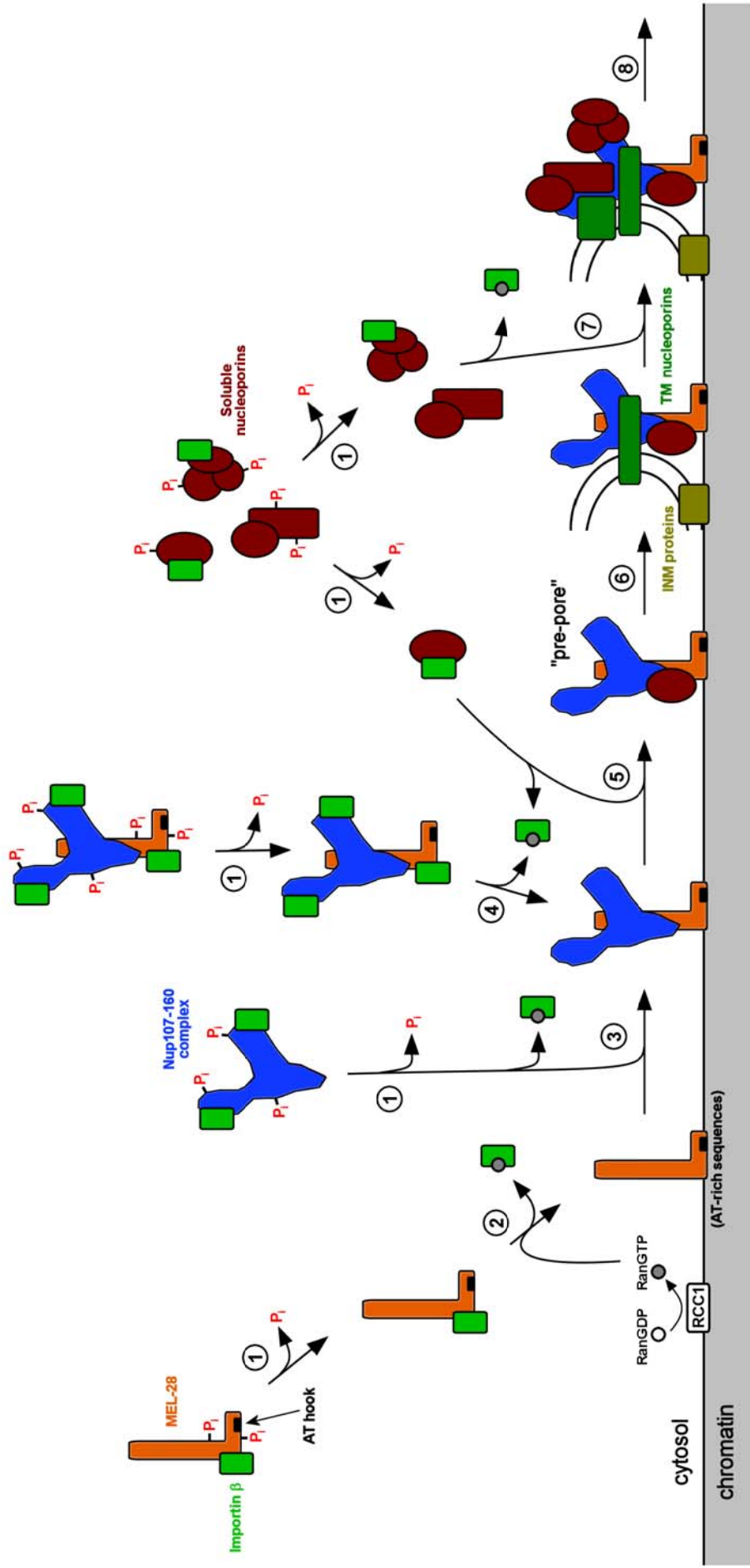


Figure 3-1. Model for early events in postmitotic NPC formation.
 An illustration of the mechanism described in detail in chapter 3.1.9.

160 complex are targeted to chromatin as one entity (step 4). Once this binding has occurred, MEL-28 and the Nup107-160 complex relocalize to foci on the chromatin surface and other nups, such as those recognized by mAb414, bind to them forming so-called pre-pores (step 5). Subsequent steps of NPC assembly require the presence of NE membranes and binding of integral membrane nups, such as Pom121 and Ndc1, to the nascent NPC (step 6). In the absence of the transmembrane nups, MEL-28 and the Nup107-160 complex prevent closure of the NE membranes (Antonin *et al.*, 2005), presumably a control mechanism which ensures accurate coordination of NPC formation with NE membrane assembly. Additional soluble nups join the forming NPC, some after being liberated from importin β by RanGTP close to chromatin (Walther *et al.*, 2003b, step 7). NPC formation is completed by addition of the cytoplasmic filaments and nuclear basket (step 8).

While regulation of its phosphorylation state may account for the temporal regulation of MEL-28 in NPC assembly, RanGTP is likely to contribute to its local control. MEL-28 appears to be directly regulated by Ran, but NPC assembly is modulated by RanGTP at multiple levels (Walther *et al.*, 2003b). MEL-28 anchors the forming NPC to chromatin during postmitotic NPC assembly.

It will be important, in the future, to integrate the contribution of individual factors to NE and NPC formation into a uniform assembly model and to elucidate the dynamic changes that nups undergo during NPC formation. In addition, we know comparatively little about the underlying regulatory mechanisms which govern nuclear assembly at the end of mitosis. The data in this thesis contribute to our mechanistic understanding of early events in postmitotic NPC formation and of how nups are targeted to chromatin during this process. It will be rewarding to closely examine the regulation of MEL-28 during the cell cycle and to investigate its involvement in cellular processes other than NPC formation.

3.2 NET5

3.2.1 NET5 is a conserved transmembrane protein of the INM

NET5/T24F1.2 is a novel transmembrane protein of the NE found in most eukaryotes. Its high degree of conservation suggests that it carries out an essential function. NET5 has six predicted transmembrane helices, a putative bipartite NLS and four highly conserved cysteine pairs in its N-terminal domain, which might form zinc finger motifs (Figure 2-22).

In cultured human cells NET5 is not evenly distributed in the plane of the NE, but localizes to foci (Figure 2-23 C) that are distinct from NPCs (Figure 2-24). It is currently unclear what the NET5-containing foci in the NE are, however we will address this question by performing immunoprecipitations against NET5 and GST-pulldown experiments with the C-terminal NET5 domain from HeLa cell lysates. According to immunogold labeling and electron microscopy NET5 localizes to the INM in HeLa cells and *C. elegans* and is enriched at nuclear pores in worm embryos. We are currently investigating whether human NET5 also partly localizes to NPCs, as this would have interesting implications for its function.

3.2.2 Specific domains mediate correct NET5 localization

The fact that NET5 domain topology can be predicted with confidence allowed us to systematically investigate the contribution of individual domains and motifs to its localization. This analysis demonstrated that the N-terminal domain (amino acids 1-213) is required for NET5 localization to the NE. The C-terminal domain targets NET5 to NE foci. The iFRAP experiments performed by Nathalie Daigle indicate that binding to foci largely immobilized NET5 in the NE, suggesting that the interaction formed by the C-terminal domain is a stable one. The C-terminal domain alone is, however, not sufficient for correct localization.

Based on the topological analysis of the *S.pombe* NET5 homologue, Ima1, by King *et al.* (2008), who concluded that the first predicted TM helix is a membrane-adhering motif and not a signal peptide, both NET5 domains should be either cytoplasmic or

nucleoplasmic. Our EM result that NET5 localizes to the INM in human cells and *C. elegans* embryos suggests that they face the inner side of the NE. Both domains might therefore interact with nuclear proteins, specific chromatin regions or the nucleoplasmic domains of other NE transmembrane proteins. In addition, our data suggest that the putative NLS in the C-terminus of NET5 is not functional, or at least not required for directing the short human NET5 isoform to the NE. Mutation of one pair of cysteines in the N-terminal domain led to redistribution of NET5 into the ER, demonstrating the importance of this protein motif for correct NET5 localization. These results provide a framework for assessing the domain requirements for NET5 localization and the available GFP-tagged fragments can also be used in future experiments to attempt rescue of the NET5 RNAi phenotype.

3.2.3 Loss of NET5 perturbs nuclear integrity

The *ima1* deletion phenotype in *S.pombe* and NET5/T24F1.2 RNAi phenotypes in human cells and *C. elegans* suggest a context in which NET5 might contribute to nuclear architecture and function. Loss of Ima1 from fission yeast cells and reduction of NET5 levels in human cells lead to similar phenotypes (King *et al.*, 2008 and Figures 2-25 and 2-26). *ima1* Δ cells display severe NE deformations and loss of spherical nuclear shape, while NET5 RNAi-treated HeLa cells have a highly lobulated and distorted NE. Deletion of *ima1* renders nuclei increasingly sensitive to microtubule-dependent forces and results in fragmentation of the MTOC attachment site at the NE (King *et al.*, 2008). HeLa cells with reduced amounts of NET5 display a dramatic reorganization of their microtubule cytoskeleton and their nuclei are no longer centrally located but instead sink to the bottom of the cells. These results demonstrate that NET5 plays a role in physically stabilizing the NE and might link the nucleus to the microtubule cytoskeleton. The observation that the *S.pombe* nup cut11 accumulates in cytoplasmic foci in *ima1* Δ cells and the fact that NPCs appear to cluster in the NE in T24F1.2 RNAi-treated *C. elegans* embryos indicate that NET5 might also influence the NPC distribution in the NE.

Another intriguing finding was that some NET5 RNAi-treated HeLa cells had large chromatin protrusions bulging out of their nuclei. These extensions seemed to

penetrate the NE through holes in the nuclear lamina (Figure 2-26 A). Accordingly, NET5 might contribute to chromatin organization or be required for confining chromatin to the nuclear compartment. King *et al.* (2008) report that the inner centromeric region is bound by Ima1 and preventing the heterochromatin-specific H3K9 methylation results in mislocalization of Ima1. In *S.pombe*, centromeres are positioned adjacent to the SPB attachment site at the NE (Funabiki *et al.*, 1993), indicating a connection between chromatin and the cytoskeleton, for which Ima1 might be essential. Whether NET5 carries out an analogous function in human cells remains to be determined, but the identification of the centromere protein T in our Yeast 2-Hybrid approach suggests that NET5 might indeed be linked to heterochromatin. It will therefore be important to examine the behavior of centromere markers in the NET5 RNAi-treated cells.

ima1 deletion leads to separation of the *S.pombe* SUN and KASH proteins Sad1 and Ksm2, which usually co-localize at the MTOC attachment site. Together with the finding that Sad1 dissociates from the centromere in *ima1* Δ cells, it is tempting to speculate that the NET5 foci in the NE of human cells might contain SUN proteins. Human Sun2 has been reported to localize to the NE in a punctuate pattern similar to NET5 (Liu *et al.*, 2007) and SUN proteins are involved in anchoring the nucleus to the cytoskeleton, which appears defective in NET5 RNAi-treated HeLa cells. RNAi against T24F1.2 did not affect the localization of Matefin, the *C. elegans* Sun orthologue, any *C. elegans* KASH domain protein, or *vice versa* (Matyas Gorjanacz, personal communication). It will nevertheless be interesting to examine if NET5 is functionally linked to SUN- or KASH-proteins in human cells.

Our RNAi experiments suggest that NET5 is not directly involved in postmitotic NE or NPC assembly. The fact that we could not identify a NET5 *Xenopus* orthologue, presumably because sequencing of the *Xenopus* genome is not complete, prevented us from analyzing a potential role of NET5 in nuclear assembly *in vitro*. In the future it will be important to investigate whether NET5-deficient cells encounter problems during cell division, if they display abnormalities in assembling the NE and NPCs at the end of mitosis, or whether the observed phenotype develops in interphase.

3.2.4 Future perspectives regarding NET5

A difficulty with the present NET5 results is the uncertainty surrounding the RNAi phenotypes generated by different siRNAs. NET5 RNAi treatment did not visibly decrease the NET5 signal in HeLa cells as judged by immunofluorescence (data not shown), suggesting that a significant fraction of NET5 has a low turnover. This is in contrast to the situation in *C. elegans* embryos, where RNAi treatment efficiently depletes T24F1.2 (Matyas Gorjanacz, personal communication). However, Western blotting of total lysates of RNAi-treated cells revealed a similar reduction of a band at the predicted size of full length NET5 with all four siRNA oligos (Figure 2-25 A). Whether the remaining signal corresponds to stable NET5 or represents an unspecific cross-reacting band is a question we will attempt to answer in the near future. It will be important to determine which NET5 isoforms are expressed in HeLa cells and to examine the specificity of the RNAi phenotype by performing rescue experiments with RNAi-resistant NET5 constructs.

Our longer term plan is to identify NET5 binding partners by means of biochemical methods and to characterize their functional relationship with NET5. In parallel we will investigate the NET5 binding candidate proteins from the Yeast 2-Hybrid approach, in particular LMO7, the Ran GTPase, RanBP1 and RanBP2. By following different experimental approaches we hope to be able to determine in more detail the mechanism by which NET5 contributes to nuclear organization.

4 Materials and methods

4.1 Materials

4.1.1 Chemicals and reagents

Acetic acid	Merck (Darmstadt, Germany)
Acetone	Merck (Darmstadt, Germany)
30% Acrylamide/bisacrylamide solution, 37.5:1	Bio-Rad (München, Germany)
Adenosine 5'-triphosphate (ATP)	Sigma-Aldrich (Steinheim, Germany)
Agar-agar	Serva (Heidelberg, Germany)
Agarose	Invitrogen (Karlsruhe, Germany)
Alexa Fluor®-coupled secondary antibodies	Invitrogen (Karlsruhe, Germany)
Ampicillin	Grünenthal (Aachen, Germany)
Ammonium chloride	Merck (Darmstadt, Germany)
Ammonium sulfate	Gibco BRL (Eggstein, Germany)
Ammonium peroxodisulfate	Sigma-Aldrich (Steinheim, Germany)
Bacto tryptone	Difco (Detroit, USA)
Bacto yeast extract	Difco (Detroit, USA)
Bench Mark™ Prestained Protein Ladder	Invitrogen (Karlsruhe, Germany)
Bovine serum albumin (BSA)	Sigma-Aldrich (Steinheim, Germany)
Bromophenol blue (3',3'',5',5''-tetrabromophenolsulfonephthalein)	Sigma-Aldrich (Steinheim, Germany)
Calcium chlorid	Merck (Darmstadt, Germany)
Chloramphenicol	Sigma-Aldrich (Steinheim, Germany)
CNBr-activated Sepharose™ 4B	Amersham Biosciences (Braunschweig, Germany)
Complete™ EDTA-free Protease Inhibitor Cocktail (use 1 tablet per 25 ml buffer)	Roche (Mannheim, Germany)
Coomassie brilliant blue G-250	Sigma-Aldrich (Steinheim, Germany)
Creatine phosphate	Roche (Mannheim, Germany)
Cycloheximid (3-(2-(3,5-dimethyl 2-oxocyclohexyl) 2-hydroxyethyl)glutarimide)	Sigma-Aldrich (Steinheim, Germany)
L-Cysteine	Merck (Darmstadt, Germany)
Cytochalasin D	Sigma-Aldrich (Steinheim, Germany)
4',6-Diamidino 2-phenylindole (DAPI)	Sigma-Aldrich (Steinheim, Germany)
Deoxynucleotides (dNTPs) 100mM	Fermentas (St. Leon-Rot, Germany)
Digitonin	Sigma-Aldrich (Steinheim, Germany)
1-(4,5-Dimethoxy 2-nitrophenyl)ethyl ester (A23187)	Invitrogen (Karlsruhe, Germany)
Dimethyl pimelimidate	Sigma-Aldrich (Steinheim, Germany)
Dimethyl sulfoxid (DMSO)	Merck (Darmstadt, Germany)
100bp DNA ladder	New England Biolabs (Ipswich, USA)
1kb DNA ladder	New England Biolabs (Ipswich, USA)
DNA oligonucleotides	MWG Biotech (Ebersberg, Germany)
DNA Polymerase I, Large (Klenow) Fragment	New England Biolabs (Ipswich, USA)
DNase I	Roche (Mannheim, Germany)
1,1'-Diocadecyl-3,3,3',3'-tetramethylindocarbocyanine perchlorate (DiIC ₁₈)	Invitrogen (Karlsruhe, Germany)
1,4-Dithio-L-threitol (DTT)	Merck (Darmstadt, Germany)
Dulbecco modified Eagle's medium (DMEM)	Invitrogen (Karlsruhe, Germany)
ECL™ anti-rabbit IgG Horseradishperoxidase linked whole antibody (from donkey)	Amersham Biosciences (Braunschweig, Germany)

ECLTM anti-mouse IgG, Horseradishperoxidase linked whole antibody (from sheep)	Amersham Biosciences (Braunschweig, Germany)
Epon	Roth (Karlsruhe, Germany)
Ethanol	Merck (Darmstadt, Germany)
Ethanolamine	Sima-Aldrich (Steinheim, Germany)
Ethidium bromide	Serva (Heidelberg, Germany)
Ethylenediamine-N,N,N',N'-tetraacetic acid (EDTA)	Sigma-Aldrich (Steinheim, Germany)
Ethylene glycol-bis(2-aminoethylether)-N,N,N',N'-tetraacetic acid (EGTA)	Sima-Aldrich (Steinheim, Germany)
Fetal calf serum (FCS)	PAA Laboratories (Cölbe, Germany)
Formvar	Serva (Heidelberg, Germany)
Fugene 6 transfection reagent	Roche (Mannheim, Germany)
L-Glutamine	Invitrogen (Karlsruhe, Germany)
Glutaraldehyde (50% aqueous solution)	Sigma-Aldrich (Steinheim, Germany)
Glutathione	Sigma-Aldrich (Steinheim, Germany)
Glutathione Sepharose 4 Fast Flow	Amersham Biosciences (Braunschweig, Germany)
Glycerol (87% aqueous solution)	Merck (Darmstadt, Germany)
Glycine	Merck (Darmstadt, Germany)
Glycogen (source: oyster, used at 200 mg/ml)	Amersham Biosciences (Braunschweig, Germany)
Guanosine 5'-diphosphate (GDP)	Sigma-Aldrich (Steinheim, Germany)
Guanosine 5'-triphosphate (GTP)	Merck (Darmstadt, Germany)
HeLa nuclear extract	Cilbiotech (Mons, Belgium)
HiPerFect Transfection Reagent	QIAGEN (Hilden, Germany)
Hoechst 33342	Sigma-Aldrich (Steinheim, Germany)
Hydrochloric acid, 37% (HCl)	Merck (Darmstadt, Germany)
Human chorionic gonadotropin (hCG)	Sigma-Aldrich (Steinheim, Germany)
4-(2-Hydroxyethyl)piperazine-1-ethansulfonic acid (HEPES)	Sigma-Aldrich (Steinheim, Germany)
Igepal CA-630 (NP-40)	Sigma-Aldrich (Steinheim, Germany)
Imidazole	Sigma-Aldrich (Steinheim, Germany)
Immersion oil	Leica (Heidelberg, Germany)
Intergonan (PMSG)	Intervet (Unterschleißheim, Germany)
Isopropyl β -D-thiogalactopyranoside (IPTG)	Sigma-Aldrich (Steinheim, Germany)
Kanamycin	Serva (Heidelberg, Germany)
Magnesium chloride	Merck (Darmstadt, Germany)
Magnesium acetate	Merck (Darmstadt, Germany)
Manganese chloride	Sigma-Aldrich (Steinheim, Germany)
2-Mercaptoethanol	Sigma-Aldrich (Steinheim, Germany)
Methanol	Merck (Darmstadt, Germany)
Microcystin LR	Sigma-Aldrich (Steinheim, Germany)
Milk powder	Frema Reform (Lüneburg, Germany)
3-(N-Morpholino)propanesulfonic acid, 4-Morpholinepropanesulfonic acid (MOPS)	Sigma-Aldrich (Steinheim, Germany)
Nail polish P2	Palmers Textil AG (Vienna, Austria)
Ni-NTA agarose	QIAGEN (Hilden, Germany)
OptiMEM	Invitrogen (Karlsruhe, Germany)
Osmium tetroxide	Serva (Heidelberg, Germany)
Paraformaldehyde, 16% solution	Electron Microscopy Sciences (Hatfield, USA)
Penicillin/Streptomycin	Sigma-Aldrich (Steinheim, Germany)
Pfu turbo polymerase	Stratagene (La Jolla, USA)

Piperazine 1,4-bis(2-ethanesulfonic acid) (PIPES)	
Phenylmethylsulfonyl fluoride (PMSF)	Sigma-Aldrich (Steinheim, Germany)
2-Phosphoglycerol	Sigma-Aldrich (Steinheim, Germany)
Polyethylene glycol 4000	Sigma-Aldrich (Steinheim, Germany)
Poly-L-Lysine solution	Roth (Karlsruhe, Germany)
Polyvinylpyrrolidon	Sigma-Aldrich (Steinheim, Germany)
Ponceau S	Merck (Darmstadt, Germany)
Potassium acetate	Sigma-Aldrich (Steinheim, Germany)
Potassium chloride	Merck (Darmstadt, Germany)
Potassium hydroxide	Merck (Darmstadt, Germany)
Precision Plus Protein Standards	Sigma-Aldrich (Steinheim, Germany)
2-Propanol	Bio-Rad (München, Germany)
Protein A Gold	Merck (Darmstadt, Germany)
Protein A Sepharose TM CL-4B	Cell Microscopy Center (University Medical Center, Utrecht, The Netherlands)
Protein Assay	Amersham Biosciences (Braunschweig, Germany)
Protein Molecular Weight Standards	Bio-Rad (München, Germany)
QIAGEN Plasmid Maxi Kit	Amersham Biosciences (Braunschweig, Germany)
QIAGEN Plasmid Midi Kit	QIAGEN (Hilden, Germany)
QIAprep Spin Miniprep Kit	QIAGEN (Hilden, Germany)
QIAquick Gel Extraction Kit	QIAGEN (Hilden, Germany)
QIAquick PCR Purification Kit	QIAGEN (Hilden, Germany)
Restriction enzymes	QIAGEN (Hilden, Germany)
RNAseH	New England Biolabs (Ipswich, USA)
RNeasy Mini kit	Invitrogen (Karlsruhe, Germany)
Shrimp alkaline phosphatase (SAP)	QIAGEN (Hilden, Germany)
Silver nitrate	USB Corporation (Cleveland, USA)
siRNA oligonucleotides	Sigma-Aldrich (Steinheim, Germany)
Sodium azide	Dharmacon (Lafayette, USA)
Sodium cacodylate	Sigma-Aldrich (Steinheim, Germany)
Sodium chloride	Sigma-Aldrich (Steinheim, Germany)
Sodium dodecylsulfate	Merck (Darmstadt, Germany)
Sodium hydroxide	Serva (Heidelberg, Germany)
Sodium thiosulfat	Sigma-Aldrich (Steinheim, Germany)
Spermidine tetrachloride	Merck (Darmstadt, Germany)
Spermine	Sigma-Aldrich (Steinheim, Germany)
Sucrose	Sigma-Aldrich (Steinheim, Germany)
SuperScript II reverse transcriptase	USB Corporation (Cleveland, USA)
SYBR Green PCR master mix	Invitrogen (Karlsruhe, Germany)
T4-DNA ligase	Applied Biosystems (Foster City, USA)
Taq polymerase	New England Biolabs (Ipswich, USA)
N,N,N',N'-Tetramethylethylenediamine (TEMED)	Roche (Mannheim, Germany)
Titer Max Gold adjuvant	Sigma-Aldrich (Steinheim, Germany)
Tris(hydroxymethyl)amino methane (Tris)	Sigma-Aldrich (Steinheim, Germany)
Triton X-100	Sigma-Aldrich (Steinheim, Germany)
Trypsin EDTA 1x GibcoTM	Sigma-Aldrich (Steinheim, Germany)
Tween®-20, Sigma-Ultra	Invitrogen (Karlsruhe, Germany)
Uranyl acetate	Sigma-Aldrich (Steinheim, Germany)
Vectashield® mounting medium H-1000	Serva (Heidelberg, Germany)
Western Lightning™ Chemiluminescence reagent	Vector Laboratories (Grünberg, Germany)

Perkin Elmer Life Science (Boston, USA)

4.1.2 Commonly used buffers, solutions and media

AB (acetate buffer)	20 mM HEPES, pH 7.4 100 mM KOAc 3 mM KCl 50 mM EGTA 150 mM Sucrose
Coomassie staining for SDS-PAGE gels	0.2% (w/v) Coomassie brilliant blue 40% (v/v) Methanol 10% (v/v) Acetic acid
Coomassie destain solution	40% (v/v) Methanol 10% (v/v) Acetic acid
Cysteine buffer	2% (w/v) Cysteine in 0.25x MMR adjusted to pH 7.8 with NaOH
DMEM + Glucose	DMEM medium 44 mM NaHCO ₃ 17 mM Glucose
6x DNA loading buffer	0.25% (w/v) Bromphenol blue 0.25% (w/v) Xylene cyanol FF 40% (w/v) Sucrose in H ₂ O
50x Energy mix	500 mM Creatine phosphate 25 mM GTP 25 mM ATP 2.5 mg/ml Creatine kinase
LB-agar (autoclaved)	1.5% (w/v) Bacto agar in LB medium
LB-medium (autoclaved)	1% (w/v) Bacto tryptone 0.5% (w/v) Bacto yeast extract 170 mM NaCl adjusted to pH 7.6 with NaOH
MMR buffer	50 mM HEPES, pH 7.9 100 mM NaCl 10 mM MgCl ₂ 20 mM CaCl ₂ 1 mM EDTA
PBS (phosphate buffered saline)	130 mM NaCl 100 mM Na ₂ HPO ₄ , pH 7.0

S250 buffer	20 mM HEPES, pH 7.5 250 mM Sucrose 50 mM KCl 2.5 mM MgCl ₂
S500 buffer	500 mM Sucrose 20 mM HEPES, pH 7.5 50 mM KCl 2.5 mM MgCl ₂
1x SDS-loading buffer	10% (v/v) Glycerol 50 mM Tris, pH 6.8 10% (w/v) SDS 1 mM DTT 0.1% (w/v) Bromphenol blue
SDS running buffer	25 mM Tris 192 mM Glycine 0.1% (w/v) SDS
Viki-fix	80 mM Pipes pH 6.8 1 mM MgCl ₂ 150 mM Sucrose 0.5% (v/v) Glutaraldehyde 2% (w/v) Paraformaldehyde
Wet blot transfer buffer	25 mM Tris 200 mM Glycine 10% (v/v) Methanol

4.1.3 Materials

0.2 ml reaction tubes (Thermo Tube™)	PEQlab (Erlangen, Germany)
0.5 ml micro tubes	Sarstedt (Nümbrecht, Germany)
1.5 ml reaction tubes	Eppendorf (Hamburg, Germany)
10 ml chromatography columns	Bio-Rad (München, Germany)
6-well or 24-well plates	Nunc (Wiesbaden, Germany)
Bottle top filters, 0.22 µm pore size	Millipore (Schwalbach, Germany)
Coverslips (11 mm diameter)	Nunc (Wiesbaden, Germany)
Homogenizer 2 ml and 40 ml, Pestle B	Kontes Glass, Co (Vineland, USA)
Filter paper	Whatman (Dassel, Germany)
General glass ware	Schott (Jena, Germany)
General plastic ware	Nunc (Wiesbaden, Germany)
Gloves (Latex or Nitrile)	Kimberley-Clark (Mainz, Germany)
KODAK BioMax MR Film	Sigma-Aldrich (Steinheim, Germany)
Lab-Tek	Nunc (Wiesbaden, Germany)
MoBiCol	MoBiTec (Göttingen, Germany)
Microlance™ sterile needles	Becton Dickinson (Heidelberg, Germany)

Microscope slides	Nunc (Wiesbaden, Germany)
Neubauer chamber	LO-Laboroptik (Friedrichsdorf, Germany)
NuPAGE 4-12% Bis-Tris gels	Invitrogen (Karlsruhe, Germany)
Parafilm	Pechiney Plastic Packaging (Chicago, USA)
Plastic cuvettes	Nunc (Wiesbaden, Germany)
Protran nitrocellulose membrane	Perkin Elmer Life Science (Boston, USA)
SDS-PAGE Minigel system	Bio-Rad (München, Germany)
Spectra/Por Membrane	Carl Roth (Karlsruhe, Germany)
Syringes	Becton Dickinson (Heidelberg, Germany)
Ultracentrifuge tubes	Beckman (Krefeld, Germany)

4.1.4 Instruments

Centrifuges:

Heraeus Megafuge 1.0 R
Heraeus BiofugeA
Beckman L8-70M
Beckman Coulter Optima TLX
Beckman Coulter Avanti J-20 XP
Du Pont Instruments Sorvall RC-5B

Rotors:

Beckman SW55Ti
Beckman SW40
Beckman JLA-8.1000
Beckman TLA100.4
Beckman TLA120.2
Beckman TLA 100
Beckman TLS-55
Sorvall SS34
Sorvall HB6

Air liquide ESPACE 331 GAZ (Liquid nitrogen tank)
Amersham Biosciences Ultraspec 2100 pro (Spectrometer)
Avestin EmulsiFlex-C5 (Homogeniser)
B. Braun, Thermomic Bu (Waterbath)
Biorad Power Pac 300 (Power supply)
Biorad gelelectrophoresis system
Biorad Transfer Cell (Western blot wet blot chamber)
Biorad Gene PulserTM
Branson Sonifier B15, Tip: Branson Converter BSB7 (Sonicator)
Carl Zeiss AG LSM 510 META (confocal microscope)
Cell culture cabinet (The Baker Company (Sanford, USA))
Eppendorf Centrifuges 5415 D and R (table top centrifuges)
Eppendorf Thermomixer compact
Eppendorf Thermostat 5320
Heidolph Polymax 2040 and Unimax 2010 (shaking tables)
Hera cell 240 (Incubator)
Infors AG HT (Shaking incubators)
Leica TCS SP2 AOBS FCS (confocal microscope)
MJ Research PTC-200 Peltier Thermal Cycler (PCR machine)
Pharmacia LKB (FPLC machine)
Philips CM-120 BioTwin (electron microscope)

Radiometer Copenhagen pH M82 Standard pH Meter
 7500 Real Time PCR system (Applied Biosystems, Foster City, USA)
 Snijders Scientific test tube rotator Model 34528
 Superose 6 gel filtration column (GE Healthcare, München, Germany)
 Thermo Scientific Hera -80°C freezer

4.1.5 Animals and cell lines

Rabbits	Harlan Winkelmann GmbH (Borchen, Germany)
<i>Xenopus laevis</i> frogs	African Reptile Park (Republic of South Africa)
<i>Drosophila</i> cells (Sf9, TniHi5, SF+, High 5)	EMBL protein expression and purification facility
HeLa Kyoto cells	Ellenberg lab (EMBL Heidelberg)
U2OS cells	Ulrike Kutay (ETH Zürich)
<i>Xenopus laevis</i> A6 cells	Karsenti lab (EMBL Heidelberg)

4.1.6 Bacterial strains

XL1Blue: genotype: *recA1 endA1 gyrA96 thi-1 hsdR17 supE44 relA1 lac (F'proAB lacI_qZDM15 Tn 10 (Tetr))* (Stratagene).

BL21 (DE3): genotype: *F- ompT hsdS_B (r_B-m_B-) gal dcm (DE3)*, a lambda prophage carrying the T7 RNA polymerase gene (Novagene).

Rosetta (DE3): genotype: *F- ompT hsdS_B (r_B-m_B-) gal dcm (DE3) pRARE₂ (Cam_R)* (Novagene).

4.1.7 Antibodies

Primary antibodies

<u>Antigen</u>	<u>Raised in</u>	<u>Source / remarks</u>
Alpha tubulin	Mouse	Sigma-Aldrich (Steinheim, Germany)
AND-1	Mouse	Kindly provided by Marion Schmidt-Zachmann (DKFZ, Heidelberg). (Köhler <i>et al.</i> , 1997)
GST	Rabbit	Kindly provided by Elisa Izaurrealde (MPI Tübingen).
Histone H2B	Rabbit	Abcam (Cambridge, UK)
Human Coilin	Rabbit	Kindly provided by Melpomeni Platani. (Platani <i>et al.</i> , 2000)
Human Emerin	Rabbit	Abcam (Cambridge, UK)
Human Lamin A	Mouse	Biozol Diagnostica (Eching, Germany)
Human Lamin B	Mouse	ImmuQuest (North Yorkshire, UK)
Human MEL-28	Rabbit	Raised against His ₆ -tagged aa 1208-1800 or aa 1572-2266 of human MEL-28. (Franz <i>et al.</i> , 2007)
Human NET5	Rabbit	Raised against N-terminally GST-tagged and C-terminally His ₆ -tagged aa 374-640 of human NET5.
Human Nup107	Rabbit	Kindly provided by Ulrike Kutay (ETH Zürich).
Human Nup133	Rabbit	Kindly provided by Martin Hetzer (SALK Institute, La Jolla).
Human Nup358	Guinea-pig	Raised against aa 2285-2314 of human Nup358. Kindly provided by Volker Cordes (MPI Göttingen).

Human Nup37	Rabbit	Cross-reacts with <i>X. laevis</i> Nup37, produced by Melpomeni Platani, available in the Mattaj lab.
Lap2	Mouse	BD Biosciences (Heidelberg, Germany)
Human LEM2	Rabbit	(Ulbert <i>et al.</i> , 2006a)
mAb414	Mouse	Covance (Berkeley, USA)
<i>X. laevis</i> Cyclin B1	Rabbit	Kindly provided by the Gruss lab (ZMBH Heidelberg)
<i>X. laevis</i> MEL-28	Rabbit	Raised against His ₆ -tagged aa 1602-2120 of <i>X. laevis</i> MEL-28. (Franz <i>et al.</i> , 2007)
<i>X. laevis</i> Ndc1	Rabbit	Raised against GST-tagged aa 361-521 of <i>X. laevis</i> Ndc1, produced by Wolfram Antonin, available in the Mattaj lab. (Mansfeld <i>et al.</i> , 2006)
Rat Nup107	Rabbit	Cross-reacts with <i>X. laevis</i> Nup107, raised against His ₆ -tagged aa 76-171 of rat Nup107, produced by Tobias Walther, available in the Mattaj lab. (Walther <i>et al.</i> , 2003a)
<i>X. laevis</i> Nup155	Rabbit	Raised against His ₆ -tagged <i>X. laevis</i> Nup155 purified from inclusion bodies, produced by Cerstin Franz, available in the Mattaj lab. (Franz <i>et al.</i> , 2005)
<i>X. laevis</i> Nup160	Rabbit	Raised against His ₆ -tagged aa 1-414 of <i>X. laevis</i> Nup160, produced by Wolfram Antonin, available in the Mattaj lab.
<i>X. laevis</i> Nup205	Rabbit	Raised against aa 1-230 of <i>X. laevis</i> Nup205, produced by Wolfram Antonin, available in the Mattaj lab.
<i>X. laevis</i> Nup50	Rabbit	Raised against His ₆ -tagged <i>X. laevis</i> Nup50. Affinity purified antibodies were used in this thesis.
<i>X. laevis</i> Nup93	Rabbit	Raised against aa 1-230 of <i>X. laevis</i> Nup93, produced by Wolfram Antonin, available in the Mattaj lab.
<i>X. laevis</i> Nup98	Rabbit	Raised against GST-tagged aa 1-185 of <i>X. laevis</i> Nup98, produced by Wolfram Antonin, available in the Mattaj lab.
Human RCC1	Rabbit	Cross-reacts with <i>X. laevis</i> RCC1, raised against His ₆ -tagged human RCC1, produced by Oliver Gruss and Christoph Schatz, available in the Mattaj lab.

Secondary antibodies (Western blotting)

ECLTM anti-rabbit IgG Horseradishperoxidase linked whole antibody (from donkey)
Amersham Biosciences (Braunschweig, Germany)
ECLTM anti-mouse IgG, Horseradishperoxidase linked whole antibody (from sheep)
Amersham Biosciences (Braunschweig, Germany)

Secondary antibodies (Immunofluorescence)

Alexa Fluor **488** goat anti-mouse or anti-rabbit IgG (Invitrogen (Karlsruhe, Germany))
Alexa Fluor **546** goat anti-mouse or anti-rabbit IgG (Invitrogen (Karlsruhe, Germany))
Alexa Fluor **488** goat anti-guinea pig IgG (Invitrogen (Karlsruhe, Germany))

4.1.8 Clones

The clones used in this thesis were ordered at the Deutsches Ressourcenzentrum für Genomforschung (RZPD), now imaGenes (Berlin, Germany).

IMAGp998K238393Q	full length <i>X. laevis</i> Nup50, in pCMV-SPORT6
IRAKp961F12217Q	short NET5 isoform (aa 1-394), in pCMV-SPORT6

4.1.9 Oligonucleotides

All oligos for cloning were ordered from MWG Biotech AG (Ebersberg, Germany).

<u>Name</u>	<u>Sequence (5' → 3')</u>
1 hELYS_R1208NdeI_fw	GCATCGCATATGCGATCAACACCTTTAGCATCTCCCT
2 hELYS_Q1800XhoI_rev	CTGCTCGAGTCACTGGTTCTGAAATAGTCCTCTGA
3 hELYS_D1572NheI_fw	CTGGCTAGCGACACTGCTGAATGTGACATTGCTG
4 hELYS_L2266XhoI_rev	CCGCTCGAGTTACAGCATTTTTCTGCGTAAAATTTG
5 Xlnup50fwd1	GCATCGCATATGGCGAAGCGAATTGCGGATAAAGAG
6 Xlnup50rev	CCGCTCGAGTTATACTTCTTTTTCTCCAGAAGGATTT
7 GST-AT-1	GATCCGGGCCCTCAAACCAAGAGGCAGACCTCCAAA CACAAAGCAAAGACGTAGC
8 GST-AT-2	TCGAGCTACGTCTTTGCTTTGTGTTTTGGAGGTCTGCCT CTTGGTTTTGAGGGCCCG
9 GSTonly1	GATCCTAGGGGCCCTCAAACCAAGAGGCAGACCTCCA AAACACAAAGCAAAGACGC
10 GSTonly2	TCGAGCGTCTTTGCTTTGTGTTTTGGAGGTCTGCCTCTT GGTTTTGAGGGCCCTAG
11 ATmutGly_Fwd	GATCCGGTCCGAGCAAACCGGGTGGTGGTCCGCCGGG TCACAAAGCAAAAACCTAGC
12 ATmutGly_Rev	TCGAGCTAGGTTTTGCTTTGTGACCCGGCGGACCACCA CCCGGTTTGCTCGGACCG
13 AT-HMGA_Fwd	GATCCAGCCCGAAACGTCCGCGTGGTCGTCCGAAAGGC AGCAAAAACAAAAGCTAGC
14 AT-HMGA_Rev	TCGAGCTAGCTTTTGTGTTTTGCTGCCTTTCGGACGACCA CGCGGACGTTTCGGGCTG
15 AT-LHX_Fwd	GATCCGTGGGTACCGTGCAGAAAGGTGTCGTCGCGTAAA CGTAAAAGCCCAGGTTAGC
16 AT-LHX_Rev	TCGAGCTAACCTGGGCTTTTACGTTTACGCGGACGACCT TTCTGCACGGTACCCACG
17 AT-ORC1_F	GATCCCGCGTGTATGCGTGGAAGGCCGCCGAGCATT AAAGATCGCAAACGTAGC
18 AT-ORC1_R	TCGAGCTACAGTTTGCATCTTTAATGCTCGGGCGGCCT TTCCACGCATACACGCGG
19 rAth FwdBamHI	ACTGGATCCCTACCTCCAGTAATCGAAGACCATT
20 F7ext_revXhoI	CCGCTCGAGTCATATCATCTTTCGGCGCATGA
21 mut Gly F2	GGGCCCTCAAACCAAGGTGGCGGTCTCCAGGTCACAA AGCAAAGACG
22 mut Gly R2	CGTCTTTGCTTTGTGACCTGGAGGACCGCCACCTGGTTT TGAGGGCCC
23 Fwd-M1	ATCGGAGCTCATGCAAACCTCAAAGCTCAGATCAC
24 Fwd-K196	ATCGGAGCTCAAATTCCTCAAGCTACGAGAAGGTG
25 Fwd-D401	ATCGGAGCTCGACATTAATCGATGGTATCAAGCGC
26 Fwd-G605	ATCGGAGCTCGGATCATGTAACCTTCATTGACCCAC
27 Fwd-S800	ATCGGAGCTCTCTGTTCCCTGCCAGTCTTATCAAATT
28 Fwd-A1007	ATCGGAGCTCGCCAAACCCTACTCATTACCATCAC
29 Fwd-R1200	ATCGGAGCTCCGCACTACACCGTTGGTCTCACCT
30 Rev-G1418	ATCGCCCGGGCTAGCCTGCAGGAGTTTCTGAAATACAC
31 nTMfwdBgIII	GTA CTAGATCTATGGAGGGAGTGAGCGCGCTGCTG
32 nTMrevBam2	ACTGGATCCGCGCAGGCTCTGGTACAGAAACAC
33 nTM_Ct_N3r	ACTGGATCCGGAAGGGCCGAAACGACCTCTCCA

34	nTMfwdXhoI	CCGCTCGAGGTATGGAGGGAGTGAGCGCGCTGCTG
35	nTMrevBam1	ACTGGATCCTGGCTGCTTCTCTGACCTTCGGGG
36	nTMsh-delNLS	ACTGGATCCTGTGGCCACAGCCGCGTGAAGC
37	nTM_Nt_N3f	GTACTAGATCTATGGCGCGGAGGATGAAGCCAACGCAC AC
38	nTM_Nt_N3r	ACTGGATCCCTGGACCGGGGACTTCACGGCGG
39	nTM_Ct_N3f	GTACTAGATCTATGACAAGGAAGGCAACGGGGCCCACGG
40	nTM3-pGEXfwd	ACTGGATCCACAAGGAAGGCAACGGGGCCCACGG
41	nTM3-pGEXrev	TACGAATTCTCAATGGTGTATGGTGTATGGTGGGAAGGGC CGAAACGACCTCTCCA
42	nTM1-Y2Hnew	TACGAATTCGCGCGGAGGATGAAGCCAACGCAC
43	nTM_Nt_C3r	ACTGGATCCTCACTGGACCGGGGACTTCACGGCGG
44	nTM3-Y2Hnew	TACGAATTCACAAGGAAGGCAACGGGGCCCACGG
45	nTM3_revBam	ACTGGATCCTCAGGAAGGGCCGAAACGACCTCTCCA
46	qPCR_278fwd	CCTGAGATCCAAGCTGGAAA
47	qPCR_278rev	TGGTGTCCACCACACAGGTA
48	qPCR_279fwd	CTCCAGCTCCGGCTCTCT
49	qPCR_279rev	GTGACGGGAACAGCAGCA
50	qPCR_001fwd	AGCTGTCTCGGTGGATTCTG
51	qPCR_001rev	TGACCTGGCAAATGTGTAGA
52	qPCR_003fwd	TGTGGAGTGGGCAGAAGG
53	qPCR_003rev	GTCACAAAGCAGGGCACAT

siRNA oligonucleotides were ordered from Dharmacon (Lafayette, USA).

Firefly Luciferase	AATCGAAGTATTCCGCGTACG
MEL-28 (1)	AATATCTACATAATTGCTCTT
MEL-28 (2)	CCCTCAAGTTCGCAATTAATT

NET5:

"278"	CCATCAAGAAAGAGGACGA
"279"	GGCTCAACCTGAAGGGACA
"3'-UTR 1"	ACTCTGCCATTCTGGGATA
"3'-UTR 2"	CCTCAGAGCTCCAGGTCT

4.1.10 Plasmids

pBluescript II KS+	Fermentas (St. Leon-Rot, Germany)
pEGFP-C3	BD Biosciences (Heidelberg, Germany)
pEGFP-N3	BD Biosciences (Heidelberg, Germany)
pET28a	Novagen (Darmstadt, Germany)
pET28d/pET28n	Kindly provided by Wolfram Antonin (FMI, Tübingen)
pFastBac 1	Invitrogen (Karlsruhe, Germany)
pFastBac HT A	Invitrogen (Karlsruhe, Germany)
pGBT9	Clontech (Saint-Germain-en-Laye, France)
pGEX-KG	EMBL, Protein Expression and Purification Facility
pmEGFP-C3	BD Biosciences (Heidelberg, Germany) for expression tagged with monomeric GFP

4.1.11 Constructs

4.1.11.1 Foreign constructs

pCRII hELYS	Full length human MEL-28 cDNA clone (Peter Asjkaer) This construct contains point mutations!
pEGFP-C3 X/MEL-28	Full length <i>X. laevis</i> MEL-28 (Cerstin Franz)
pET28a xMel(1602-2120aa)	Amino acids 1602-2102 of <i>X. laevis</i> MEL-28 (Cerstin Franz)
pQE32 RanQ69L	For expression as His ₆ -tagged protein in <i>E. coli</i>
pQE32 RanT24N	For expression as His ₆ -tagged protein in <i>E. coli</i>
pQE Impβ	For expression as His ₆ -tagged protein in <i>E. coli</i>
pGEX-KG xMel(1-195aa)	Amino acids 1-195 of <i>X. laevis</i> MEL-28 (Cerstin Franz)

4.1.11.2 Constructs generated as part of this thesis

<u>Vector</u>	<u>Oligos</u>	<u>Restriction sites</u>	<u>Description</u>
pET28 a	1+2	NdeI/XhoI	Amino acids 1208-1800 of human MEL-28
pET28 a	3+4	NheI/XhoI	Amino acids 1572-2266 of human MEL-28
pET28 a	5+6	NdeI/XhoI	Full length <i>X. laevis</i> Nup50
pGEX-KG	7+8	BamHI/XhoI	GST without multiple cloning site ("GST-stop")
pGEX-KG	9+10	BamHI/XhoI	GST-AT hook (MEL-28)
pGEX-KG	11+12	BamHI/XhoI	GST-AT hook _{MUT} (MEL-28)
pGEX-KG	13+14	BamHI/XhoI	GST-AT hook (HMGA 2β)
pGEX-KG	15+16	BamHI/XhoI	GST-AT hook (LHX 2)
pGEX-KG	17+18	BamHI/XhoI	GST-AT hook (ORC-1)

The oligos for the GST-AT hook constructs were designed to yield DNA fragments with sticky ends for direct ligation. Two corresponding oligos were mixed at 17.5 ng/μl in 1x TE buffer, the mixture heated to 95°C in a heat block for 5 min and allowed to slowly cool down to RT. 5 μl of the annealed oligos were used in a ligation reaction.

pGEX-KG	19+20	BamHI/XhoI	GST-rAth (the C-terminal 208 amino acids of <i>X. laevis</i> MEL-28)
pGEX-KG	21+22	-	GST-rAth _{MUT} (the C-terminal 208 amino acids of <i>X. laevis</i> MEL-28 with three point mutations in the AT hook)

pGEX-KG GST-rAth_{MUT} was generated from pGEX-KG GST-rAth by site-directed mutagenesis. The wild type construct was used as template in a PCR reaction and the PCR product was purified with a QIAquick PCR Purification Kit according to the manufacturer's instructions. The purified DNA was digested with DpnI in NEB4 at 37°C for 3 h. 5 μl of the digested DNA were used to transform competent *E. coli* cells.

pEGFP-C3	-	SpeI/BamHI	Amino acids 1-660 of <i>X. laevis</i> MEL-28
pEGFP-C3	-	PmlI/BamHI	Amino acids 1-1010 of <i>X. laevis</i> MEL-28

pEGFP-C3	-	SbfI/BamHI	Amino acids 1-1420 of <i>X. laevis</i> MEL-28
pEGFP-C3	-	EcoNI/BamHI	Amino acids 1-1760 of <i>X. laevis</i> MEL-28

These constructs were generated from the pEGFP-C3 full length MEL-28 construct by removing fragments via restriction digest with the indicated enzymes. The overhangs were filled using Klenow fragment (1u/μg DNA) by incubating the DNA with 33 μM dNTPs in NEB2 for 15 min at 25°C. The reaction was stopped by addition of EDTA to 10 mM and heating to 75°C for 20 min. The DNA was purified from an agarose gel with a QIAquick Gel Extraction Kit according to the manufacturer's instructions, followed by ligation and transformation of competent *E. coli* cells.

pEGFP-C3	23+30	SacI/XmaI	Amino acids 1-1418 of <i>X. laevis</i> MEL-28
pEGFP-C3	24+30	SacI/XmaI	Amino acids 196-1418 of <i>X. laevis</i> MEL-28
pEGFP-C3	25+30	SacI/XmaI	Amino acids 401-1418 of <i>X. laevis</i> MEL-28
pEGFP-C3	26+30	SacI/XmaI	Amino acids 605-1418 of <i>X. laevis</i> MEL-28
pEGFP-C3	27+30	SacI/XmaI	Amino acids 800-1418 of <i>X. laevis</i> MEL-28
pEGFP-C3	28+30	SacI/XmaI	Amino acids 1007-1418 of <i>X. laevis</i> MEL-28
pEGFP-C3	29+30	SacI/XmaI	Amino acids 1200-1418 of <i>X. laevis</i> MEL-28
pmEGFP-N3	31+32	BglII/BamHI	Full length human NET5
pmEGFP-N3	31+33	XhoI/BamHI	Amino acids 1-640 of human NET5
pmEGFP-N3	34+35	XhoI/BamHI	Amino acids 1-394 of human NET5
pmEGFP-N3	34+36	XhoI/BamHI	Amino acids 1-374 of human NET5
pmEGFP-N3	37+32	BglII/BamHI	Amino acids 36-666 of human NET5
pmEGFP-N3	34+38	XhoI/BamHI	Amino acids 1-213 of human NET5
pmEGFP-N3	37+38	BglII/BamHI	Amino acids 36-213 of human NET5
pmEGFP-N3	39+33	BglII/BamHI	Amino acids 374-640 of human NET5
pGEX-KG	40+41	BamHI/EcoRI	Amino acids 374-640 of human NET5, expressible with a C-terminal His ₆ -tag
pGBT9	42+43	EcoRI/BamHI	Amino acids 36-213 of human NET5
	44+45	EcoRI/BamHI	Amino acids 374-640 of human NET5

The sequences of all constructs were verified by sequencing at the EMBL genomics core facility.

4.2 Methods

4.2.1 Molecular biology methods

4.2.1.1 Purification of plasmid DNA

Purification of plasmid DNA from bacteria was carried out with the QIAGEN plasmid Maxi, Midi or QIAprep Spin Miniprep Kits according to the manufacturer's instructions.

4.2.1.2 Restriction digest

For a typical restriction digest, 1 μg DNA was digested with 2 μl restriction enzyme(s)

in 50 μ l at 37°C for 2 h or overnight. To prevent self-ligation, vectors were treated with shrimp alkaline phosphatase (SAP). 10x SAP buffer was directly added to the restriction reaction and the sample was incubated at 37°C for 45 min, followed by purification of the DNA using a QIAquick PCR Purification Kit according to the manufacturer's instructions.

4.2.1.3 Ligation of DNA fragments

Ligation reactions were carried out in 10 μ l reaction volume containing 1 μ l 10x T4 DNA ligase buffer (New England Biolabs), 0.5 μ l vector (20 ng), 7.5 μ l insert and 1 μ l T4 DNA ligase. The ligation reaction was incubated at 16°C overnight and used directly for transforming competent *E. coli* cells.

4.2.1.4 Preparation of chemically competent cells

A single colony of the bacterial strain of interest was picked from a fresh LB-agar plate and used for growing a 10 ml overnight culture in LB medium at 37°C. A 1 l culture was inoculated with 2-3 ml of the overnight culture and grown under vigorous rotation at 18°C until OD₆₀₀ \approx 0.12 (typically 24 h). The culture flask was chilled in ice water for 10 min and the cells were harvested by centrifugation in chilled, sterile centrifuge buckets at 5000 rpm for 10 min. All subsequent steps were carried out on ice in the coldroom. The cell pellet was resuspended in 150 ml cold transformation buffer (10 mM PIPES pH 6.7, 250 mM KCl, 15 mM CaCl₂, 55 mM MnCl₂), centrifuged at 5000 rpm for 10 min and resuspended again in 15 ml cold transformation buffer. After addition of 1 ml DMSO to the resuspended cells and careful mixing, 100 μ l aliquots of cells were frozen in liquid nitrogen and stored at -80°C.

4.2.1.5 Transformation of chemically competent bacteria

Chemically competent *E. coli* cells were thawed on ice. 50 ng plasmid DNA or 5 μ l ligation reaction were added to 50 μ l bacteria and the mixture was incubated on ice for 15 min. A heat shock was performed in a water bath at 42°C for 45 s and the cells were transferred to ice for 2 min. 150 μ l of warm (37°C) LB medium were added to the cells, incubated at 37°C for 1 h on a Thermomixer followed by plating of the bacteria.

4.2.1.6 PCR

PCR-reactions were carried out in 50 μ l reaction volume containing: 5 μ l 10x *Pfu* buffer, 5 μ l dNTPs (2 mM each), 2x 10 μ l primers (0.5 μ M), 18 μ l dH₂O and 1 μ l template (10 ng plasmid DNA). 1 μ l *Pfu* polymerase (2.5u/ μ l) was added, the reaction was mixed and transferred to the PCR machine.

Standard PCR reactions were performed according to the following program: 95°C, 1 min; 5 cycles of [95°C, 45 s; 54°C, 45 s; 72°C, X+1 min]; 25 cycles of [95°C, 45 s; 58°C, 45 s; 72°C, X+1 min]; 72°C, 2X min; 4°C forever. The extension time X was chosen based on the product size (1 min per 1 kb of product size). The amplified PCR product was analyzed on an agarose gel and purified with a QIAquick PCR Purification Kit according to the manufacturer's instructions.

4.2.1.7 RT-PCR

First-strand cDNA synthesis was carried out with the SuperScript II Reverse transcriptase (Invitrogen) according to the manufacturer's instructions. 5 µg of total RNA were used in a 20 µl RT-PCR reaction. The total RNA for cloning of the full length human NET5 cDNA and for monitoring the NET5 RNAi experiments was collected from HeLa cells with the RNeasy Mini kit (QIAGEN) according to the manufacturer's instructions. The concentration of the isolated total RNA sample was determined by measuring the OD₂₆₀.

4.2.1.8 Real time quantitative PCR

Real time quantitative PCR reactions were carried out with the SYBR Green PCR master mix using a 7500 Real Time PCR system (Applied Biosystems) in the EMBL genomics core facility. The reactions were set up in 25 µl with 12.5 µl SYBR Green PCR master mix. The cDNA and primer concentrations were optimized starting with 12.5 ng cDNA per reaction and 200 nM primers. The NET5 primers used were oligos 46-53 from chapter 4.1.9 and the EMBL genomics core facility standard actin and GAPDH primers served as controls. The reactions were carried out according to the gene core standard qPCR protocol with 40 cycles of amplification.

4.2.2 Biochemical methods

4.2.2.1 Biochemical standard methods

4.2.2.1.1 Protein expression in *E. coli*

A small scale culture in LB medium (+ antibiotics) was inoculated with a single colony from a fresh plate and incubated overnight shaking at 37°C. An expression culture (LB with antibiotics) was inoculated with the overnight culture to OD₆₀₀=0.1 and grown at 37°C under vigorous rotation. At OD₆₀₀=0.4 the culture was allowed to cool down to RT and at OD₆₀₀=0.8 expression was induced by addition of 0.25 mM IPTG (final conc.). After 2.5 h of expression the bacteria were harvested by centrifugation (JLA-8.1000, 4000 rpm, 15 min, 4°C). The cell pellet was resuspended in cold Ni wash buffer (20 mM Tris pH 7.5, 0.5 M NaCl, 1 mM MgCl₂, 8 mM imidazole) in the case of His₆-tagged proteins or PBS + 1 mM EDTA for GST-tagged proteins and pelleted again (Heraeus Megafuge 1.0 R, 4000 rpm, 10 min, 4°C). The washed bacteria pellet was frozen in liquid nitrogen and stored at -80°C.

4.2.2.1.2 Purification of His₆-tagged proteins

The cell pellet was resuspended in cold Ni wash buffer (20 mM Tris pH 7.5, 0.5 M NaCl, 1 mM MgCl₂, 8 mM imidazole; 20 ml per 1000 OD₆₀₀ cells), 200 µM PMSF were added and the bacteria were lysed by passing the suspension twice through an Emulsiflex-C5 homogenizer. The lysate was cleared by centrifugation (SS34, 15000 rpm, 15 min, 4°C) and the supernatant incubated with Ni-NTA agarose (1 ml 50% slurry per 1000 OD₆₀₀ cells) at 4°C for 1 h. The resin was washed twice in batch with 10 bed volumes of Ni wash buffer and transferred to a Bio-Rad chromatography

column. The resin was washed in the column with 10 bed volumes Ni wash buffer and the bound protein was eluted with Ni wash buffer + 250 mM imidazole in 1 ml fractions. The fractions were analyzed by SDS-PAGE and Coomassie staining and pooled accordingly. The eluted protein was dialyzed overnight at 4°C against 10 mM Tris pH 7.5, 150 mM NaCl, 1 mM MgCl₂, 5% (v/v) glycerol, frozen in liquid nitrogen and stored at -80°C.

His₆-tagged RanQ69L, RanT24N and Importin β were expressed and prepared as described in Walther *et al.* (2003b) and the references therein.

4.2.2.1.3 Purification of GST-tagged proteins

The bacteria pellet was resuspended in cold PBS, 200 μM PMSF were added and the bacteria were lysed by passing the suspension twice through an Emulsiflex-C5 homogenizer. The lysate was cleared by centrifugation (SS34, 15000 rpm, 15 min, 4°C) and the supernatant incubated with Glutathione Sepharose (0.5 ml 50% slurry per 1000 OD₆₀₀ cells) at 4°C for 1 h. The resin was washed twice in batch with 10 bed volumes of PBS and transferred to a Bio-Rad chromatography column. The resin was washed in the column with 10 bed volumes PBS and the bound protein was eluted with 50 mM Tris pH 8, 150 mM NaCl, 20 mM glutathione in 1 ml fractions. The fractions were analyzed by SDS-PAGE and Coomassie staining and pooled accordingly. The eluted protein was dialyzed overnight at 4°C against 10 mM Tris pH 7.5, 150 mM NaCl, 1 mM MgCl₂, 5% (v/v) glycerol, frozen in liquid nitrogen and stored at -80°C.

4.2.2.1.4 Determination of protein concentration

Protein concentrations were typically determined in a Bradford assay using the Bio-Rad Protein Assay. 1 volume of the Protein Assay reagent was diluted with 4 volumes of water. The protein samples were diluted to 100 μl in plastic cuvettes and 0.9 ml of diluted reagent were added. After 3 min incubation at RT, the absorption at 595 nm was measured in an Ultraspec 2100 pro spectrometer and the protein concentration determined with the help of a BSA concentration gradient.

4.2.2.1.5 Sodium dodecyl sulfate polyacrylamide gel electrophoresis (SDS-PAGE)

SDS-PAGE separating and stacking gels for 4 mini gels (0.75mm spacer) with the Bio-Rad gel system were prepared according to the following table:

	<u>Stacking gel</u>	<u>Separating gel</u>
Percentage acrylamide	3.9%	6 / 8 / 12%
30% Acrylamide/bis	1.3 ml	4 / 5.35 / 8 ml
1.5M Tris pH 8.8	-	5 ml
1M Tris pH 6.8	1.25 ml	-
10% (w/v) SDS	100 μl	200 μl
dH ₂ O	7.25 ml	10.6 / 9.25 / 6.6 ml
TEMED	10 μl	20 μl
10% (w/v) APS	100 μl	200 μl
Σ	10 ml	20 ml

All separating gel components except for APS were mixed and polymerization was initiated by addition of APS. The separating gel solution was filled into the assembled gel plates and overlaid with 2-propanol. After polymerization of the separating gel, the 2-propanol was removed by washing with water, the stacking gel solution was prepared, pipetted on top of the separating gel and the combs were inserted. Gels were stored in the coldroom for up to one week wrapped in wet tissue paper. For gels of different percentages the amounts of acrylamide were adjusted and for larger gels the volumes of all components were scaled up accordingly. The gels were run at 120 V until the dye front had entered the separating gel, followed by 200 V.

For experiments, in which low amounts of proteins had to be detected by Western blotting, NuPAGE 4-12% Bis-Tris gels (Invitrogen) were used to electrophoretically separate proteins.

Coomassie-staining:

SDS-PAGE gels were stained with Coomassie by incubation in Coomassie staining solution for 30 min and destaining in Coomassie destain solution.

4.2.2.1.6 Silver staining

The SDS-PAGE gel was fixed for 20 min in methanol-acetic acid-dH₂O (40:10:50) and rinsed several times with water (time: 3-4 h). Sensitizing was carried out for 2 min in 0.02% (w/v) sodium thiosulfate in dH₂O followed by 2 washes with water (1 min each). The gel was incubated for 30 min in chilled (4°C) 0.1% (w/v) silver nitrate solution and washed twice with water (1 min each). The staining was developed by incubation in 0.04% (v/v) formaldehyde in an aqueous 2% (w/v) sodium carbonate solution and the reaction stopped by addition of 1% (v/v) acetic acid. Silver-stained gels were stored in 1% (v/v) acetic acid at 4°C.

4.2.2.1.7 Western blotting

Western blotting was carried out using the wet blot method. The SDS-PAGE gel was incubated in transfer buffer (25 mM Tris, 200 mM glycine, 10% (v/v) methanol) for 5 min. A nitrocellulose membrane, Whatman filter papers and sponges were soaked in transfer buffer and assembled in the blotting cassette in the following order: cathode – sponge – 3 filter papers – gel – membrane – 3 filter papers – sponge – anode. The transfer was carried out for 4 h at 250 mA for small gels and for 4 h at 370 mA in the case of large gels. To control the transfer efficiency, the membrane was briefly stained with 0.1% (w/v) Ponceau S in 1% (v/v) acetic acid and the staining was washed off with water.

The membrane was blocked at 4°C overnight with 5% (w/v) milk powder in PBS-Tween (0.1% (v/v) Tween-20). Incubation with primary antibodies was for 2 h at RT or overnight at 4°C in blocking solution, followed by 3 washes (10 min each) with PBS-Tween. Incubation with secondary antibodies was for 1 h at RT, followed by several washes with PBS-Tween (time > 2 h). The wash buffer was dripped off the membrane and Western Lightning™ Chemiluminescence reagent was added. After 1 min of incubation, the reagent was removed and the membrane covered with cling film. A

Kodak BioMax MR film was exposed to the membrane in the darkroom and the film was developed automatically.

Stripping of antibodies from membranes for re-probing was performed by washing the membranes for 30 min in pre-warmed (55°C) stripping buffer (60 mM Tris pH 6.8, 2% (w/v) SDS, 100 mM 2-mercaptoethanol). The membranes were washed several times with PBS-Tween prior to re-blocking and re-probing.

4.2.2.1.8 Affinity purification of polyclonal antibodies

The antigen was dialyzed against buffer A (100 mM NaHCO₃ pH 8.3, 0.5 M NaCl, 2 mM MgCl₂) overnight at 4°C. CNBr-activated Sepharose 4B was swelled in ice cold 1 mM HCl pH 2-3 and equilibrated with buffer A (0.3 g Sepharose per 10 mg antigen). The antigen solution was incubated with the CNBr-Sepharose at 3.5 mg/ml for 1 h at RT. The supernatant was removed and the beads washed with 5 bed volumes buffer A. All washes were performed in batch in a Heraeus Megafuge 1.0 R (1000 rpm, 2 min, 4°C). The Sepharose beads were incubated with 1 M ethanolamine pH 8 in buffer A for 2 h at RT to block remaining free binding sites. The resin was washed twice in buffer A, twice in buffer B (100 mM sodium acetate pH 4.2, 0.5 M NaCl), twice in buffer A and again twice in buffer B (10 ml per wash). The antigen beads were pre-eluted with 200 mM glycine pH 2.3, 150 mM NaCl and equilibrated in PBS.

Antiserum was added to the antigen column (10 ml serum per 1 ml beads) and rotated overnight at 4°C. The beads were washed with 5 bed volumes cold PBS, packed into a Bio-Rad chromatography column and washed with 20 bed volumes PBS. The column was drained and eluted with 3x 1 ml 200 mM glycine pH 2.7, 150 mM NaCl. The elution fractions were neutralized with 1.5 M Tris pH 8.8 (30 µl/ml eluate), pooled and immediately dialyzed against PBS (twice for 1h). The column was eluted with 5x 1 ml 200 mM glycine pH 2.3, 150 mM NaCl, the elution fractions neutralized with 1.5 M Tris pH 8.8 (60 µl/ml eluate), combined and dialyzed against PBS (twice for 1h). The column was washed extensively with PBS and stored in PBS + 0.1% (w/v) sodium azide + protease inhibitors.

4.2.2.1.9 Preparation of antibody beads

Affinity purified antibodies or antiserum were bound to protein A Sepharose overnight at 4°C (4 mg purified antibodies or 1 ml serum per 50% slurry protein A). The beads were washed twice with coupling buffer (200 mM NaHCO₃ pH 9.3, 100 mM NaCl) and incubated with 10 mM Dimethylpimelimidate (DMP) in coupling buffer for 10 min at RT. The beads were washed again with coupling buffer and the cross-linking was repeated. The beads were washed twice with buffer B (100 mM sodium acetate pH 4.2, 0.5 M NaCl), twice in buffer A (100 mM NaHCO₃ pH 8.3, 0.5 M NaCl), twice in buffer B and again twice in buffer A. The antibody beads were equilibrated with S250 and blocked with 3% BSA (w/v) in S250 supplemented with protease inhibitors. Blocked antibody beads were stored at 4°C in 3% BSA (w/v) in S250 + protease inhibitors.

4.2.2.1.10 Immunodepletion of MEL-28 or the Nup107-160 complex from egg extract

MEL-28 was immunodepleted from interphase egg extract with affinity purified anti-*Xenopus* MEL-28 antibodies cross-linked to protein A Sepharose. The extract was incubated with the antibody beads (beads:extract 1:2) in MoBiCol columns for 30 min at 4°C under rotation. Two rounds of depletion were necessary to remove MEL-28 from the extract.

The Nup107-160 complex was depleted with anti-Rat Nup107 antiserum (ODBF, 3rd bleed) cross-linked to protein A Sepharose. Two rounds of incubation (30 min at 4°C) were required to immunodeplete the Nup107-160 complex. Immunodepletions were carried out in MoBiCol columns.

4.2.2.1.11 Immunoprecipitation

Egg extract was diluted with an equal volume of cold PBS, supplemented with protease inhibitors and centrifuged to remove membranes (TLA100.4, 100000 rpm, 30 min, 4°C). The immunoprecipitations were carried out in MoBiCol columns and draining of the beads was performed by centrifugation in a table top centrifuge (5000 rpm, 30 sec, 4°C). For immunoprecipitation with antibodies cross-linked to beads, 0.7 ml supernatant was directly added to 50 µl beads. When serum was used, 50 µl serum in 0.5 ml PBS was incubated with protein A Sepharose under rotation for 30 min at 4°C to bind the antibodies. The unbound was removed and 0.7 ml membrane-free diluted egg extract were added to the beads. Beads and extract were incubated under rotation for 1 h at 4°C. The beads were washed 10 times with PBS and the bound proteins eluted with 50 µl 1x SDS-loading buffer or with 40 µl 200 mM glycine pH 2.3, 150 mM NaCl into 5 µl 1.5 M Tris pH 8.8. When serum was used for the immunoprecipitation, protein A peroxidase was used as secondary antibody in Western blotting.

Immunoprecipitation from human nuclear extract (Cilbiotech) was performed using affinity purified anti-human MEL-28 antibodies cross-linked to protein A Sepharose in MoBiCol columns. 0.7 ml nuclear extract were supplemented with 20 mM Tris pH 7.5, 150 mM KCl, 0.2 mM MgCl₂, 0.04 u/µl DNaseI and protease inhibitors. The mixture was centrifuged in a table top centrifuge (13200 rpm, 10 min, 4°C) and the supernatant was added to 50 µl antibody beads, followed by a 1 h incubation at 4°C under rotation. The beads were washed 8 times with 20 mM Tris pH 7.5, 150 mM KCl, 0.2 mM MgCl₂. The bound proteins were eluted with 50 µl 200 mM glycine pH 2.3, 150 mM NaCl into 5 µl 1.5 M Tris pH 8.8. 10 µl 4x SDS-loading buffer were added to the eluate and 10 µl were loaded per SDS-PAGE gel lane.

4.2.2.2 Specific biochemical methods

4.2.2.2.1 Protein expression and purification using the Baculo system

Expression of proteins in insect cells was carried out using the Bac-to-Bac Baculovirus Expression system (Invitrogen). Generating the bacmid and virus followed the Bac-to-Bac protocol according to the manufacturer's instructions.

Expression tests with Sf9, TniHi5, SF+ and High 5 cells at 0, 24, 40, 48 and 72 h time points were carried out. N-terminally His₆-tagged MEL-28 was expressed in Hi 5 cells for 24 h, typically in 6x 175 cm² flask scale. The cells were harvested by scraping from the plates and frozen in liquid nitrogen.

The cell pellet was resuspended in insect cell lysis buffer (20 mM Tris pH 7.5, 0.35 M NaCl, 0.5% (v/v) Triton X-100, 1 mM MgCl₂, 5 mM imidazole, 5 mM, 0.1 u/μl DNase I and EDTA-free complete protease inhibitors). 1 ml cell pellet was taken up in 10 ml lysis buffer, sonicated 3x with 15 pulses and homogenized in a potter with pestle B. After rotation for 20 min at 4°C, the cell lysate was centrifuged (SS34, 18000 rpm, 20 min, 4°C) and the supernatant incubated with Ni-NTA agarose beads for 30 min at 4°C (0.2 ml 50% slurry per 1 ml cell pellet). The beads were filled into a Bio-Rad chromatography column and washed with 15 column volumes Ni wash buffer (20 mM Tris pH 7.5, 0.5 M NaCl, 1 mM MgCl₂, 8 mM imidazole). The protein was eluted with 250 mM imidazole in Ni wash buffer in 150 μl fractions. The elution fractions were dialyzed individually twice for 1 h against 10 mM Tris pH 7.5, 0.35 M NaCl, 1 mM MgCl₂, 10% (v/v) glycerol, frozen in liquid nitrogen and stored at -80°C.

4.2.2.2.2 Preparation of interphase *Xenopus laevis* egg extract

Extract preparation was carried out with a modified protocol from Newmeyer and Wilson (1991) and Hartl *et. al.* (1994).

Female *Xenopus laevis* frogs were primed by injection with pregnant mare serum gonadotropin (PMSG). To induce laying of eggs, the frogs were injected with 0.5 ml (500u/ml in H₂O) human chorionic gonadotropin and placed in plastic boxes with 0.5 l MMR at 16°C for 14-16 h. Batches of eggs containing apoptotic eggs were discarded. The eggs were collected and washed intensively with 1xMMR to remove dirt and debris and apoptotic eggs (large white) were removed continuously. Dejelling of eggs was performed for 10 min under continuous swirling with 1 l freshly prepared 2% (w/v) cysteine in 0.25x MMR. The eggs were washed carefully 4 more times with 1x MMR and activated (in 100ml MMR) by addition of 8 μl of the calcium ionophore A23187 (2 mg/ml in EtOH) for 10 min. This step mimics fertilization and releases the eggs from metaphase of meiosis II into interphase. Activation was visible by contraction of the animal pole. The eggs were washed 4 more times with 1x MMR, incubated at RT for 20 min and washed twice with cold S250. All subsequent steps were carried out on ice. With a cut plastic pasteur pipette, the eggs were carefully transferred into SW55Ti tubes into which 50 μl S250, 50 μl protease inhibitors (PI), 5 μl DTT, 12.5 μl Cycloheximide and 2.5 μl Cytochalasin D had been filled. The eggs were packed by centrifugation in a Heraeus Megafuge 1.0 R (800 rpm, 30 sec, immediately followed by 1600 rpm, 30 sec, both at 4°C). Excess buffer was removed and the tubes were filled with remaining eggs. A crude low speed extract was generated by centrifugation in a Beckmann L8-70M ultracentrifuge (SW55Ti, 25000 g (15000 rpm), 20 min, 4°C). The low speed extract was removed from the tubes using a syringe, avoiding lipids, yolk and pigments. The low speed extract was supplemented with fresh DTT, PI, cycloheximide and cytochalasin D and centrifuged again (SW55Ti, 225000 g (45000 rpm), 40 min, 4°C). Cytosol and membranes were removed from the tubes using a syringe, were diluted with AB buffer (0.3 ml per 1 ml of extract) and centrifuged again (SW55Ti, 225000 g (45000 rpm), 40 min, 4°C), yielding a high speed extract which consisted of a cytosolic and a membrane fraction. Cytosol was removed,

supplemented with 3% (v/v) glycerol, frozen in aliquots and stored in liquid nitrogen. Cytosol for immunoprecipitation was immediately processed as described in chapter 4.2.2.1.10. Membranes were processed as described in chapter 4.2.2.2.4.

Stock solutions of reagents:

A23187	2 mg/ml in EtOH, use 1/2500
Cycloheximide	20 mg/ml in EtOH, use 1/400
Cytochalasin D	10 mg/ml in EtOH, use 1/2000
DTT	1 M, use 1/1000
Protease inhibitors (PI)	dissolve 1 tablet in 0.5 ml H ₂ O, use 1/100

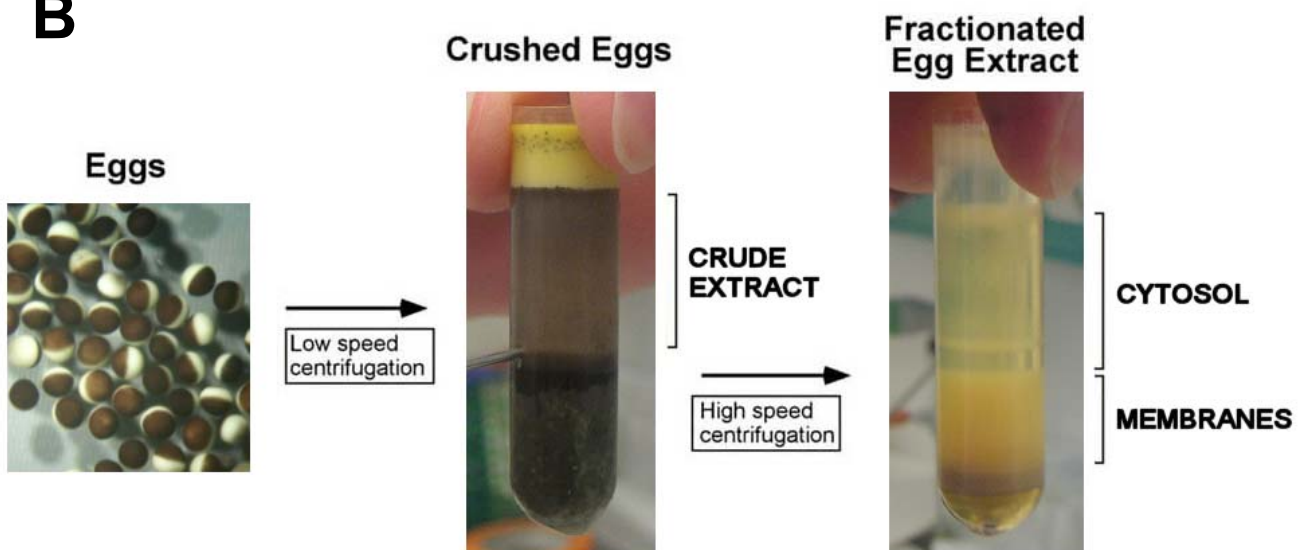
A**B**

Figure 4-1. Preparation of interphase *Xenopus laevis* egg extract. (A) Female *Xenopus laevis* frogs. (B) Fractionation of *Xenopus laevis* eggs by differential centrifugation. Eggs were packed into centrifuge tubes and lysed by low speed centrifugation yielding a crude extract, lipids (yellow top phase), pigments (black) and yolk (bottom pellet). Further centrifugation of the crude extract at high speed allows separation into a cytosolic and membrane fraction and removal of lipids (white phase on top), mitochondria (brown, below membranes) and glycogen+ribosomes (clear yellow pellet at bottom of tube). The membranes can be separated further on a stepwise sucrose gradient. Cytosol and membranes may be used for *in vitro* nuclear assembly reactions together with demembrated sperm head chromatin.

4.2.2.2.3 Preparation of mitotic *Xenopus leavis* egg extract

Mitotic egg extract was prepared as described in Desai *et al.* (1999). When used in experiments (immunoprecipitation or chromatin recruitment), mitotic extracts were supplemented with 1 μ M microcystin, 20 mM 2-phospho-glycerol and EDTA-free protease inhibitors and were centrifuged to remove membranes (TLA 120.2, 100000 rpm, 20 min, 4°C).

4.2.2.2.4 Floatation of interphase membranes

The membrane fraction was removed from the SW55Ti tube avoiding mitochondria and lipids. Total membranes were prepared by diluting the membranes 10 fold with S250 + 1 mM DTT + PI, mixing and douncing the mixture with pestle B on ice. The membranes were placed on top of 1 ml S500 + 1 mM DTT + PI in SW40 tubes and centrifuged (SW40, 18000 g (11000 rpm), 20 min, 4°C). The pelleted total membranes were taken up in a small volume of S250 + 1 mM DTT + PI and homogenized again in a small potter. The volume of the total membrane suspension was brought to 20% of the corresponding volume of cytosol, aliquoted and frozen and stored in liquid nitrogen.

In order to separate total membranes on a stepwise sucrose gradient (preparation of "floated membranes"), the membrane fraction from the second high speed spin was mixed with 2.1 M sucrose (1 ml membranes + 2.08 ml of 2.1 M sucrose solution). Membranes were homogenized in a large chilled potter with pestle B and filled into SW40 tubes (2 ml per tube). The membranes were overlaid with a stepwise sucrose gradient of decreasing density (each concentration prepared by dissolving additional sucrose in S250 + 1 mM DTT + PI): 1.4 M, 1.3 M, 1.1 M, 0.9 M, 0.7 M (1.6 ml each). The tubes were filled with S250 buffer and centrifuged (SW40, 225000 g (38000 rpm), 4 h, 4°C), setting the centrifuge to minimum deceleration (to avoid perturbation of the separated membranes). This step allowed separation of the total membrane fraction into six separate membrane layers. The two upper layers were collected individually, mixed 1:2.5 with S250 + 1 mM DTT + PI and centrifuged (TLA100.4, 420000 g (100000 rpm), 30 min, 4°C). The pelleted membranes were resuspended in S250 + 1 mM DTT + PI (1/30 of the cytosol volume for each membrane layer), homogenized in a chilled small douncer using pestle B and frozen as 15 μ l aliquots in liquid nitrogen. The membranes were stored in liquid nitrogen.

4.2.2.2.5 Labeling of floated membranes

For labeling membranes with the lipophilic membrane dye DiI_{C18}, floated membranes were supplemented with DiI_{C18} dissolved in DMSO + 1 mM DTT + PI at a final concentration of 5 μ g/ml and incubated on ice for 10 min. The labeled membranes were mixed 1:1 with S250 + 1 mM DTT + PI, laid on top of 1.2 ml S500 and centrifuged (TLA100.4, 420000 g (100000 rpm), 30 min, 4°C). The pelleted membranes were resuspended and homogenized as above and frozen in liquid nitrogen in 5 μ l aliquots. When used in nuclear assembly reactions, 1 volume of labeled membranes was diluted with 4 volumes of unlabeled membranes.

4.2.2.2.6 Preparation of sperm chromatin

This protocol was modified from Gurdon *et al.* (1976). Testis were removed from male *Xenopus laevis* frogs and separated into smaller pieces with forceps in HPS buffer (15 mM HEPES pH 7.4, 250 mM sucrose, 0.5 mM spermidine tetrachloride, 0.2 mM spermine). The testis fragments were further disrupted by pressing the suspension through a 1 ml syringe onto a glass plate. The suspension was filtered through cheese cloth to remove debris. Cells were pelleted by centrifugation in a Heraeus Megafuge 1.0 R (2000 rpm, 10 min, 4°C). The cell pellet was resuspended in 1 ml HSP supplemented with 0.3 mM PMSF and 50 µl 10 mg/ml lysolecithin. Plasma membranes were permeabilized at RT for 5 min and the reaction was stopped by addition of 10 ml chilled HSP buffer containing 0.3 mM PMSF and 3% BSA. The cells were pelleted repeatedly as above and washed with 3 ml HSP, 0.3 mM PMSF, 0.3% (w/v) BSA. The sperm heads were resuspended in 2.5 ml HSP buffer, 0.3% (w/v) BSA and 30% (v/v) glycerol, diluted and counted in a Neubauer chamber according to the manufacturer's instructions. Staining with trypan blue showed whether cells had been properly permeabilized. The preparation was diluted to 3000 sperm heads per µl, aliquoted, frozen in liquid nitrogen and stored at -80°C.

4.2.2.2.7 *In vitro* nuclear assembly

For a typical assembly reaction 20 µl interphase egg extract were added to 1 µl sperm head chromatin (3000/µl) and incubated at 20°C for 10 min. In this initial decondensation step, nucleoplasmin in the extract exchanges protamines bound to the chromatin with histones (Philpott *et al.*, 1991). Following the decondensation, 2 µl floated membranes, 0.4 µl 50x energy mix and 0.4 µl glycogen (200 mg/ml) were added and the reaction was incubated at 20°C for 90 min. The steps of nuclear assembly *in vitro* are depicted in Figure 4-2. In order to fluorescently label membranes following the nuclear assembly reaction, 1 µl of 0.1 µg/ml DilC₁₈ was added to the nuclei after the 90 min incubation, the sample was mixed and incubated at RT for 10 min. When using pre-labeled membranes, this step was omitted. Samples with labeled membranes or those designated for immunostaining with mAb414 were fixed with Viki fix on ice for 20min (0.5 ml of Viki fix per nuclear assembly reaction). For labeling with other antibodies, the nuclei were fixed with 4% PFA in PBS (0.5 ml per assembly reaction) at RT for 10 min. The fixed nuclei were placed on top of an 0.8 ml 30% (w/v) sucrose cushion in PBS and centrifuged onto poly L-Lysine-coated coverslips in a Heraeus Megafuge 1.0 R (3500 rpm, 15 min). The coverslips were washed once with water, mounted and sealed with nail polish.

Alternatively, the assembled nuclei were fixed and processed for immunofluorescence (chapter 4.2.3.4) or electron microscopy (chapter 4.2.3.6).

The exclusion assay on *in vitro* assembled nuclei was carried out as described in Franz *et al.* (2007).

4.2.2.2.8 Formation of annulate lamellae *in vitro*

Interphase egg extract was centrifuged to remove membranes (TLA120.2, 100000 rpm, 30 min, 4°C). 35 µl of membrane-free supernatant were supplemented with 0.7 µl 50x energy mix and 0.7 µl glycogen and up to 4 µl proteins/buffer (as required for the

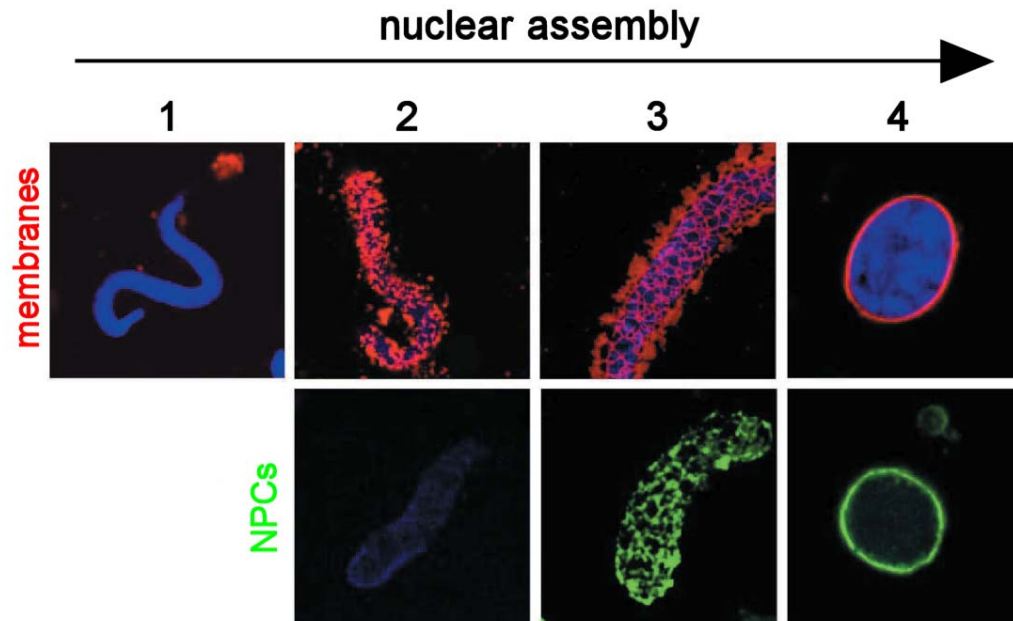


Figure 4-2. Steps of nuclear assembly *in vitro*. Decondensed, demembranated sperm heads (1) were incubated with DilC₁₈-labeled membranes (red) and cytosolic extracts, and the time course of NE assembly was recorded. During nuclear assembly, membranes bind to chromatin (2), form a network on the chromatin surface (3) and give rise to a closed NE (4). The *in vitro* assembled nuclei contain functional NPCs (green). After closure of the membranes, the nuclei grow and the NE expands in a transport-dependent manner. DNA is coloured in blue. (Modified from Hetzer *et al.*, 2002).

experiment). 35 μ l of the mixture were combined with 4 μ l floated membranes and incubated for 45 min at 20°C. The reaction was diluted with 0.95 ml S250, placed on top of a 0.8 ml 0.5 M sucrose cushion and centrifuged (TLS-55, 34000 g (22000 rpm), 20 min, 4°C). The pelleted AL were taken up in 50 μ l 1x SDS loading buffer and 10 μ l were loaded per lane of an SDS-PAGE gel.

4.2.2.2.9 Re-isolation of chromatin for Western blotting

For chromatin recruitment experiments *Xenopus laevis* egg extract was centrifuged to remove membranes (TLA120.2, 100000 rpm, 20 min, 4°C). Proteins, inhibitors or buffer (as required for the experiment) were added to the membrane-free cytosol and the mixture was incubated on ice for 5 min. A typical recruitment reaction was set up as follows: 60 μ l cytosol with additives were supplemented with 1.2 μ l 50x energy mix and 1.2 μ l glycogen, added to 3 μ l sperm head chromatin (3000/ μ l) and incubated at 20°C for 10min. The reaction was diluted with 0.94 ml S250 buffer and placed on top of a 0.6 ml 1.7 M sucrose cushion in TLS-55 rotor tubes. The chromatin templates were separated from the soluble extract by centrifugation (TLS-55, 10000 g (13000 rpm), 10 min, 4°C). Supernatant and sucrose cushion were carefully aspirated and the pelleted chromatin washed once with 1 ml S250 buffer, followed by a second round of centrifugation (TLS-55, 10000 g (13000 rpm), 10 min, 4°C). After removal of the S250 supernatant, the chromatin pellet was taken up in 60 μ l 1x SDS-loading buffer. 10 μ l sample were loaded per SDS-PAGE gel lane.

In order to analyze complete nuclei by Western blotting, a modified protocol was used. 40 μ l cytosol were added to 2 μ l sperm head chromatin (3000/ μ l) and incubated at 20°C for 10 min. 4 μ l floated membranes, 0.8 μ l 50x energy mix and 0.8 μ l glycogen were added and the reaction incubated at 20°C for 60 min. The assembly reaction was diluted with 0.95 ml isolation buffer (20 mM Tris pH 7.4, 70 mM KCl, 10 mM EDTA, 2 mM DTT, 2% (w/v) polyvinylpyrrolidone) and placed on a 0.5 ml 1.3 M sucrose cushion (in isolation buffer) in TLS-55 tubes. Following centrifugation (TLS-55, 5000 g (9000 rpm), 10 min, 4°C), supernatant and cushion were removed and the pelleted nuclei taken up in 50 μ l 1x SDS-loading buffer. 10 μ l sample were loaded per lane.

4.2.3 Other methods

4.2.3.1 Generation of polyclonal antibodies in rabbits

Immunization of rabbits was carried out with purified recombinant proteins expressed in *E. coli*. The antigen was dialyzed against PBS + 0.35 M NaCl, diluted to 2 mg/ml, frozen in 0.6 ml aliquots in liquid nitrogen and stored at -80°C. 0.6 ml antigen solution were mixed with 0.6 ml Titer Max Gold adjuvant and passed several times through an 0.8 mm needle until the emulsion remained viscous. A pre-bleed was taken prior to immunization. 0.6 ml antigen-Titer Max Gold emulsion were injected per rabbit and boost. Rabbits were boosted four times every 14 days before the first bleed was taken, followed by boosting and bleeding every 28 days. Antigen injection and bleeding of the rabbits were performed by EMBL Laboratory Animal Resources technicians. The blood was incubated in a water bath for 45 min at 37°C and

centrifuged twice in a Heraeus Megafuge 1.0 R (4000 rpm, 20 min, 4°C). The serum was frozen in liquid nitrogen and stored at -80°C.

Purified proteins used as antigen in this study were His₆-Hs MEL-28(aa 1208-1800), His₆-Hs MEL-28(aa 1572-2266), His₆-XI MEL-28(aa 1572-2266), His₆-XI Nup50 and GST-Hs NET5(aa 374-640)-His₆.

4.2.3.2 Cell culture

HeLa and U2OS cells were maintained in Dulbecco's modified Eagle medium (DMEM), high glucose, obtained from the EMBL media kitchen, supplemented with 10% fetal calf serum, 2 mM glutamine, 100 µg/ml penicillin and 100 U/ml streptomycin. Cells were grown in a Hera cell 240 incubator at 37 °C under 5% CO₂.

Xenopus laevis A6 cells were obtained from the Karsenti lab (EMBL Heidelberg) and maintained according to published protocols (Miller and Daniel, 1977).

4.2.3.3 Transient transfection of human cells

Transfection of HeLa cells with plasmids was carried out with the Fugene 6 transfection reagent (Roche) according to the manufacturer's instructions. 100 µl serum-free OptiMEM medium were mixed with 1 µg plasmid DNA and 3 µl Fugene 6 reagent and incubated at RT for 15 min. The entire mixture was added to 5 ml DMEM medium, mixed and added to the cells.

Transfection of HeLa or U2OS cells with siRNA oligonucleotides (at 50 nM final concentration) was performed with the HiPerFect Transfection Reagent (QIAGEN) according to the manufacturer's instructions.

4.2.3.4 Immunofluorescence

Fixed cells or *in vitro* assembled nuclei were incubated for 5 min in 50 mM ammonium chloride in PBS to quench remaining PFA. Blocking was carried out for 30 min in 3% (w/v) BSA in PBS-Tx (0.1% (v/v) Triton X-100). The samples were incubated with the primary antibodies in blocking solution at RT for 2 h and washed 6 times with PBS-Tx. Incubation with secondary antibodies in blocking solution was performed for 1 h, followed by 10 washes with PBS-Tx. In order to stain DNA, the samples were incubated for 10 min with 0.1 µg/ml DAPI in PBS or 5 ng/ml Hoechst 33342. The samples were washed twice with water, mounted and sealed with nail polisher.

For the selective permeabilization experiment, cells were treated for 10 min with either PBS + 0.25% (v/v) Triton X-100 or with 0.025% (w/v) digitonin in PBS on ice. Cells treated with digitonin were washed and incubated in PBS without Triton X-100.

4.2.3.5 Light microscopy

Image acquisition of microscopy samples was performed with Carl Zeiss LSM 510 META and Leica TCS SP2 AOBs FCS confocal microscopes. The fluorophores, predominantly DAPI, Alexa 488 and Alexa 568, were excited with the laser lines at 405 nm, 488 nm and 532 nm, respectively.

4.2.3.6 Electron microscopy

HeLa and A6 cells designated for immunogold labeling were prepared according to Tokuyasu (1973) and Tokuyasu (1978). Immunogold labeling was carried out as described in Slot *et al.* (1983).

For morphological studies by electron microscopy, HeLa cells rinsed twice with PBS and fixed with 2.5% glutaraldehyde in cacodylate buffer (50 mM sodium cacodylate pH 7.2) for 30 min. After fixation, they were washed 5 times (5 min each) with cacodylate buffer and then stained with 1% osmium tetroxide in cacodylate buffer for 40 min. After osmium staining, cells were rinsed 4 times with water, stained with 0.5% uranyl acetate in water for 40 min, and rinsed again 4 times with water. All fixation and staining steps were carried out on ice. Finally, the coverslips were taken through a series of dehydration steps with EtOH (40%, 50%, 70%, 80%, 90%), 5 min each step. Cells were further dehydrated twice with 96% EtOH and 100% dried EtOH. Coverslips were then dipped in propylene oxide and quickly placed on top of a BEEM capsule filled with Epon (Roth). Blocks were incubated for 48 h at 60°C. Serial sections were cut 60 nm thick and placed on a copper palladium slot grid coated with 1% Formvar (Serva).

In vitro assembled nuclei were prepared for electron microscopy according to Macaulay and Forbes (1996).

Imaging of the electron microscopy samples was performed with a CM-120 Biotwin (Phillips) electron microscope.

4.2.3.7 Bioinformatic tools

The following prediction algorithms were used to predict the structure and properties of MEL-28 and NET5:

For predicting MEL-28 protein disorder:

<http://dis.embl.de/>, <http://globplot.embl.de/>, <http://www.strubi.ox.ac.uk/RONN>,
<http://bip.weizmann.ac.il/fldbin/findex>,
<http://www.ist.temple.edu/disprot/predictorVSL2.php>, <http://iupred.enzim.hu/>,
<http://www.pondr.com/>, <http://bioinf.cs.ucl.ac.uk/disopred/disopred.html>

For predicting a signal peptide in NET5:

<http://www.cbs.dtu.dk/services/SignalP/>

5 References

- Akhtar, A. and S. M. Gasser (2007). "The nuclear envelope and transcriptional control." *Nat Rev Genet* **8**(7): 507-17.
- Alber, F., S. Dokudovskaya, et al. (2007). "The molecular architecture of the nuclear pore complex." *Nature* **450**(7170): 695-701.
- Anderson, D. J. and M. W. Hetzer (2007). "Nuclear envelope formation by chromatin-mediated reorganization of the endoplasmic reticulum." *Nat Cell Biol* **9**(10): 1160-6.
- Anderson, D. J. and M. W. Hetzer (2008). "Reshaping of the endoplasmic reticulum limits the rate for nuclear envelope formation." *J Cell Biol* **182**(5): 911-24.
- Antonin, W., C. Franz, et al. (2005). "The integral membrane nucleoporin pom121 functionally links nuclear pore complex assembly and nuclear envelope formation." *Mol Cell* **17**(1): 83-92.
- Aravind, L. and D. Landsman (1998). "AT-hook motifs identified in a wide variety of DNA-binding proteins." *Nucleic Acids Res* **26**(19): 4413-21.
- Askjaer, P., V. Galy, et al. (2002). "Ran GTPase cycle and importins alpha and beta are essential for spindle formation and nuclear envelope assembly in living *Caenorhabditis elegans* embryos." *Mol Biol Cell* **13**(12): 4355-70.
- Audhya, A., A. Desai, et al. (2007). "A role for Rab5 in structuring the endoplasmic reticulum." *J Cell Biol* **178**(1): 43-56.
- Bamba, C., Y. Bobinnec, et al. (2002). "The GTPase Ran regulates chromosome positioning and nuclear envelope assembly in vivo." *Curr Biol* **12**(6): 503-7.
- Baur, T., K. Ramadan, et al. (2007). "NSF- and SNARE-mediated membrane fusion is required for nuclear envelope formation and completion of nuclear pore complex assembly in *Xenopus laevis* egg extracts." *J Cell Sci* **120**(Pt 16): 2895-903.
- Bayliss, R., T. Littlewood, et al. (2000). "Structural basis for the interaction between FxFG nucleoporin repeats and importin-beta in nuclear trafficking." *Cell* **102**(1): 99-108.
- Bayliss, R., S. W. Leung, et al. (2002). "Structural basis for the interaction between NTF2 and nucleoporin FxFG repeats." *Embo J* **21**(12): 2843-53.
- Beaudouin, J., D. Gerlich, et al. (2002). "Nuclear envelope breakdown proceeds by microtubule-induced tearing of the lamina." *Cell* **108**(1): 83-96.
- Beck, M., F. Forster, et al. (2004). "Nuclear pore complex structure and dynamics revealed by cryoelectron tomography." *Science* **306**(5700): 1387-90.
- Beck, M., V. Lucic, et al. (2007). "Snapshots of nuclear pore complexes in action captured by cryo-electron tomography." *Nature* **449**(7162): 611-5.
- Belgareh, N., G. Rabut, et al. (2001). "An evolutionarily conserved NPC subcomplex, which redistributes in part to kinetochores in mammalian cells." *J Cell Biol* **154**(6): 1147-60.
- Ben-Efraim, I. and L. Gerace (2001). "Gradient of increasing affinity of importin beta for nucleoporins along the pathway of nuclear import." *J Cell Biol* **152**(2): 411-7.
- Bernad, R., H. van der Velde, et al. (2004). "Nup358/RanBP2 attaches to the nuclear pore complex via association with Nup88 and Nup214/CAN and plays a supporting role in CRM1-mediated nuclear protein export." *Mol Cell Biol* **24**(6): 2373-84.
- Bischoff, F. R. and H. Ponstingl (1991). "Catalysis of guanine nucleotide exchange on Ran by the mitotic regulator RCC1." *Nature* **354**(6348): 80-2.
- Blobel, G. (1985). "Gene gating: a hypothesis." *Proc Natl Acad Sci U S A* **82**(24): 8527-9.

- Blower, M. D., M. Nachury, et al. (2005). "A Rae1-containing ribonucleoprotein complex is required for mitotic spindle assembly." *Cell* **121**(2): 223-34.
- Bodoor, K., S. Shaikh, et al. (1999). "Sequential recruitment of NPC proteins to the nuclear periphery at the end of mitosis." *J Cell Sci* **112** (Pt 13): 2253-64.
- Böhmer, T., S. Jeudy, et al. (2008). "Structural and functional studies of Nup107/Nup133 interaction and its implications for the architecture of the nuclear pore complex." *Mol Cell* **30**(6): 721-31.
- Boman, A. L., M. R. Delannoy, et al. (1992). "GTP hydrolysis is required for vesicle fusion during nuclear envelope assembly in vitro." *J Cell Biol* **116**(2): 281-94.
- Brohawn, S. G., N. C. Leksa, et al. (2008). "Structural evidence for common ancestry of the nuclear pore complex and vesicle coats." *Science* **322**(5906): 1369-73.
- Burke, B. and C. L. Stewart (2002). "Life at the edge: the nuclear envelope and human disease." *Nat Rev Mol Cell Biol* **3**(8): 575-85.
- Campbell, M. S., G. K. Chan, et al. (2001). "Mitotic checkpoint proteins HsMAD1 and HsMAD2 are associated with nuclear pore complexes in interphase." *J Cell Sci* **114**(Pt 5): 953-63.
- Casolari, J. M., C. R. Brown, et al. (2004). "Genome-wide localization of the nuclear transport machinery couples transcriptional status and nuclear organization." *Cell* **117**(4): 427-39.
- Chakraborty, P., Y. Wang, et al. (2008). "Nucleoporin levels regulate cell cycle progression and phase-specific gene expression." *Dev Cell* **15**(5): 657-67.
- Chial, H. J., M. P. Rout, et al. (1998). "Saccharomyces cerevisiae Ndc1p is a shared component of nuclear pore complexes and spindle pole bodies." *J Cell Biol* **143**(7): 1789-800.
- Clarke, P. R. and C. Zhang (2008). "Spatial and temporal coordination of mitosis by Ran GTPase." *Nat Rev Mol Cell Biol* **9**(6): 464-77.
- Cook, A., F. Bono, et al. (2007). "Structural biology of nucleocytoplasmic transport." *Annu Rev Biochem* **76**: 647-71.
- Cordes, V. C., S. Reidenbach, et al. (1997). "Identification of protein p270/Tpr as a constitutive component of the nuclear pore complex-attached intranuclear filaments." *J Cell Biol* **136**(3): 515-29.
- Coutavas, E., M. Ren, et al. (1993). "Characterization of proteins that interact with the cell-cycle regulatory protein Ran/TC4." *Nature* **366**(6455): 585-7.
- Crisp, M., Q. Liu, et al. (2006). "Coupling of the nucleus and cytoplasm: role of the LINC complex." *J Cell Biol* **172**(1): 41-53.
- Cronshaw, J. M., A. N. Krutchinsky, et al. (2002). "Proteomic analysis of the mammalian nuclear pore complex." *J Cell Biol* **158**(5): 915-27.
- D'Angelo, M. A., D. J. Anderson, et al. (2006). "Nuclear pores form de novo from both sides of the nuclear envelope." *Science* **312**(5772): 440-3.
- Davis, L. I. and G. Blobel (1986). "Identification and characterization of a nuclear pore complex protein." *Cell* **45**(5): 699-709.
- Davuluri, G., W. Gong, et al. (2008). "Mutation of the zebrafish nucleoporin elys sensitizes tissue progenitors to replication stress." *PLoS Genet* **4**(10): e1000240.
- Dawlaty, M. M., L. Malureanu, et al. (2008). "Resolution of sister centromeres requires RanBP2-mediated SUMOylation of topoisomerase IIalpha." *Cell* **133**(1): 103-15.
- de Jong-Curtain, T. A., A. C. Parslow, et al. (2008). "Abnormal Nuclear Pore Formation Triggers Apoptosis in the Intestinal Epithelium of elys-Deficient

- Zebra Fish." Gastroenterology.
- De Souza, C. P., A. H. Osmani, et al. (2004). "Partial nuclear pore complex disassembly during closed mitosis in *Aspergillus nidulans*." Curr Biol **14**(22): 1973-84.
- Debler, E. W., Y. Ma, et al. (2008). "A fence-like coat for the nuclear pore membrane." Mol Cell **32**(6): 815-26.
- Denning, D. P., S. S. Patel, et al. (2003). "Disorder in the nuclear pore complex: the FG repeat regions of nucleoporins are natively unfolded." Proc Natl Acad Sci U S A **100**(5): 2450-5.
- Desai, A., A. Murray, et al. (1999). "The use of *Xenopus* egg extracts to study mitotic spindle assembly and function in vitro." Methods Cell Biol **61**: 385-412.
- Devos, D., S. Dokudovskaya, et al. (2004). "Components of coated vesicles and nuclear pore complexes share a common molecular architecture." PLoS Biol **2**(12): e380.
- Devos, D., S. Dokudovskaya, et al. (2006). "Simple fold composition and modular architecture of the nuclear pore complex." Proc Natl Acad Sci U S A **103**(7): 2172-7.
- Drin, G., J. F. Casella, et al. (2007). "A general amphipathic alpha-helical motif for sensing membrane curvature." Nat Struct Mol Biol **14**(2): 138-46.
- Dultz, E., E. Zanin, et al. (2008). "Systematic kinetic analysis of mitotic dis- and reassembly of the nuclear pore in living cells." J Cell Biol **180**(5): 857-65.
- Ellenberg, J., E. D. Siggia, et al. (1997). "Nuclear membrane dynamics and reassembly in living cells: targeting of an inner nuclear membrane protein in interphase and mitosis." J Cell Biol **138**(6): 1193-206.
- Englmeier, L., J. C. Olivo, et al. (1999). "Receptor-mediated substrate translocation through the nuclear pore complex without nucleotide triphosphate hydrolysis." Curr Biol **9**(1): 30-41.
- Eriksson, C., C. Rustom, et al. (2004). "Dynamic properties of nuclear pore complex proteins in gp210 deficient cells." FEBS Lett **572**(1-3): 261-5.
- Faria, A. M., A. Levay, et al. (2006). "The nucleoporin Nup96 is required for proper expression of interferon-regulated proteins and functions." Immunity **24**(3): 295-304.
- Favreau, C., H. J. Worman, et al. (1996). "Cell cycle-dependent phosphorylation of nucleoporins and nuclear pore membrane protein Gp210." Biochemistry **35**(24): 8035-44.
- Fernandez, A. G. and F. Piano (2006). "MEL-28 is downstream of the Ran cycle and is required for nuclear-envelope function and chromatin maintenance." Curr Biol **16**(17): 1757-63.
- Finlay, D. R., E. Meier, et al. (1991). "A complex of nuclear pore proteins required for pore function." J Cell Biol **114**(1): 169-83.
- Fornierod, M., M. Ohno, et al. (1997). "CRM1 is an export receptor for leucine-rich nuclear export signals." Cell **90**(6): 1051-60.
- Franke, W. W. (1966). "Isolated nuclear membranes." J Cell Biol **31**(3): 619-23.
- Franz, C., P. Askjaer, et al. (2005). "Nup155 regulates nuclear envelope and nuclear pore complex formation in nematodes and vertebrates." Embo J **24**(20): 3519-31.
- Franz, C., R. Walczak, et al. (2007). "MEL-28/ELYS is required for the recruitment of nucleoporins to chromatin and postmitotic nuclear pore complex assembly." EMBO Rep **8**(2): 165-72.

- Frey, S., R. P. Richter, et al. (2006). "FG-rich repeats of nuclear pore proteins form a three-dimensional meshwork with hydrogel-like properties." Science **314**(5800): 815-7.
- Frey, S. and D. Görlich (2007). "A saturated FG-repeat hydrogel can reproduce the permeability properties of nuclear pore complexes." Cell **130**(3): 512-23.
- Funabiki, H., I. Hagan, et al. (1993). "Cell cycle-dependent specific positioning and clustering of centromeres and telomeres in fission yeast." J Cell Biol **121**(5): 961-76.
- Galy, V., I. W. Mattaj, et al. (2003). "Caenorhabditis elegans nucleoporins Nup93 and Nup205 determine the limit of nuclear pore complex size exclusion in vivo." Mol Biol Cell **14**(12): 5104-15.
- Galy, V., P. Askjaer, et al. (2006). "MEL-28, a novel nuclear-envelope and kinetochore protein essential for zygotic nuclear-envelope assembly in *C. elegans*." Curr Biol **16**(17): 1748-56.
- Galy, V., W. Antonin, et al. (2008). "A role for gp210 in mitotic nuclear-envelope breakdown." J Cell Sci **121**(Pt 3): 317-28.
- Gerace, L. and G. Blobel (1980). "The nuclear envelope lamina is reversibly depolymerized during mitosis." Cell **19**(1): 277-87.
- Gillespie, P. J., G. A. Khoudoli, et al. (2007). "ELYS/MEL-28 chromatin association coordinates nuclear pore complex assembly and replication licensing." Curr Biol **17**(19): 1657-62.
- Glavy, J. S., A. N. Krutchinsky, et al. (2007). "Cell-cycle-dependent phosphorylation of the nuclear pore Nup107-160 subcomplex." Proc Natl Acad Sci U S A **104**(10): 3811-6.
- Goldberg, M. W., C. Wiese, et al. (1997). "Dimples, pores, star-rings, and thin rings on growing nuclear envelopes: evidence for structural intermediates in nuclear pore complex assembly." J Cell Sci **110** (Pt 4): 409-20.
- Goldfarb, D. S., A. H. Corbett, et al. (2004). "Importin alpha: a multipurpose nuclear-transport receptor." Trends Cell Biol **14**(9): 505-14.
- Gong, D., J. R. Pomerening, et al. (2007). "Cyclin A2 regulates nuclear-envelope breakdown and the nuclear accumulation of cyclin B1." Curr Biol **17**(1): 85-91.
- Gorjanacz, M., E. P. Klerkx, et al. (2007). "Caenorhabditis elegans BAF-1 and its kinase VRK-1 participate directly in post-mitotic nuclear envelope assembly." Embo J **26**(1): 132-43.
- Görlich, D. and U. Kutay (1999). "Transport between the cell nucleus and the cytoplasm." Annu Rev Cell Dev Biol **15**: 607-60.
- Grandi, P., T. Dang, et al. (1997). "Nup93, a vertebrate homologue of yeast Nic96p, forms a complex with a novel 205-kDa protein and is required for correct nuclear pore assembly." Mol Biol Cell **8**(10): 2017-38.
- Gruenbaum, Y., A. Margalit, et al. (2005). "The nuclear lamina comes of age." Nat Rev Mol Cell Biol **6**(1): 21-31.
- Guan, T., S. Muller, et al. (1995). "Structural analysis of the p62 complex, an assembly of O-linked glycoproteins that localizes near the central gated channel of the nuclear pore complex." Mol Biol Cell **6**(11): 1591-603.
- Gunsalus, K. C., H. Ge, et al. (2005). "Predictive models of molecular machines involved in Caenorhabditis elegans early embryogenesis." Nature **436**(7052): 861-5.
- Gurdon, J. B. (1976). "Injected nuclei in frog oocytes: fate, enlargement, and chromatin dispersal." J Embryol Exp Morphol **36**(3): 523-40.

- Guzik, B. W., L. Levesque, et al. (2001). "NXT1 (p15) is a crucial cellular cofactor in TAP-dependent export of intron-containing RNA in mammalian cells." Mol Cell Biol **21**(7): 2545-54.
- Hachet, V., T. Kocher, et al. (2004). "Importin alpha associates with membranes and participates in nuclear envelope assembly in vitro." Embo J **23**(7): 1526-35.
- Hachet, V., C. Canard, et al. (2007). "Centrosomes promote timely mitotic entry in *C. elegans* embryos." Dev Cell **12**(4): 531-41.
- Haque, F., D. J. Lloyd, et al. (2006). "SUN1 interacts with nuclear lamin A and cytoplasmic nesprins to provide a physical connection between the nuclear lamina and the cytoskeleton." Mol Cell Biol **26**(10): 3738-51.
- Harel, A., A. V. Orjalo, et al. (2003a). "Removal of a single pore subcomplex results in vertebrate nuclei devoid of nuclear pores." Mol Cell **11**(4): 853-64.
- Harel, A., R. C. Chan, et al. (2003b). "Importin beta negatively regulates nuclear membrane fusion and nuclear pore complex assembly." Mol Biol Cell **14**(11): 4387-96.
- Hartl, P., E. Olson, et al. (1994). "Nuclear assembly with lambda DNA in fractionated *Xenopus* egg extracts: an unexpected role for glycogen in formation of a higher order chromatin intermediate." J Cell Biol **124**(3): 235-48.
- Hawryluk-Gara, L. A., E. K. Shibuya, et al. (2005). "Vertebrate Nup53 interacts with the nuclear lamina and is required for the assembly of a Nup93-containing complex." Mol Biol Cell **16**(5): 2382-94.
- Hawryluk-Gara, L. A., M. Platani, et al. (2008). "Nup53 is required for nuclear envelope and nuclear pore complex assembly." Mol Biol Cell **19**(4): 1753-62.
- Hetzer, M., D. Bilbao-Cortes, et al. (2000). "GTP hydrolysis by Ran is required for nuclear envelope assembly." Mol Cell **5**(6): 1013-24.
- Hetzer, M., H. H. Meyer, et al. (2001). "Distinct AAA-ATPase p97 complexes function in discrete steps of nuclear assembly." Nat Cell Biol **3**(12): 1086-91.
- Hetzer, M., O. J. Gruss, et al. (2002). "The Ran GTPase as a marker of chromosome position in spindle formation and nuclear envelope assembly." Nat Cell Biol **4**(7): E177-84.
- Holaska, J. M., K. L. Wilson, et al. (2002). "The nuclear envelope, lamins and nuclear assembly." Curr Opin Cell Biol **14**(3): 357-64.
- Hsia, K. C., P. Stavropoulos, et al. (2007). "Architecture of a coat for the nuclear pore membrane." Cell **131**(7): 1313-26.
- Huth, J. R., C. A. Bewley, et al. (1997). "The solution structure of an HMG-I(Y)-DNA complex defines a new architectural minor groove binding motif." Nat Struct Biol **4**(8): 657-65.
- Iouk, T., O. Kerscher, et al. (2002). "The yeast nuclear pore complex functionally interacts with components of the spindle assembly checkpoint." J Cell Biol **159**(5): 807-19.
- Ishii, K., G. Arib, et al. (2002). "Chromatin boundaries in budding yeast: the nuclear pore connection." Cell **109**(5): 551-62.
- Jeganathan, K. B., L. Malureanu, et al. (2005). "The Rae1-Nup98 complex prevents aneuploidy by inhibiting securin degradation." Nature **438**(7070): 1036-9.
- Joseph, J., S. T. Liu, et al. (2004). "The RanGAP1-RanBP2 complex is essential for microtubule-kinetochore interactions in vivo." Curr Biol **14**(7): 611-7.
- Kalab, P., K. Weis, et al. (2002). "Visualization of a Ran-GTP gradient in interphase and mitotic *Xenopus* egg extracts." Science **295**(5564): 2452-6.
- Kalab, P., A. Pralle, et al. (2006). "Analysis of a RanGTP-regulated gradient in mitotic

- somatic cells." Nature **440**(7084): 697-701.
- Katahira, J., K. Strasser, et al. (1999). "The Mex67p-mediated nuclear mRNA export pathway is conserved from yeast to human." Embo J **18**(9): 2593-609.
- Kessel, R. G. (1992). "Annulate lamellae: a last frontier in cellular organelles." Int Rev Cytol **133**: 43-120.
- Kimura, N., M. Takizawa, et al. (2002). "Identification of a novel transcription factor, ELYS, expressed predominantly in mouse foetal haematopoietic tissues." Genes Cells **7**(4): 435-46.
- King, M. C., C. P. Lusk, et al. (2006). "Karyopherin-mediated import of integral inner nuclear membrane proteins." Nature **442**(7106): 1003-7.
- King, M. C., T. G. Drivas, et al. (2008). "A network of nuclear envelope membrane proteins linking centromeres to microtubules." Cell **134**(3): 427-38.
- Kiseleva, E., S. Rutherford, et al. (2001). "Steps of nuclear pore complex disassembly and reassembly during mitosis in early *Drosophila* embryos." J Cell Sci **114**(Pt 20): 3607-18.
- Klebe, C., H. Prinz, et al. (1995). "The kinetic mechanism of Ran--nucleotide exchange catalyzed by RCC1." Biochemistry **34**(39): 12543-52.
- Köhler, A., M. S. Schmidt-Zachmann, et al. (1997). "AND-1, a natural chimeric DNA-binding protein, combines an HMG-box with regulatory WD-repeats." J Cell Sci **110** (Pt 9): 1051-62.
- Kutay, U. and M. W. Hetzer (2008). "Reorganization of the nuclear envelope during open mitosis." Curr Opin Cell Biol **20**(6): 669-77.
- Lenart, P., G. Rabut, et al. (2003). "Nuclear envelope breakdown in starfish oocytes proceeds by partial NPC disassembly followed by a rapidly spreading fenestration of nuclear membranes." J Cell Biol **160**(7): 1055-68.
- Liu, Q., N. Pante, et al. (2007). "Functional association of Sun1 with nuclear pore complexes." J Cell Biol **178**(5): 785-98.
- Liu, H. L., C. P. De Souza, et al. (2009). "The three fungal transmembrane nuclear pore complex proteins of *aspergillus nidulans* are dispensable in the presence of an intact An-Nup84-120 complex." Mol Biol Cell **20**(2): 616-30.
- Lohka, M. J. and Y. Masui (1983). "Formation in vitro of sperm pronuclei and mitotic chromosomes induced by amphibian ooplasmic components." Science **220**(4598): 719-21.
- Loiodice, I., A. Alves, et al. (2004). "The entire Nup107-160 complex, including three new members, is targeted as one entity to kinetochores in mitosis." Mol Biol Cell **15**(7): 3333-44.
- Lopez-Soler, R. I., R. D. Moir, et al. (2001). "A role for nuclear lamins in nuclear envelope assembly." J Cell Biol **154**(1): 61-70.
- Lutzmann, M., R. Kunze, et al. (2002). "Modular self-assembly of a Y-shaped multiprotein complex from seven nucleoporins." Embo J **21**(3): 387-97.
- Macaulay, C. and D. J. Forbes (1996). "Assembly of the nuclear pore: biochemically distinct steps revealed with NEM, GTP gamma S, and BAPTA." J Cell Biol **132**(1-2): 5-20.
- Madrid, A. S., J. Mancuso, et al. (2006). "The role of the integral membrane nucleoporins Ndc1p and Pom152p in nuclear pore complex assembly and function." J Cell Biol **173**(3): 361-71.
- Mahajan, R., C. Delphin, et al. (1997). "A small ubiquitin-related polypeptide involved in targeting RanGAP1 to nuclear pore complex protein RanBP2." Cell **88**(1): 97-107.

- Malone, C. J., L. Misner, et al. (2003). "The *C. elegans* hook protein, ZYG-12, mediates the essential attachment between the centrosome and nucleus." Cell **115**(7): 825-36.
- Mans, B. J., V. Anantharaman, et al. (2004). "Comparative genomics, evolution and origins of the nuclear envelope and nuclear pore complex." Cell Cycle **3**(12): 1612-37.
- Mansfeld, J., S. Guttinger, et al. (2006). "The conserved transmembrane nucleoporin NDC1 is required for nuclear pore complex assembly in vertebrate cells." Mol Cell **22**(1): 93-103.
- Mattaj, I. W. and L. Englmeier (1998). "Nucleocytoplasmic transport: the soluble phase." Annu Rev Biochem **67**: 265-306.
- Mattaj, I. W. (2004). "Sorting out the nuclear envelope from the endoplasmic reticulum." Nat Rev Mol Cell Biol **5**(1): 65-9.
- Matunis, M. J., E. Coutavas, et al. (1996). "A novel ubiquitin-like modification modulates the partitioning of the Ran-GTPase-activating protein RanGAP1 between the cytosol and the nuclear pore complex." J Cell Biol **135**(6 Pt 1): 1457-70.
- Maul, G. G., H. M. Maul, et al. (1972). "Time sequence of nuclear pore formation in phytohemagglutinin-stimulated lymphocytes and in HeLa cells during the cell cycle." J Cell Biol **55**(2): 433-47.
- Meier, E., B. R. Miller, et al. (1995). "Nuclear pore complex assembly studied with a biochemical assay for annulate lamellae formation." J Cell Biol **129**(6): 1459-72.
- Melcak, I., A. Hoelz, et al. (2007). "Structure of Nup58/45 suggests flexible nuclear pore diameter by intermolecular sliding." Science **315**(5819): 1729-32.
- Mendjan, S., M. Taipale, et al. (2006). "Nuclear pore components are involved in the transcriptional regulation of dosage compensation in *Drosophila*." Mol Cell **21**(6): 811-23.
- Miller, L. and J. C. Daniel (1977). "Comparison of in vivo and in vitro ribosomal RNA synthesis in nucleolar mutants of *Xenopus laevis*." In Vitro **13**(9): 557-63.
- Moir, R. D., M. Yoon, et al. (2000). "Nuclear lamins A and B1: different pathways of assembly during nuclear envelope formation in living cells." J Cell Biol **151**(6): 1155-68.
- Mühlhauser, P. and U. Kutay (2007). "An in vitro nuclear disassembly system reveals a role for the RanGTPase system and microtubule-dependent steps in nuclear envelope breakdown." J Cell Biol **178**(4): 595-610.
- Nachury, M. V. and K. Weis (1999). "The direction of transport through the nuclear pore can be inverted." Proc Natl Acad Sci U S A **96**(17): 9622-7.
- Napetschnig, J., G. Blobel, et al. (2007). "Crystal structure of the N-terminal domain of the human protooncogene Nup214/CAN." Proc Natl Acad Sci U S A **104**(6): 1783-8.
- Newmeyer, D. D. and K. L. Wilson (1991). "Egg extracts for nuclear import and nuclear assembly reactions." Methods Cell Biol **36**: 607-34.
- Newport, J. and W. Dunphy (1992). "Characterization of the membrane binding and fusion events during nuclear envelope assembly using purified components." J Cell Biol **116**(2): 295-306.
- Nousiainen, M., H. H. Sillje, et al. (2006). "Phosphoproteome analysis of the human mitotic spindle." Proc Natl Acad Sci U S A **103**(14): 5391-6.
- Ohba, T., E. C. Schirmer, et al. (2004). "Energy- and temperature-dependent transport of integral proteins to the inner nuclear membrane via the nuclear pore." J Cell

- Biol **167**(6): 1051-62.
- Okita, K., I. Nobuhisa, et al. (2003). "Genomic organization and characterization of the mouse ELYS gene." Biochem Biophys Res Commun **305**(2): 327-32.
- Okita, K., H. Kiyonari, et al. (2004). "Targeted disruption of the mouse ELYS gene results in embryonic death at peri-implantation development." Genes Cells **9**(11): 1083-91.
- Orjalo, A. V., A. Arnaoutov, et al. (2006). "The Nup107-160 nucleoporin complex is required for correct bipolar spindle assembly." Mol Biol Cell **17**(9): 3806-18.
- Palancade, B., X. Liu, et al. (2007). "Nucleoporins prevent DNA damage accumulation by modulating Ulp1-dependent sumoylation processes." Mol Biol Cell **18**(8): 2912-23.
- Palancade, B. and V. Doye (2008). "Sumoylating and desumoylating enzymes at nuclear pores: underpinning their unexpected duties?" Trends Cell Biol **18**(4): 174-83.
- Patel, S. S., B. J. Belmont, et al. (2007). "Natively unfolded nucleoporins gate protein diffusion across the nuclear pore complex." Cell **129**(1): 83-96.
- Philpott, A., G. H. Leno, et al. (1991). "Sperm decondensation in *Xenopus* egg cytoplasm is mediated by nucleoplasmin." Cell **65**(4): 569-78.
- Pickersgill, H., B. Kalverda, et al. (2006). "Characterization of the *Drosophila melanogaster* genome at the nuclear lamina." Nat Genet **38**(9): 1005-14.
- Platani, M., I. Goldberg, et al. (2000). "In vivo analysis of Cajal body movement, separation, and joining in live human cells." J Cell Biol **151**(7): 1561-74.
- Portier, N., A. Audhya, et al. (2007). "A microtubule-independent role for centrosomes and aurora a in nuclear envelope breakdown." Dev Cell **12**(4): 515-29.
- Prunuske, A. J. and K. S. Ullman (2006). "The nuclear envelope: form and reformation." Curr Opin Cell Biol **18**(1): 108-16.
- Puhka, M., H. Vihinen, et al. (2007). "Endoplasmic reticulum remains continuous and undergoes sheet-to-tubule transformation during cell division in mammalian cells." J Cell Biol **179**(5): 895-909.
- Rabut, G., V. Doye, et al. (2004). "Mapping the dynamic organization of the nuclear pore complex inside single living cells." Nat Cell Biol **6**(11): 1114-21.
- Ramadan, K., R. Bruderer, et al. (2007). "Cdc48/p97 promotes reformation of the nucleus by extracting the kinase Aurora B from chromatin." Nature **450**(7173): 1258-62.
- Rasala, B. A., A. V. Orjalo, et al. (2006). "ELYS is a dual nucleoporin/kinetochore protein required for nuclear pore assembly and proper cell division." Proc Natl Acad Sci U S A **103**(47): 17801-6.
- Rasala, B. A., C. Ramos, et al. (2008). "Capture of AT-rich chromatin by ELYS recruits POM121 and NDC1 to initiate nuclear pore assembly." Mol Biol Cell **19**(9): 3982-96.
- Reddy, K. L., J. M. Zullo, et al. (2008). "Transcriptional repression mediated by repositioning of genes to the nuclear lamina." Nature **452**(7184): 243-7.
- Reichelt, R., A. Holzenburg, et al. (1990). "Correlation between structure and mass distribution of the nuclear pore complex and of distinct pore complex components." J Cell Biol **110**(4): 883-94.
- Rexach, M. and G. Blobel (1995). "Protein import into nuclei: association and dissociation reactions involving transport substrate, transport factors, and nucleoporins." Cell **83**(5): 683-92.
- Ribbeck, K., G. Lipowsky, et al. (1998). "NTF2 mediates nuclear import of Ran." Embo

- J **17**(22): 6587-98.
- Ribbeck, K., U. Kutay, et al. (1999). "The translocation of transportin-cargo complexes through nuclear pores is independent of both Ran and energy." Curr Biol **9**(1): 47-50.
- Ribbeck, K. and D. Görlich (2001). "Kinetic analysis of translocation through nuclear pore complexes." Embo J **20**(6): 1320-30.
- Rout, M. P., J. D. Aitchison, et al. (2000). "The yeast nuclear pore complex: composition, architecture, and transport mechanism." J Cell Biol **148**(4): 635-51.
- Ryan, K. J., J. M. McCaffery, et al. (2003). "The Ran GTPase cycle is required for yeast nuclear pore complex assembly." J Cell Biol **160**(7): 1041-53.
- Ryan, K. J., Y. Zhou, et al. (2007). "The karyopherin Kap95 regulates nuclear pore complex assembly into intact nuclear envelopes in vivo." Mol Biol Cell **18**(3): 886-98.
- Salina, D., K. Bodoor, et al. (2002). "Cytoplasmic dynein as a facilitator of nuclear envelope breakdown." Cell **108**(1): 97-107.
- Salina, D., P. Enarson, et al. (2003). "Nup358 integrates nuclear envelope breakdown with kinetochore assembly." J Cell Biol **162**(6): 991-1001.
- Schirmer, E. C., L. Florens, et al. (2003). "Nuclear membrane proteins with potential disease links found by subtractive proteomics." Science **301**(5638): 1380-2.
- Schrader, N., P. Stelter, et al. (2008). "Structural basis of the nic96 subcomplex organization in the nuclear pore channel." Mol Cell **29**(1): 46-55.
- Schwartz, T. U. (2005). "Modularity within the architecture of the nuclear pore complex." Curr Opin Struct Biol **15**(2): 221-6.
- Shah, S., S. Tugendreich, et al. (1998). "Major binding sites for the nuclear import receptor are the internal nucleoporin Nup153 and the adjacent nuclear filament protein Tpr." J Cell Biol **141**(1): 31-49.
- Siniosoglou, S., C. Wimmer, et al. (1996). "A novel complex of nucleoporins, which includes Sec13p and a Sec13p homolog, is essential for normal nuclear pores." Cell **84**(2): 265-75.
- Siniosoglou, S., M. Lutzmann, et al. (2000). "Structure and assembly of the Nup84p complex." J Cell Biol **149**(1): 41-54.
- Slot, J. W. and H. J. Geuze (1983). "Immunoelectron microscopic exploration of the Golgi complex." J Histochem Cytochem **31**(8): 1049-56.
- Smith, A. E., B. M. Slepchenko, et al. (2002). "Systems analysis of Ran transport." Science **295**(5554): 488-91.
- Soullam, B. and H. J. Worman (1993). "The amino-terminal domain of the lamin B receptor is a nuclear envelope targeting signal." J Cell Biol **120**(5): 1093-100.
- Starr, D. A. and M. Han (2002). "Role of ANC-1 in tethering nuclei to the actin cytoskeleton." Science **298**(5592): 406-9.
- Starr, D. A. (2007). "Communication between the cytoskeleton and the nuclear envelope to position the nucleus." Mol Biosyst **3**(9): 583-9.
- Stavru, F., G. Nautrup-Pedersen, et al. (2006a). "Nuclear pore complex assembly and maintenance in POM121- and gp210-deficient cells." J Cell Biol **173**(4): 477-83.
- Stavru, F., B. B. Hulsmann, et al. (2006b). "NDC1: a crucial membrane-integral nucleoporin of metazoan nuclear pore complexes." J Cell Biol **173**(4): 509-19.
- Strasser, K. and E. Hurt (2000). "Yra1p, a conserved nuclear RNA-binding protein, interacts directly with Mex67p and is required for mRNA export." Embo J **19**(3): 410-20.

- Strawn, L. A., T. Shen, et al. (2004). "Minimal nuclear pore complexes define FG repeat domains essential for transport." Nat Cell Biol **6**(3): 197-206.
- Taddei, A., G. Van Houwe, et al. (2006). "Nuclear pore association confers optimal expression levels for an inducible yeast gene." Nature **441**(7094): 774-8.
- Tarendeau, F., J. Boudet, et al. (2007). "Structure and nuclear import function of the C-terminal domain of influenza virus polymerase PB2 subunit." Nat Struct Mol Biol **14**(3): 229-33.
- Tokuyasu, K. T. (1973). "A technique for ultracryotomy of cell suspensions and tissues." J Cell Biol **57**(2): 551-65.
- Tokuyasu, K. T. (1978). "A study of positive staining of ultrathin frozen sections." J Ultrastruct Res **63**(3): 287-307.
- Ulbert, S., W. Antonin, et al. (2006a). "The inner nuclear membrane protein Lem2 is critical for normal nuclear envelope morphology." FEBS Lett **580**(27): 6435-41.
- Ulbert, S., M. Platani, et al. (2006b). "Direct membrane protein-DNA interactions required early in nuclear envelope assembly." J Cell Biol **173**(4): 469-76.
- Vasu, S., S. Shah, et al. (2001). "Novel vertebrate nucleoporins Nup133 and Nup160 play a role in mRNA export." J Cell Biol **155**(3): 339-54.
- Vigers, G. P. and M. J. Lohka (1991). "A distinct vesicle population targets membranes and pore complexes to the nuclear envelope in *Xenopus* eggs." J Cell Biol **112**(4): 545-56.
- Voeltz, G. K., W. A. Prinz, et al. (2006). "A class of membrane proteins shaping the tubular endoplasmic reticulum." Cell **124**(3): 573-86.
- Walther, T. C., M. Fornerod, et al. (2001). "The nucleoporin Nup153 is required for nuclear pore basket formation, nuclear pore complex anchoring and import of a subset of nuclear proteins." Embo J **20**(20): 5703-14.
- Walther, T. C., H. S. Pickersgill, et al. (2002). "The cytoplasmic filaments of the nuclear pore complex are dispensable for selective nuclear protein import." J Cell Biol **158**(1): 63-77.
- Walther, T. C., A. Alves, et al. (2003a). "The conserved Nup107-160 complex is critical for nuclear pore complex assembly." Cell **113**(2): 195-206.
- Walther, T. C., P. Askjaer, et al. (2003b). "RanGTP mediates nuclear pore complex assembly." Nature **424**(6949): 689-94.
- Watson, M. L. (1959). "Further observations on the nuclear envelope of the animal cell." J Biophys Biochem Cytol **6**: 147-56.
- Weis, K. (2003). "Regulating access to the genome: nucleocytoplasmic transport throughout the cell cycle." Cell **112**(4): 441-51.
- Wiese, C., M. W. Goldberg, et al. (1997). "Nuclear envelope assembly in *Xenopus* extracts visualized by scanning EM reveals a transport-dependent 'envelope smoothing' event." J Cell Sci **110** (Pt 13): 1489-502.
- Winey, M., D. Yarar, et al. (1997). "Nuclear pore complex number and distribution throughout the *Saccharomyces cerevisiae* cell cycle by three-dimensional reconstruction from electron micrographs of nuclear envelopes." Mol Biol Cell **8**(11): 2119-32.
- Yang, L., T. Guan, et al. (1997). "Integral membrane proteins of the nuclear envelope are dispersed throughout the endoplasmic reticulum during mitosis." J Cell Biol **137**(6): 1199-210.
- Ye, Q. and H. J. Worman (1996). "Interaction between an integral protein of the nuclear envelope inner membrane and human chromodomain proteins homologous to *Drosophila* HP1." J Biol Chem **271**(25): 14653-6.

- Yokoyama, N., N. Hayashi, et al. (1995). "A giant nucleopore protein that binds Ran/TC4." Nature **376**(6536): 184-8.
- Zabel, U., V. Doye, et al. (1996). "Nic96p is required for nuclear pore formation and functionally interacts with a novel nucleoporin, Nup188p." J Cell Biol **133**(6): 1141-52.
- Zhang, X., S. Chen, et al. (2008). "Mutation in nuclear pore component NUP155 leads to atrial fibrillation and early sudden cardiac death." Cell **135**(6): 1017-27.
- Zuccolo, M., A. Alves, et al. (2007). "The human Nup107-160 nuclear pore subcomplex contributes to proper kinetochore functions." Embo J **26**(7): 1853-64.

Declaration

I, Rudolf Walczak, declare I am the author of this thesis and all cited references with the exemption of purely technical references have been consulted. The work presented in this thesis is the original work undertaken under the supervision of Prof. Iain W. Mattaj and work carried out by others is clearly stated. This dissertation, in whole or in part, has not been previously accepted for a higher degree.

Erklärung

Hiermit bestätige ich, Rudolf Walczak, die vorliegende Arbeit selbständig verfasst und keine anderen als die angegebenen Quellen und Hilfsmittel verwendet zu haben. Die Ergebnisse anderer und die aus zitierten Werken wörtlich oder inhaltlich entnommenen Stellen wurden als solche kenntlich gemacht.

Heidelberg, January 2009

Rudolf Walczak

Publications

Franz C*, **Walczak R***, Yavuz S, Santarella R, Gentzel M, Askjaer P, Galy V, Hetzer M, Mattaj IW and Antonin W (2007). "MEL-28/ELYS is required for the recruitment of nucleoporins to chromatin and postmitotic nuclear pore complex assembly." EMBO Rep **8**: 165-72.

* authors contributed equally

Platani M, Santarella-Mellwig R, Posch M, **Walczak R**, Swedlow JR and Mattaj IW (2008). "The Nup107-160 nucleoporin complex promotes mitotic events via control of the localisation and modification of the chromosome passenger complex." (submitted)

Poster presentation

Walczak R*, Franz C*, Yavuz S, Santarella R, Mattaj IW and Antonin W (2006). "MEL-28 is essential for postmitotic nuclear pore complex assembly."

* authors contributed equally

Poster presented at the 11th International *Xenopus* conference in Kisarazu, Japan, 2006.

Acknowledgements

I wish to thank Iain Mattaj for giving me the opportunity to undertake my PhD research in his laboratory and for his continuous support and encouragement. Working at EMBL under his supervision is an invaluable experience from which I will profit for the rest of my professional life.

I am indebted to my thesis advisory committee members Jan Ellenberg, Jürg Müller and Elmar Schiebel for their feedback and guidance throughout my PhD.

I thank Cerstin Franz for initiating the MEL-28 project, which became the majority of my PhD and I am very grateful to Wolfram Antonin whose help, motivation and supervision were invaluable during the first year of my PhD.

I would like to thank all past and present members of the Mattaj lab (Andi, Andri, Birgit, Cerstin, Claudia, Claudio, Iain D, Katharina, Katrien, Matyas, Melpi, Moritz, Rachel, Sebastian, Sevil, Uli and Wolfram) for their help, discussions and for providing a very pleasant working atmosphere. I wish all of them all the best for their projects and future work. I want to thank Moritz, Iain and Rachel for the good time we had in our bay and Moritz & Iain for the daily avalanche of (mostly funny) puns and jokes.

I am thankful to Matyas Gorjanacz, Nathalie Daigle and Rachel Mellwig for collaborating with me on the NET5 project.

EMBL is a wonderful place full of motivated, competent and helpful people. I thank every one of them who has contributed to my PhD, in particular Kreso for keeping the frogs happy, Rachel Mellwig for her excellent EM analysis of so many of my samples, Vladimir Benes and Gene Core for their help relating to molecular biology, Ann-Marie Lawrence for expressing MEL-28 with the Baculo system, Marc Gentzel for identifying proteins by mass spectrometry, Darren Hart for the collaboration with the ESPRIT method and Tobias Doerks for his help with bioinformatics.

I thank Iain Mattaj, Iain Davidson and Moritz Mall for critically reading this manuscript and for helpful comments and suggestions.

I thank my friends Raju Tomer and Alexandru Denes for our interesting discussions and the many memorable moments during the past three years.

Last but not least, I especially wish to thank Claudia for our happy time in Heidelberg and her and my family for their constant encouragement and support.